Sampling the Physical Ocean in CMIP6 Simulations

CLIVAR Ocean Model Development Panel (OMDP)
Committee on CMIP6 Ocean Model Output

Stephen M. Griffies (NOAA Geophysical Fluid Dynamics Laboratory, USA)
Alistair J. Adcroft (NOAA/GFDL and Princeton University, USA)
V. Balaji (NOAA/GFDL and Princeton University, USA)
Gokhan Danabasoglu (National Center for Atmospheric Research, USA)
Paul J. Durack (LLNL/Program for Climate Model Diagnosis and Intercomparison, USA)
Peter J. Gleckler (LLNL/Program for Climate Model Diagnosis and Intercomparison, USA)
Jonathan M. Gregory (Hadley Centre and University of Reading, UK)
John P. Krasting (NOAA Geophysical Fluid Dynamics Laboratory, USA)
Trevor J. McDougall (University of New South Wales, AUS)
Ronald J. Stouffer (NOAA Geophysical Fluid Dynamics Laboratory, USA)
Karl E. Taylor (LLNL/Program for Climate Model Diagnosis and Intercomparison, USA)

Version 1.0
March 6, 2015

Abstract

We present recommendations for sampling physical ocean fields for the World Climate Research Program (WCRP) Coupled Model Intercomparison Project #6 (CMIP6), including its DECK experiment suite, the historical simulation (1850-2014), as well as any CMIP6 satellite MIPs that include a physical ocean model component. Such MIPs in particular include the Ocean Model Intercomparison Project (OMIP), Coupled Climate Carbon Cycle Model Intercomparison Project (C4MIP), Decadal Climate Prediction Project (DCPP), High Resolution Model Intercomparison Project (HighResMIP), and the Flux Anomoly Forcing Model Intercomparison Project (FAFMIP). We motivate the diagnostics by presenting salient scientific reasons for their relevance, and present a practical framework for meaningful comparisons across climate models and observational based measurements. We focus on diagnostics related to physical properties and processes within the simulated ocean, along with associated ocean boundary fluxes. The audience for this document includes the WCRP Working Group for Coupled Modeling (WGCM), the CMIP panel, CLIVAR Scientific Steering Group (SSG), CLIVAR Ocean Model Development Panel (OMDP), scientists contributing model results to CMIP, and scientists analyzing ocean climate simulations.

History of this document

This document started from the CMIP5 recommendations of Griffies et al. (2009a). The co-authors iterated during September 2014 to prepare the draft presented to WGCM and CLIVAR SSG in late September 2014. Further iterations followed from this initial release to the community, leading up to Version 1.0 released March 6, 2015.

Acknowledgements

We thank the modelling groups at GFDL, NCAR, and the Hadley Centre for feedback on this document.

How to cite

S.M. Griffies, A.J. Adcroft, V. Balaji, G. Danabasoglu, P.J. Durack, P.J. Gleckler, J.M. Gregory, J.P. Krasting, T.J. McDougall, R.J. Stouffer, K.E. Taylor, 2015: **Sampling the Physical Ocean in CMIP6 Simulations**, WCRP Publication Number (TBD), 68 pages. Version 1.0 from March 6, 2015.

Contents

Chapter 1

Sampling and archiving ocean fields

Contents

We here present certain recommendations about sampling numerical ocean models in time and space. We also address questions regarding the computational precision of the archived model data. Temporal sampling recommendations are identical to CMIP5. Spatial sampling recommendations for CMIP6 are modified relative to CMIP5, with the aim to facilitate both primary and secondary analyses using the archived diagnostics. Finally, we detail issues related to the TEOS-10 seawater thermodynamics.

1.1 Primary and secondary analyses

In this document, we consider the often conflicting needs for those undertaking *primary analyses* versus those interested in *secondary analyses*. We introduce the needs in this section, and offer our recommendations for sampling ocean models and archiving the model data.

1.1.1 The needs of primary and secondary analyses

Primary analyses make direct use of CMIP diagnostics for comparisons between models and observation-based estimates. Such comparisons generally involve taking differences to determine statistics (e.g., mean square bias), thus rendering quantitative measures of the distance between models (model-model comparisons), or between model and observation. Such *metric-based* primary analyses are the dominant means for assessing the accuracy of CMIP simulations.

As a point of practice, primary analyses require diagnostics to be placed on a common grid, with the grid generally corresponding to the observation-based estimate. Although there are notable exceptions, most observation-based estimates use depth/pressure for the vertical and spherical (latitude-longitude) in the horizontal. Hence, CMIP has traditionally recommended model diagnostics be archived on depth/pressure levels in the vertical, and spherical coordinates in the horizontal. The fundamental issues with spatial sampling concern the following.

- There is an increasing complexity of ocean model vertical and horizontal grids. Notably, spherical grids are rarely used for ocean simulations, yet they are most commonly used for observation-based analysis products. Furthermore, native ocean model grids (both horizontal and vertical) commonly used today are somewhat complex and hence quite difficult to use by the novice.
- There is a continued refinement of grids that in turn admit higher frequency fluctuations intrinsic to the ocean (e.g., mesoscale eddies).
- The above two trends within the modelling community must be balanced by the desire to supply CMIP diagnostics that facilitate a broad suite of analysis capabilities.

CMIP5 ocean diagnostics were generally remapped to depth/pressure vertical levels for those models not based on one of the vertical coordinates z, z^*, p, or p^* (Section 1.5.5).[1] However, horizontal sampling deviated from the spherical coordinate sampling of earlier CMIPs. Namely, all 2d (horizontal) and 3d ocean diagnostics in CMIP5 were requested on the native ocean model grid in the horizontal, with native grids generally deviating from spherical latitude-longitude grids. Although very inconvenient for primary analyses, the CMIP5 recommendation allowed for the horizontally native fields to be manipulated for use in *secondary analyses*, defined here as requiring multiplicative manipulations of primary diagnostics. An example of a secondary analysis is the offline estimation of regional budgets or tracer transports, in which case secondary or derived diagnostics are computed by multiplying primary diagnostics (e.g., native grid velocity times native grid tracer concentration times native grid cell face area to approximate an advective tracer transport).

Diagnostics based on secondary analyses are generally less accurate than when the analogous diagnostics are directly sampled from online model algorithms. The reasons for the loss of accuracy concern missing temporal correlations and/or offline numerical methods that poorly approximate online numerics. Many of today's ocean models possess rather sophisticated numerical methods and physical parameterizations. Additionally, refined resolution introduces enhanced power at the high frequency. Both attributes of modern ocean models make offline estimates of transports and budgets rather poor approximations to their online values, thus making model inter-comparison of secondary diagnostics even less robust.

Secondary analyses would be unnecessary if all desired diagnostics were computed and saved online from the ocean model simulation. In particular, we strongly urge model centres to submit to CMIP6 the requested transports (Section 3.3) and budget terms (Section 3.6) using online diagnostic methods. Doing so will remove the need to compute these terms using offline approximations. Unfortunately, it is difficult to anticipate all desired diagnostics prior to running a simulation. Furthermore, many contributing models to CMIP will contribute only a subset of requested diagnostics. It is therefore useful, as a pragmatic step, to save certain model native fields to facilitate approximate offline computations.

1.1.2 Our recommendation

One means for resolving the conflict between the needs for primary and secondary analyses is to insist that CMIP cater just to one. This approach has *de facto* been taken for much of the atmosphere diagnostics, where spherical grids are the norm for CMIP atmospheric diagnostics.[2] A huge suite of primary analyses have been supported by this approach, thus serving well the needs for comparing model results and developing metrics. Conversely, multiplicative manipulations of CMIP atmospheric diagnostics are generally avoided. Such secondary analyses of atmospheric fields are known to be very inaccurate, particularly given the high frequency variability inherent in the atmosphere.

In an ideal world, we would have a robust and efficient software tool to serve the native ocean model diagnostics onto a standard horizontal and vertical grid with a standard topography, using conservative remapping to ensure that integrated terms (e.g., heat) are unchanged. This tool is unavailable for most modern vertical coordinates, whose grid cell mass/volumes are functions of space and time. In this case, conservative vertical remapping must be performed online in order to preserve scalar content (e.g., heat, water, salt). However, horizontal grid cell dimensions are static in CMIP models. Mapping from native horizontal grids to a spherical grid could thus be performed conservatively offline, given sufficient information about grid cell areas.

Unfortunately, as we prepare for CMIP6, there is no community standard of sufficient gen-

erality and maturity that can routinely provide accurate conservative remapping for general horizontal grids onto a spherical grid. Instead, each modelling group generally has their own methods that differ in accuracy, efficiency, and nomenclature. Additionally, there is no community standard horizontal grid and topography onto which we can suggest centres map onto. Hence, we are unable to rely on community standards, and it is outside our scope to develop such standards for CMIP6.

We have struggled with these issues, and our recommendation is not satisfying from the perspective of reducing CMIP archive loads. Our basic conundrum is that we remain unwilling to abandon the needs of either primary or secondary analysis.

- **We recommend archiving horizontally native grid ocean diagnostics for all 2d and 3d fields, as well as archiving a subset of these diagnostics remapped to a spherical grid, with remapping for scalars performed conservatively.**
- **We recommend conservative vertical remapping to depth or pressure vertical coordinates for all 3d fields (Section 1.5.5). The only exception is to provide the overturning streamfunction on both depth/pressure and isopycnal (σ_{2000}) coordinates (Section 3.3.6).**

Correspondingly, CMIP6 will archive *derived diagnostics* based on remapping or averaging (in space and/or time) certain of the primary diagnostics. That is, primary diagnostics mapped from native to spherical longitude-latitude grids will be supported in CMIP6. Remapping to a sphere is most trustworthy if sanctioned by the respective modelling centres for accuracy and conservation (for scalar fields), which generally means the remapping is performed directly by the model centres prior to submitting data to CMIP. The alternative is for the centres to provide sufficient grid information for analysts to perform accurate remapping on the native diagnostics. This second approach is prone to more errors given that the analysts are generally not expert in the details of the ocean model grids. We therefore strongly urge all model centres to submit both native grid diagnostics as well as the recommended subset of spherical remapped diagnostics. Doing so will greatly enhance the utility of CMIP ocean fields for *both* primary and secondary analyses.

1.2 Summary of the CMIP6 sampling needs

Here is a summary of the key recommendations for sampling and archiving the ocean diagnostics. A discussion of these recommendations follows in the remaining sections of this chapter.

- TIME SAMPLING
  - There is no sub-sampling when computing time averages; all model time steps are accumulated to compute the average.
  - To determine extreme values over a chosen time range, all time steps within the time range are sampled in order to determine the precise extrema.
- SPATIAL INTEGRATION

  Spatial integrals for regional diagnostics or transports across lines (e.g., poleward transports in ocean basins, as discussed in Section 3.3.6) are computed using all grid points within the region or line. There is no sub-sampling.
- VERTICAL SAMPLING
  - For models using z, z^*, p, or p^* vertical coordinates (Section 1.5.5), output can be saved on the model native vertical grid.
  - For all other vertical grids (e.g., isopycnal, terrain following, generalized), then diagnostics are archived on a z^* (Boussinesq) or p^* (non-Boussinesq) vertical grid. The remapping is performed conservatively online during each model time step.
  - There is one exception to the above remapping requirement; namely, the overturning mass transport is of scientific interest on both depth/pressure surfaces, and potential density surfaces (referenced to 2000 dbar) (see Section 3.3.6). Any remapping must be performed online using conservative methods, accumulating each model time step.
- HORIZONTAL SAMPLING
  - PRIMARY ANALYSES: To support primary analyses of CMIP diagnostics (Section 1.1), all level-0 diagnostic fields should be archived on a spherical (longitude-latitude) grid. Scalar fields must be remapped conservatively. Vector fields can be interpolated onto a common A-grid or B-grid (with north-south and east-west components) using conservative or non-conservative interpolation. Diagnostic variables that are stored in both native and spherical grids can have the same standard name and the same CMIP/CMOR name. Within files, the gridded fields will be distinguished by the cell_measures, coordinates, and auxiliary CF attributes. The same variable in native and standard form can never coexist in the same file. The WGCM Infrastructure Panel (WIP) will provide means to distinguished the gridded fields.
  - SECONDARY ANALYSES: To support secondary analyses of CMIP diagnostics (Section 1.1), all model diagnostics are to be available on the native model grid.
- PRECISION OF THE ARCHIVED DIAGNOSTICS: All model data submitted to CMIP6 should follow the netCDF4 protocol (Section 1.6). Precision of the data should be sufficient to ensure robust statistical analyses are available. For most applications, single precision (seven signficant digits) is sufficient.

1.3 Details for time sampling

Time sampling is straightforward.

- **Time averages**: Time averages include all model time steps over the given range of the average. Products of time dependent fields are time averaged as a product, using all model time steps to build the average.
- **Extreme values**: Extreme values over a time range are obtained by computing the extrema over each time step within a chosen interval.

1.4 Specification of grid area and volume

In order to calculate ocean area integrals and volume integrals, information is needed to weight the grid cells in a manner consistent with conservation properties of the model. All CMIP6 ocean models have a fixed horizontal grid and hence constant horizontal cell areas. Cell areas (areacello) should be stored in each data file (Table 2.1) in order to keep this important information within each diagnostic file. In contrast, the cell thicknesses (thkcello), and hence cell volumes and masses (masscello), may be time dependent for many ocean models. We discuss in this section how to specify ocean grid cell volumes and masses for CMIP6.

1.4.1 Volume-conserving Boussinesq ocean models

Boussinesq ocean models are based on volume-conserving kinematics, with these models having been used since the early days of ocean modelling (Bryan, 1969). For budget purposes, Boussinesq models use a constant reference density for seawater, ρ_o. Hence, their grid cell masses, $\mathrm{d}M$, are equal to the grid cell volume, $\mathrm{d}V$, multiplied by the constant reference density (Section 3.2.3)

$$\mathrm{d}M = \rho_o \, \mathrm{d}V \qquad \text{Boussinesq models (kg).} \tag{1.1}$$

A netCDF scalar variable containing the constant

$$\rho_o = \text{reference\_sea\_water\_density\_for\_boussinesq\_approximation} \ \ (\mathrm{kg\ m^{-3}}) \tag{1.2}$$

should be archived in the same file (Table 2.1).

1.4.1.1 Boussinesq models with static grid cell volumes

Certain Boussinesq ocean models assume that grid cells have time-independent volumes, meaning they have static grid cell thicknesses. This property holds for geopotential Boussinesq ocean models based on barotropic dynamics using either the rigid lid approximation (Bryan, 1969; Pinardi et al., 1995) or linearized free surface (Dukowicz and Smith, 1994; Roullet and Madec, 2000). By construction, these models do not allow for changes in the volume associated with boundary water fluxes. Consequently, they must make use of virtual tracer flux boundary conditions (Huang and Schmitt, 1993; Griffies et al., 2001).[3]

If the Boussinesq model has time-independent grid cell volumes, then the grid cell masses (equation (1.1)) are also constant in time. For these models, the CMIP6 masscello field for cell mass (sea_water_mass_per_unit_area) is to be saved as a static XYZ variable measuring the mass of the tracer grid cell (Table 2.1). Furthermore, for cells which occupy the entire vertical extent of the grid cell layer (i.e. except for partial cells at the top or bottom of the ocean), the cell thickness can be calculated as the difference of the depth-bounds for the layer. This thickness should equal the cell mass per unit area divided by the Boussinesq reference density. For these models, the cell_thickness variable thkcello is not required.

1.4.1.2 Boussinesq models with time-dependent grid cell volumes

Many Boussinesq models have time dependent cell volumes, with examples including isopycnal models, terrain-following sigma models, and stretched depth-coordinate z^* models (Section 1.5.5). For these models, the cell thickness, thkcello (Table 2.2), is time dependent. A separate masscello file is required for each distinct set of time coordinates at which other monthly XYZ scalar fields are provided (Tables 2.2, 2.10, 2.11, and 2.12). Doing so provides a one-to-one correspondence between the variable to be weighted (e.g. thetao) and the variable providing the weights (masscello). For Boussinesq models, the reference_sea_water_density_for_boussinesq_approximation should also be saved in each masscello file. The cell thickness, thkcello, is not required, since it can be easily diagnosed through

$$\text{thkcello} = \text{masscello}/(\text{areacello} * \rho_o) \quad (\mathrm{m}). \tag{1.3}$$

In contrast, for typical non-Boussinesq models (see Section 1.4.2), both masscello and thkcello are required on the same time frequency as the primary fields (e.g., monthly).

1.4.2 Mass-conserving non-Boussinesq ocean models

Non-Boussinesq models are based on mass-conserving kinematics (Griffies and Greatbatch, 2012). When hydrostatic, such models are naturally formulated using pressure, or a function of pressure, as the vertical coordinate (Huang et al., 2001; DeSzoeke and Samelson, 2002; Marshall et al., 2004). If based on pressure, then the mass of a grid cell remains constant in time, with the equations isomorphic to the depth-coordinate Boussinesq ocean equations.

In general, the cell thickness, thkcello, and cell mass, masscello (Table 2.2), are time dependent. A separate masscello file is required for each distinct set of time coordinates at which

other XYZ scalar fields are provided (Tables 2.2, 2.10, 2.11, and 2.12). Doing so provides a one-to-one correspondence between the variable to be weighted (e.g. thetao) and the variable providing the weights (masscello).

1.4.3 Details of the grid information

The link between a scalar data variable and the corresponding areacello and masscello variables is made using the cell_measures and associated_files attributes available in a netCDF file. For a field on an XY longitude-latitude horizontal grid, the file should contain variables written as

```
float pr(time,latitude,longitude);
  pr:cell_measures="area: areacello";
  pr:standard_name="rainfall_flux";
  pr:units="kg m-2 s-1";
float areacello(latitude,longitude);
  areacello:standard_name="cell_area";
  areacello:units="m2";
```

The areacello variable is not required to have the variable name areacello. In cell_measures, "area: VARNAME" identifies the variable by name.

For a field on an XYZ grid, the file should contain variables written as

```
float thetao(time,depth,latitude,longitude);
  thetao:cell_measures="area: areacello mass_per_unit_area: masscello";
  thetao:associated_files="BASENAME";
  thetao:standard_name="sea_water_potential_temperature";
  thetao:units="degC";
float areacello(latitude,longitude);
  areacello:standard_name="cell_area";
  areacello:units="m2";
```

The field BASENAME is the basename (the last element of the path) of the file containing masscello for the same times as for the primary field. That mass file contains

```
float masscello(time,depth,latitude,longitude);
  masscello:standard_name="sea_water_mass_per_unit_area";
  masscello:units="kg m-2";
```

where the time dimension and coordinate variable must have the same names and contents for the two files.

1.5 Details for spatial sampling

As introduced in Section 1.1, spatial sampling of ocean model diagnostics raises nontrivial questions. In this section, we detail issues that arise when considering how to sample scalar and vector fields in space. Our discussion raises questions about both vertical and horizontal sampling.

1.5.1 Integration over spatial regions

We start with an easy question: how to sample fields to be integrated over a spatial region, such as a basin or section? The answer is to compute the integral using all model grid points within the relevant domain (e.g., Atlantic-Arctic, Indian-Pacific, Global), and time average using all model time steps. There should be zero sub-sampling.

1.5.2 Scalar fields

1. HORIZONTAL: We recommend all scalar fields be archived on their native grids. A selection of 2d and 3d scalar fields (e.g., sea level, 3D temperature and salinity, commonly accessed boundary fluxes) will also be archived on a longitude-latitude (spherical) grid using conservative remapping techniques.
2. VERTICAL: We recommend that for the vertical, conservative remapping be performed onto a depth or pressure vertical coordinate in cases where depth or pressure are not native. In particular, for models with time dependent grid cell thicknesses (e.g., isopycnal or sigma coordinate models), vertical remapping must be realized via conservative remapping computed online each model time step. Such remapping is required to ensure scalar content (e.g., heat, salt, water) is preserved across the native and remapped grids.

The archival of both native grid and, for some diagnostics spherical grid, diagnostics aims to support the needs of *both* primary and secondary analyses (Section 1.1). Notably, when computed in a conservative manner, remapping of scalar fields retains key information from the native model results, while greatly facilitating analysis across the suite of CMIP models.

We now offer the following comments/pointers.

- THE CRITICAL NEED FOR CONSERVATIVE REMAPPING
  - Remapping must be conservative in all space directions, so that spatial integrals of scalar fields remains unchanged relative to the native grids.
  - Remapping is performed using the same remapping operator for all scalar fields.

  - In models with time dependent grid cell volumes/masses (e.g., isopycnal models, sigma coordinate models, vertical ALE models), it is critical that vertical remapping occur online for each model time step in order to include correlations between the fluctuating grid cell geometry and the scalar field. Remapping subsampled fields in such cases generally leads to erroneous results; it must be avoided.

- HORIZONTAL REMAPPING
  - For the static horizontal grids used in CMIP ocean climate modelling, remapping to a spherical grid can occur offline.
  - Remapping must be conservative, which means that all horizontal area factors must be properly handled, with care required especially in the presence of the complex ocean geometry.

- VERTICAL REMAPPING
  - For models based on z (geopotential coordinate), stretched depth z^*, pressure, or stretched pressure p^*, there is no need to perform a depth remapping. Indeed, it is preferred that the output remain on the model native depth grid for such vertical coordinate models. See Section 1.5.5 for more details of these coordinates.
  - For models with a time dependent grid cell thickness that do not use z, z^*, p, or p^* vertical coordinates (e.g., isopycnal and terrain following), the vertical remapping step should be computed each model time step to ensure exact conservation.
  - Vertical remapping should occur onto a vertical coordinate based on depth (for Boussinesq models) or pressure (for non-Boussinesq models).
  - Pressure based vertical grids should be measured in dbar, in order to facilitate easy comparison to depth-based models using metres.
  - Depth and pressure increase downward from the ocean surface, whereas the vertical geopotential z increases upward starting from the resting ocean surface.

1.5.3 Vector fields

It is mathematically straightforward to transform a continuum vector field from one coordinate system to another using basic methods of tensor analysis (e.g., Chapter 20 in Griffies (2004)). Unfortunately, these continuum mathematical methods are ambiguous for discrete vector fields. For example, the commonly used C-grid has horizontal velocity components sitting at distinct spatial positions, thus breaking the tensorial character of the continuum vector field. Tracer fluxes are likewise positioned at the sides of tracer cells for all finite volume models. There is correspondingly no consensus in the ocean modelling community regarding a preferred transformation algorithm to map discretized vector fields from the native model grid onto a non-native spherical grid.

We recommend that any remapping of vector components onto a sphere (into north-south and east-west vector components) be based on a high order interpolation scheme, thus ensuring smoothness and accuracy. Conservation is generally not needed for vector components. Furthermore, for native vector components sitting on a C-grid, these components should be mapped onto an A-grid or B-grid, depending on what is more convenient based on the native model grid. Interpolating vector components to a single point greatly facilitates routine interpretation.

1.5.4 Zig-zag method for estimating poleward transports

We recommend that each group using non-spherical grids develop a native-grid algorithm that computes the closest native grid approximation to the basin integrated poleward transports. That is, transports across a section (e.g. meridional overturning at a given latitude, transport through a passage, or vertically integrated poleward heat transport) should be computed consistent with the native grid by finding a nearly equivalent path to the section that has been "snapped" to the native grid (often resulting in a "zig-zag" path). This approach retains the native grid variables, and so allows for conservation of transports. It also avoids ambiguities associated with defining a remapped land/sea mask. The resulting transports should be made available as a function of latitude (even though the integrations are not exactly along latitude circles). The latitude spacing should be comparable to that of the model's grid spacing.

1.5.5 More details for vertical sampling

There are two questions to answer regarding the vertical coordinate:

- Should model output be remapped in the vertical to a common vertical coordinate?
- If remapped, then what is a scientifically relevant vertical coordinate?

There is no ambiguity regarding the vertical grid when working with Boussinesq rigid lid geopotential-coordinate ocean models, as each grid has a fixed vertical position. It was thus sensible for WGCM (2007) to recommend that output in the vertical be on a geopotential grid, preferably remapped to the 33 depth levels used by Levitus (1982).[4] The more recent trend towards free surface geopotential models raises only trivial issues with the surface grid cell, and these issues can be ignored without much loss of accuracy.[5] However, the move towards pressure, isopycnal, terrain following, and general/hybrid models increases the complexity of vertical coordinate questions.

We make the following observations and clarifications regarding the recommendations for vertical remapping.

- For isopycnal, terrain following, and general/hybrid models, we recommend remapping to a more standard vertical coordinate. This recommendation recognizes that the majority of ocean climate models used for IPCC assessments remain level coordinate geopotential models, and the majority of observation-based datasets are archived on geopotential or pressure levels. Hence, the application of analysis methods is prejudiced towards these vertical coordinates. However, the answer does *not* reflect our belief that geopotential/pressure based analysis is the most relevant for all purposes. Indeed, many purposes are best served by analyzing output on alternative vertical coordinates, especially on isopycnal coordinates for characterizing water masses. To support the evolution towards a more balanced analysis methodology, in Sections 3.3.6 and 3.3.7, we recommend certain fields (e.g., overturning streamfunction) be archived on both geopotential/pressure *and* density surfaces.
- Conservative vertical remapping with straightforward linear interpolation is reasonably accurate so long as the remapping is done every model time step. Remapping subsampled fields can lead to erroneous analysis, especially with isopycnal models.
- Contrary to the situation in the horizontal, separate vector components can be treated as scalars for the purpose of remapping in the vertical.
- RESCALED GEOPOTENTIAL FOR BOUSSINESQ MODELS: For Boussinesq models, it is natural to consider remapping to the *rescaled geopotential* coordinate (Stacey et al., 1995; Adcroft and Campin, 2004)

$$z^* = H\left(\frac{z-\eta}{H+\eta}\right). \tag{1.4}$$

  In this equation, z is the geopotential, $z=-H(x,y)$ is the ocean bottom, and $z=\eta(x,y,t)$ is the deviation of the free surface from a resting ocean at $z=0$. To better understand the ratio, note that $z-\eta$ is the thickness of seawater above a particular geopotential, and $H+\eta$ is the total thickness of seawater in the fluid column. Surfaces of constant z^* correspond to geopotentials when $\eta=0$. For most practical applications of global ocean modelling, z^* surfaces only slightly deviate from constant geopotential surfaces even with nonzero η fluctuations. The advantage of z^* over geopotential is that it has a time independent range $-H \le z^* \le 0$, thus allowing for a more straightforward mapping from a free surface isopycnal or terrain following model.
- RESCALED PRESSURE FOR NON-BOUSSINESQ MODELS: The *rescaled pressure* coordinate is defined as

$$p^* = p_b^o\left(\frac{p-p_a}{p_b-p_a}\right), \tag{1.5}$$

  where p is the pressure at a grid point; $p_a(x,y,t)$ is the pressure applied at the ocean surface due to overlying atmosphere, sea ice, and/or ice shelves; $p_b(x,y,t)$ is the pressure at the ocean bottom; and $p_b^o(x,y)$ is a static reference bottom pressure, such as the initial bottom pressure. To better understand the ratio, note that in a hydrostatic ocean, $g^{-1}(p-p_a)$ is the mass per horizontal area of seawater situated above a pressure level p, and $g^{-1}(p_b-p_a)$ is the total mass per horizontal area of seawater in the fluid column. For most practical applications of global modelling, constant p^* surfaces only slightly deviate from constant pressure surfaces, even with nonzero fluctuations of p_b. The advantage of p^* over pressure is that p^* has a time independent range $0 \le p^* \le p_b^o$, thus allowing for a more straightforward mapping from a non-Boussinesq model.
- For visualization purposes, the distinction between geopotential (or rescaled geopotential) and pressure (or rescaled pressure) can be ignored to within a few percentage accuracy, so long as geopotential is measured in metres and pressure is measured in decibars.
- For analysis purposes, the distinction between geopotential (or rescaled geopotential) and pressure (or rescaled pressure) can be ignored when working with model native scalars and fluxes. The differences *cannot* be ignored when performing off-line integration of velocity components to approximate fluxes. This is a central reason that we recommend archiving mass fluxes in addition to velocity components (Section 3.3).

1.6 Data precision of the archived diagnostics

Besides ensuring proper practices for temporal and spatial sampling, it is important to understand the needs for data precision of the archived diagnostics. This issue is important for two reasons, firstly to ensure that analysts are able to maintain accuracy when calculating derived diagnostics, and secondly to minimize storage footprint, particularly as model resolution and diagnostic requests increase.

1.6.1 Features of netCDF4

We request all model data for CMIP6 follow the netCDF4 protocol. This recommendation contrasts to the use of netCDF3 in CMIP5, which was a sensible recommendation since netCDF4 has matured during the recent years after the CMIP5 recommendations were finalized in 2009. The CMIP5 archives adhered to the netCDF3 classic protocol, meaning that CMIP5 data was written using single precision (32-bit float) format. In contrast, key features of netCDF4 that motivate its use for CMIP6 include lossless compression (deflation) and file access/read performance tools of chunking and shuffling. Furthermore, most standard analysis packages now support netCDF4 formatted data (see Section 1.6.2), thus placing no burden on the analyst.

In Table 1.1, we provide information about precision features of different data formatting within the netCDF4 protocol. For most analysis purposes, single precision (seven significant digits) is sufficient. However, length and area factors from grids may usefully be saved in

double precision, given that area factors are the basis for statistical analyses and remapping. Notably, it is rare to find observational-based data with significance greater than half precision (three significant digits).

1.6.2 Software packages supporting NetCDF4

NetCDF4 is now a standard library for many software packages, including

1. Ferret >6.6
2. Matlab >R2010b
3. UV-CDAT >1.0
4. CDAT >5.2
5. IDL ~7+
6. NCO >3.1
7. CDO >1.5
8. NCL >6.1.1.

Consequently, using netCDF4 deflation (and reducing file sizes by roughly 50% in a lossless format) should pose no hindrance for CMIP6 analysis. Note that the 50% compression assumes that the supplied netCDF4 libraries are built with HDF5 and zlib support, which are needed to garner the compression functionality.

DATA PRECISION								
NAME	DESCRIPTION	NETCDF4 TYPE	PRECISION	MINIMUM	MAXIMUM	DECIMAL DIGITS		SALINITY EXAMPLE (E.G. 35.1234567891)
i8	8-bit signed integer	NC_byte (byte)	-	-128	127	-		35.0708661417
u8	8-bit unsigned integer	NC_ubyte (unsigned byte)	-	0	255	-		35.0708661417
i16	16-bit signed integer	NC_short (short)	-	-32768	32767	-		35.1235694449
u16	16-bit unsigned integer	NC_ushort (unsigned short)	-	0	65535	-		35.1235694449
i32	32-bit signed integer	NC_int (int)	-	-2147483648	2147483647	-		35.123456786
u32	32-bit unsigned integer	NC_uint (unsigned int)	-	0	4294967295	-		35.123456786
i64	64-bit signed integer	NC_int64 (long long)	-	-9223372036854775808	9223372036854775807	-		35.1234567891
u64	64-bit unsigned integer	NC_uint64 (unsigned long long)	-	0	18446744073709551615	-		35.1234567891
f16/binary16	16-bit floating-point	-	half	$-\infty$	∞	3.31		35.125
f32/binary32	32-bit floating-point	NC_float (float)	single	$-\infty$	∞	7.22		35.1235
f64/binary64	64-bit floating-point	NC_double (double)	double	$-\infty$	∞	15.95		35.1234567891

Table 1.1: Listing of available data types using the netCDF4 data model, and example data precision for ocean salinity using these data types. Plausible observed salinity ranges (PSS–78; Lewis and Perkin (1981)) are between 2 and 42 (open ocean salinities normally range from 32 to 38), which is the range over which the Practical Salinity Scale (1978) provides coverage. This scale is used to define the valid_min and valid_max from which the representative salinity precision (last column) is calculated. For reference, the PSS–78 scale specifies an *in-situ* temperature range of $-2°C$ to $35°C$, and a pressure range of 0 to 10^4 dbar (Lewis and Perkin, 1981). Sources: http://en.wikipedia.org/wiki/IEEE_floating_point#Basic_formats https://www.unidata.ucar.edu/software/netcdf/docs/netcdfc/NetCDF_002d4AtomicTypes.html

1.7 CMIP and seawater thermodynamics

The purpose of this section is to offer recommendations for how to sample the simulated ocean temperature, salinity, and associated heat and salt transports. These recommendations are made in light of the endorsement by the international oceanography community of the Thermodynamic Equation of State 2010 (TEOS-10) (IOC et al., 2010). TEOS-10 is based on a consistent theory of seawater thermodynamics, as well as empirical measurements updated since the UNESCO-80 equation of state. TEOS-10 represents a major move forward in the fundamental science and practice of seawater thermodynamics.

1.7.1 Balancing the needs

This document aims to provide a rational and practical framework for meaningful comparisons across climate models and observational based measurements. Meeting this aim supports the primary means whereby analysis of CMIP simulations contributes to climate science. We addressed some of these issues in relation to the native versus spherical grid questions in Sections 1.1 and 1.5. In offering recommendations for seawater thermodynamics, we must balance the desire to remain true to IOC et al. (2010), while acknowledging the practical needs for a successful CMIP.

Many modelling groups are just now incorporating TEOS-10 into their CMIP6 models, with `http://www.teos-10.org/pubs/Getting_Started.pdf` providing a useful starting point. The work of Roquet et al. (2014) is an example of specific steps towards the use of TEOS-10 in an ocean climate model. Hence, CMIP6 will contain models based on TEOS-10, and others based on preTEOS-10. Furthermore, there remain unanswered research questions raised by IOC et al. (2010), in particular regarding the treatment of salinity. For CMIP6, we cannot impose strict standards defining what it means to be "TEOS-10 compliant", when research remains incomplete. Indeed, at this time, there are zero peer-reviewed publications using ocean climate simulations based on the suite of recommendations from TEOS-10. In short, the community is in a transition stage from preTEOS-10 to TEOS-10. For CMIP6, we thus offer a cosmopolitan approach rather than one based on a well defined territory.

1.7.2 Recommendations

Here is a summary of our recommendations.

1.7.2.1 Temperature

Regardless the model thermodynamics, modellers should archive potential temperature, θ. For models using preTEOS-10 ocean thermodynamics, no change is required relative to previous CMIPs. For models using TEOS-10 thermodynamics, in which Conservative Temperature, Θ, is the model prognostic field, we still recommend archiving potential temperature to allow for meaningful comparisons. Doing so requires an online diagnostic calculation to convert at each time step from Conservative Temperature to potential temperature.

1.7.2.2 Heat content

The air-sea flux of heat is exactly the air-sea flux of potential enthalpy (since the reference gauge pressure of potential enthalpy is 0 dbar). Apart from warming caused by the dissipation of turbulent kinetic energy (as well as another smaller term), potential enthalpy is a conservative variable in the ocean (McDougall, 2003; Graham and McDougall, 2013), meaning that it satisfies a scalar conservation equation analogous to a source-free material tracer. Because of these properties of potential enthalpy, we are justified in calling it the heat content of seawater. That is, the heat content (in Joules) of a seawater parcel or an ocean model grid cell is

$$\text{seawater heat content} = h^o \, \rho \, \mathrm{d}V \tag{1.6a}$$

$$= c_p^o \, \Theta \, \rho \, \mathrm{d}V, \tag{1.6b}$$

with

$$h^o = c_p^o \, \Theta \tag{1.7}$$

the potential enthalpy per mass, Θ the Conservative Temperature, $\mathrm{d}V$ the parcel or grid cell volume, and ρ the *in situ* seawater density. The heat capacity *defined* by TEOS-10 is the constant

$$c_p^o = 3991.86795711963 \text{ J kg}^{-1} \text{ K}^{-1}. \tag{1.8}$$

The 15 significant digits in c_p^o is a based on a numerical fit. The observation-based data used in this fit are measured to a precision no greater than three or four significant digits (see Table 1.1). Hence, there is no physics in c_p^o beyond roughly four significant digits.

Ocean climate models measure heat content (in Joules) of a grid cell according to

$$\text{ocean model heat content} = C_p^o * \text{prognostic temperature} * \rho \, \mathrm{d}V. \tag{1.9}$$

We now comment on this model practice and relate it to TEOS-10 and CMIP6.

- For a Boussinesq fluid, the *in situ* density, ρ, is set to a constant reference density, ρ_o. Not all groups use the same constant (see Roquet et al. (2014) for a discussion of various choices). Modellers should therefore archive in CMIP this constant according to the request in Table 2.1.
- The ocean model heat capacity, C_p^o, is constant. However, the ocean model heat capacity is not always equal to the TEOS-10 recommended value (1.8). We thus ask to archive in CMIP the model heat capacity in Table 2.1. We note that the TEOS-10 heat capacity c_p^o (equation (1.8)) was chosen so that the surface area average (and ocean mass average) of $c_p^o \, \theta$ closely matches the corresponding surface area (and ocean mass) averages of potential enthalpy. We thus highly recommend models choose $C_p^o = c_p^o$ for both preTEOS-10 and TEOS-10 usage.
- Expression (1.9) is the heat content for the respective TEOS-10 and preTEOS-10 ocean models. This expression is relevant for CMIP6 since the model's prognostic temperature field evolves according to grid cell budgets. Hence, preTEOS-10 models should *not* archive heat content by diagnosing the Conservative Temperature. Rather, they should measure heat content as always done for previous CMIPs, using the model's prognostic potential temperature. Likewise, TEOS-10 models should measure heat content using the TEOS-10 recommendation (1.7), using the model's prognostic Conservative Temperature field.

- As noted by McDougall (2003), boundary heat fluxes affect the ocean potential temperature, with a tendency proportional to the reciprocal of the specific isobaric heat capacity of seawater. Importantly, this heat capacity varies by 5% over the ocean. However, no ocean climate model makes use of a non-constant specific isobaric heat capacity, even though the temperature field of ocean models is most often interpreted as potential temperature. This inconsistency is motivated by the desire to have the model ocean heat content related directly to the model's prognostic temperature field, with that temperature field time stepped according to conserved budget equations. Turning this inconsistency into an opportunity, McDougall (2003) noted that ocean models using a constant heat capacity, C_p^o, may in fact be interpreted as using Conservative Temperature rather than potential temperature. There are errors associated with this interpretation arising from the calculation of *in situ* density and boundary heat fluxes. Nonetheless, these errors may in fact be smaller than those associated with ignoring the non-constant heat capacity. Research is needed to further pursue this interpretation.
- Heat transport and its convergence are determined by various transport processes (e.g., advection, diffusion) impacting on the grid cell heat content (1.9). We ask for the archival of such transports and convergences in Tables 2.3 and 2.10.

1.7.2.3 Salinity

Ocean models based on preTEOS-10 thermodynamics carry only Practical Salinity. Hence, to facilitate comparisons across all models, we must compare Practical Salinity regardless the model thermodynamics. Furthermore, there are no plans in the ocean modelling community to carry a second prognostic salinity variable encompassing the Absolute Salinity anomaly discussed in (IOC et al., 2010). Further research is required before doing so. Hence, the salinity output from CMIP6 models, regardless whether preTEOS-10 or TEOS-10, should be treated as Practical Salinity. These salinity fields should in turn be compared to observations of Practical Salinity. This practice represents exact correspondence to earlier CMIPs.

1.7.2.4 Salt content

The salt content in a grid cell is *not* given by the grid cell mass times Practical Salinity. Instead, it is given by the grid cell mass times Absolute Salinity. However, for CMIP6, the differences between Practical Salinity and Absolute Salinity will likely be ignored by all modelling groups, given the early stages of such research. In this case, salt content is approximated by the grid cell mass times the Practical Salinity.

Notes

[1] There is one exception for the vertical; namely, the overturning mass transport is of scientific interest on both depth/pressure surfaces and potential density surfaces (with 2000 dbar referencing). We detail this diagnostic in Section 3.3.6.

[2] The spherical grids are not the same, however, with each group generating their own.

[3] Some models based on fully nonlinear split-explicit free surface methods also retain virtual salt fluxes.

[4] This recommendation was not a requirement, so many groups participating in CMIP3 chose to report their output on the model's native vertical grid.

[5] We know of no group that considers the question of remapping model fields in the top model cell of a free surface geopotential model to a pre-defined geopotential level. Indeed, there is little reason to do so, as the top cell, whether it has a center at $z = -1$m or $z = 1$m, for example, still represents the model's version of the sea surface.

Chapter 2

Summary of the ocean diagnostics

Contents

We here provide a summary of the ocean-related diagnostics requested for CMIP6, with full details given in Chapter 3.

2.1 Prioritizing the ocean diagnostics

We make use of three priorities for CMIP6 physical ocean diagnostics.[6]

More specifically, these three priority classes are characterized by the following qualities.

- **Priority=1** diagnostics serve as a baseline for the CMIP physical ocean diagnostics. These diagnostics are of highest priority as they support a broad baseline of CMIP ocean related studies. Specifically, they provide the following qualities:
  - characterize the model configuration;
  - provide a broad assessment of the simulated climate state;
  - provide a broad assessment of the simulated climate change;
  - In the horizontal, all priority=1 fields should be archived on both native *and* longitude-latitude (spherical) grids.
- **Priority=2** diagnostics are of intermediate priority. They support more in-depth understanding of the simulations. Specifically, they provide the following qualities:
  - render a measure of the mass and tracer transports over the globe, within semi-enclosed basins, or across sections;
  - quantify mass, heat, salt, and momentum budget terms on global and/or regional scales;
  - document auxiliary fields that render a more complete quantitative characterization of the simulation, such as ventilation;
  - subsets of priority=1 fields that facilitate a more convenient means of performing a quick assessment.
- **Priority=3** diagnostics serve process-based analyses of CMIP ocean simulations. Specifically, they provide the following qualities:
  - quantify 3d heat and salt budgets;
  - provide for a study of sub-monthly transients and/or variability.

- document parameterized eddy coefficients to characterize subgrid scale schemes
- quantify impacts on eddy energetics.

2.2 Sponsors for particular diagnostics

Our recommended diagnostics reflect the needs and interests of numerous analysts participating in the CMIP process, including the authors of this document. The recommendations generally result from surveys and discussions within the ocean and climate community, particularly as they reflect feedback from the CMIP5 process. Furthermore, the list reflects our expert judgement regarding what diagnostics can be of use for scientifically assessing the simulations, and for providing mechanistic understanding of various physical processes.

Although tempting to ask for an extensive suite of diagnostics that allow for complete process-based examination of the simulations, any such list must confront the reality of finite archive space. Furthermore, diagnostics ideally should have an identified customer (e.g., panel, MIP), to analyze the model output in order to scientifically digest the results through publications or reports. Any such identification should not be mistaken for ownership, as the CMIP archive is public. Nor is the identification exclusive or complete. Rather, the named "champion" identifies a group who has lobbied for the diagnostics and so whose science is directly served. We identify the following CMIP sanctioned MIPs having directly sponsored ocean diagnostics listed in this document.

1. OMIP: OMIP is a new MIP for CMIP6. It is based on the Coordinated Ocean-ice Reference Experiments (CORE) (Griffies et al., 2009b; Danabasoglu et al., 2014). **OMIP is central ocean-related MIP that is sponsoring all ocean related variables in this document.** Additionally, OMIP is coordinating the diagnostics related to inter-chemical tracers and ocean biogeochemical tracers. In particular, OMIP ensures that the standard Priority=1 diagnostics available from previous CMIPs (e.g., SST, sea level) are available for CMIP6 even if they are not asked by another MIP. In support of OMIP and related ocean climate science, we request that ocean variables in this document be archived from *all* CMIP6 simulations that make use of an ocean model component.
2. FAFMIP (Flux-Anomaly-Forced Model Intercomparison Project): This MIP supports the WCRP Grand Challenge on sea level rise and regional impacts, with particular interest in identifying mechanisms for regional sea level variations/projections. Critical needs for this MIP include the budget terms for heat and salt (Table 2.10). These terms will help to understand the mechanisms for the large spread in ocean heat uptake efficiency found in CMIP5 simulations (Kuhlbrodt and Gregory, 2012), which in turn impact on the spread in projected sea level rise (Slangen et al., 2012, 2014).
3. C4MIP (Coupled Climate Carbon Cycle Model Intercomparison Project): This MIP aims to improve and accelerate development of global-scale, three-dimensional, coupled earth system models that include the carbon cycle and related biogeochemical and ecosystem components.
4. DCPP (Decadal Climate Prediction Project): This MIP aims to improve and accelerate development of global-scale, three-dimensional, coupled earth system models that include the carbon cycle and related biogeochemical and ecosystem components.
5. HIGHRESMIP (High Resolution Model Intercomparison Project): Assess the robustness of improvements in the representation of important climate processes with weather-resolving global model resolutions (25km or finer), within a simplified framework using the physical climate system with constrained aerosol forcing. Key processes include ENSO, TIWs, the Gulf Stream and its influence on the atmosphere, the global water cycle, extra-tropical cyclones and storm tracks, and Euro-Atlantic blocking.

Although not explicitly sponsoring a MIP for CMIP6, the following communities have provided input to the process of developing the variable list in this document. We identify them here in hopes that doing so will spread the responsibility for making use of the ocean diagnostics.

1. GSOP (Global Synthesis and Observational Panel): This panel has encouraged the archiving and analysis of various physical processes, such as those proposed by FAFMIP in support of understanding the role of physical processes in affecting heat and salt budgets (Table 2.10).
2. AMOC (Atlantic Meridional Overturning Circulation): This community has emphasized the needs for diagnostics measuring the mass, heat, and salt transport in the Atlantic. In particular, the US AMOC community (http://www.usclivar.org/amoc) has expressed strong desire to have models archive these diagnostics at a level of priority enhanced relative to that in CMIP5. The budget terms in Table 2.10 will also be of prime interest for regional AMOC and Arctic analysis. These diagnostics will presumably be of use to diagnose the role of ocean processes in impacting the AMOC (Roberts et al., 2013, 2014)
3. SOUTHERN OCEAN: The Southern Ocean community, as led by members of the CLIVAR/CliC/SCAR Southern Ocean Region Panel (http://www.clivar.org/panels-and-working-groups/southern), has a particular interest in the detailed workings of mesoscale eddy parameterizations, particularly as they impact on vertical heat transport (e.g., Gregory (2000)), and response of the ACC and Southern Ocean MOC to changes in surface forcing (e.g., Downes and Hogg (2013)).
4. ECOSYSTEM COMMUNITY: Certain physical fields are of direct use for assessing the impacts of physical climate on ecosystems, such as the bottom temperature and salinity fields.

5. OCEAN MIXING COMMUNITY: There is a large contingent of analysts who focus on ocean processes, such as mixing. This community is served by providing basic information regarding the subgrid scale parameterizations used by the models. In CMIP5, there were numerous fields requested to serve this community (see Tables 2.11 and 2.12). Unfortunately, few model submissions were made, thus leading to little published analysis of these fields.[7] For CMIP6, we ask for a subset of the CMIP5 information in hopes that model groups will be more able to submit these fields, thus better serving the needs of subgrid scale parameterization studies.

2.3 Diagnostic names

The CF metadata conventions "standard names" are listed for the diagnostic fields, where available. Additional names according to the CMOR convention are shorter and correspond to those used by the PCMDI diagnostic packages. The shorter CMOR names are becoming standard in the community given the widespread development of CMIP analysis software.

2.4 Tabulation of the CMIP6 ocean diagnostics

In the remainder of this chapter, we present a tabulated list of ocean model diagnostics recommended for the CMIP6 archive, with the tables containing the following information.

- diagnostic name according to the CF standard name
- diagnostic name according to the CMOR short name
- main community sponsoring the diagnostic (Section 2.2)
- relation to CMIP5 as detailed in Griffies et al. (2009a) (same, new, or modification)
- physical units
- time sampling for output (time mean over day or month, or max over a day or month)
- spatial shape
- recommended grid (native, spherical, depth/pressure)
- prioritization guidance
- experiment the diagnostic should be saved (all experiments, just the historical experiment, or only one entry as a representation for all experiments). Unless otherwise specified, results should be submitted for the full length of each experiment.

All fields should be reported as "missing" over grid cells that are entirely land. The spatial shape of a field that has no horizontal dimension(s) is indicated by a 0 (i.e., a time series); one-dimensional spatial fields are denoted by Y (e.g., meridional heat transport); horizontal two dimensional fields are denoted XY; vertical two dimensional fields are denoted YZ or Yρ; three-dimensional fields are denoted XYZ.[8]

STATIC DIAGNOSTICS									
CF STANDARD NAME	CMOR NAME	SPONSOR	CMIP5/CMIP6	UNITS	TIME	SHAPE	GRID	PRIORITY	EXPT
sea_water_equation_of_state		OMIP	same	$\rho(S,\Theta,p)$ or $\rho(S,\Theta,z)$				1	once
sea_water_freezing_temperature_equation		OMIP	same	function of (S,p) or (S,z)				1	once
reference_sea_water_density_for_boussinesq_approximation	rhozero	OMIP	same	kg/m^3	static	0	0	1	once
specific_heat_capacity_of_sea_water	cpocean	OMIP	new	J/(kg K)	static	0	0	1	once
sea_floor_depth_below_geoid	deptho	OMIP	same	m	static	XY	native & sphere	1	once
region	basin	OMIP	same	dimensionless	static	XY	native & sphere	1	once
cell_area	areacello	OMIP	same	m^2	static	XY	native & sphere	1	once
sea_water_mass_per_unit_area	masscello	OMIP	same	kg/m^2	static	XYZ	native & sphere, z/p	1	once

Table 2.1: Static fields and functions to be saved for the ocean model component in CMIP6. These fields provide basic information about the model configuration, and need only be archived once for all the model experiments in the CMIP6 repository (hence the "once" entry for the experiment column). Listed are the CF standard name, CMOR name, main community sponsoring the diagnostic (Section 2.2), relation to the CMIP5 request (same, new, modification), units, time sampling, spatial shape of the field, spatial grid (spherical longitude-latitude and/or model native, depth/pressure or isopycnal, with details in Section 1.5), prioritization (Section 2.1), and experiment for which to archive the diagnostic. For this table, the diagnostics need to be archived only once, since the diagnostics are static and so the same across all CMIP experiments. Blank entries signal a characteristic that is not applicable for this particular diagnostic. Refer to Section 3.1 for more details on these diagnostics. Furthermore, the bottom topography, grid length and areas, and basin regions should be made available on *both* the model native grid and on the spherical grid onto which scalars are remapped. The entry for masscello applies only to Boussinesq models with static grid cell volumes (Section 1.4.1.1). For other kinds of models, masscello is generally time-dependent and the entry in Table 2.2 applies instead.

SCALAR FIELDS									
CF STANDARD NAME	CMOR NAME	SPONSOR	CMIP5/CMIP6	UNITS	TIME	SHAPE	GRID	PRIORITY	EXPT
sea_water_pressure_at_sea_floor	pbo	OMIP	dbar → Pa	Pa	month	XY	native & sphere	1	all
sea_water_pressure_at_sea_water_surface	pso	OMIP	dbar → Pa	Pa	month	XY	native & sphere	1	all
sea_water_mass_per_unit_area	masscello	OMIP	same	kg/m^2	month	XYZ	native & sphere, z/p	1	all
sea_water_mass	masso	OMIP	same	kg	month	0		1	all
cell_thickness	thkcello	OMIP	same	m	month	XYZ	native & sphere, z/p	1	all
sea_water_volume	volo	OMIP	same	m^3	month	0		1	all
sea_surface_height_above_geoid	zos	OMIP	same	m	month	XY	native & sphere	1	all
square_of_sea_surface_height_above_geoid	zossq	OMIP	same	m^2	month	XY	native & sphere	3	all
global_average_thermosteric_sea_level_change	zostoga	OMIP	same	m	month	0		1	all
sea_water_potential_temperature	thetao	OMIP	K → °C	°C	month	XYZ	native & sphere, z/p	1	all
sea_water_potential_temperature	thetaoga	OMIP	K → °C	°C	month	0		1	all
sea_water_conservative_temperature	bigthetaoga	OMIP	new	°C	month	0		1	all
sea_surface_temperature	tos	OMIP	K → °C	°C	month	XY	native & sphere	1	all
sea_surface_temperature	tosga	OMIP	new	°C	month	0		1	all
sea_surface_temperature	tos	OMIP	K → °C	°C	day	XY	native & sphere	3	all
square_of_sea_surface_temperature	tossq	OMIP	K → °C	$°C^2$	month	XY	native & sphere	3	all
square_of_sea_surface_temperature	tossq	OMIP	K → °C	$°C^2$	day	XY	native & sphere	3	all
sea_water_potential_temperature_at_sea_floor	tob	OMIP	new	°C	month	XY	native & sphere	1	all
integral_wrt_depth_of_product_of_sea_water_density_and_potential_temperature	opottempmint	FAFMIP	new	$(kg\ m^{-2})\ °C$	month	XY	native & sphere	1	all
integral_wrt_depth_of_product_of_sea_water_density_and_conservative_temperature	ocontempmint	FAFMIP	new	$(kg\ m^{-2})\ °C$	month	XY	native & sphere	1	all
sea_water_salinity	so	OMIP	same	1e-3	month	XYZ	native & sphere, z/p	1	all
sea_water_salinity	soga	OMIP	same	1e-3	month	0		1	all
sea_surface_salinity Text	sos	OMIP	same	1e-3	month	XY	native & sphere	1	all
sea_surface_salinity	sosga	OMIP	new	1e-3	month	0		1	all
sea_water_salinity_at_sea_floor	sob	OMIP	new	1e-3	month	XY	native & sphere	1	all
integral_wrt_depth_of_product_of_sea_water_density_and_salinity	somint	FAFMIP	new	$(kg\ m^{-2}) * (1e-3)$	month	XY	native & sphere	1	all
square_of_brunt_vaisala_frequency_in_sea_water	obvfsq	OMIP	new	s^{-2}	month	XYZ	native & sphere, z/p	1	all
sea_water_age_since_surface_contact	agessc	OMIP	same	year	month	XYZ	native & sphere, z/p	1	all
moles_per_unit_mass_of_cfc11_in_sea_water	cfc11	OMIP	same	mol/kg	month	XYZ	native & sphere, z/p	1	hist & omip
moles_per_unit_mass_of_cfc12_in_sea_water	cfc12	OMIP	same	mol/kg	month	XYZ	native & sphere, z/p	2	hist & omip
moles_per_unit_mass_of_sf6_in_sea_water	sf6	OMIP	same	mol/kg	month	XYZ	native & sphere, z/p	2	hist & omip
ocean_mixed_layer_thickness_defined_by_sigma_t	mlotst	OMIP	same	m	month	XY	native & sphere	2	all
square_of_ocean_mixed_layer_thickness_defined_by_sigma_t	mlotstsq	OMIP	same	m^2	month	XY	native & sphere	3	all
ocean_barotropic_mass_streamfunction	msftbarot	OMIP	same	kg/s	month	XY	native & sphere	1	all

Table 2.2: Scalar fields to be saved from the ocean component in CMIP6 ocean model simulations. Listed are the CF standard name, CMOR name, main community sponsoring the diagnostic (Section 2.2), relation to the CMIP5 request (same, new, modification), units, time sampling, spatial shape of the field, spatial grid (spherical longitude-latitude and/or model native, depth/pressure or isopycnal, with details in Section 1.5), prioritization (Section 2.1), and experiment for which to archive the diagnostic. The column indicating the experiment for saving the diagnostics generally says "all", in which we recommend the diagnostic be saved for ALL experiments in which there is an ocean model component. The only exceptions are CFC-11, CFC-12, and SF6, which should be archived only for the CMIP6/historical and CMIP6/OMIP simulations. Blank entries signal a characteristic that is not applicable for this particular diagnostic. As noted in Section 1.5.2, we recommend all scalar fields be conservatively mapped to a latitude-longitude-depth/pressure grid. Squared diagnostics are computed online by accumulating each time step, so that they can be of use for computing variance fields. The entry for masscello applies for models with time-dependent cell masses (Sections 1.4.1.2 and 1.4.2). For Boussinesq models with static grid cell volumes (Section 1.4.1.1), the entry in Table 2.1 applies instead. The time series, bigthetaoga, is requested only for models enacting the TEOS-10 Conservative Temperature field as a prognostic model variable (see Section 3.2.11). Heavy horizontal lines separate physically distinct fields. See Section 3.2 for more details on these scalar diagnostics.

COMPONENTS OF VECTOR FIELDS									
CF STANDARD NAME	CMOR NAME	SPONSOR	CMIP5/CMIP6	UNITS	TIME	SHAPE	GRID	PRIORITY	EXPT
sea_water_x_velocity	uo	OMIP	same	m/s	month	XYZ	native & sphere, z/p	1	all
sea_water_y_velocity	vo	OMIP	same	m/s	month	XYZ	native & sphere, z/p	1	all
ocean_mass_x_transport	umo	OMIP	resolved + parameterized	kg/s	month	XYZ	native, z/p	2	all
ocean_mass_y_transport	vmo	OMIP	resolved + parameterized	kg/s	month	XYZ	native, z/p	2	all
upward_ocean_mass_transport	wmo	OMIP	resolved + parameterized	kg/s	month	XYZ	native & sphere, z/p	1	all
ocean_meridional_overturning_mass_streamfunction	msftmyz	OMIP	level 1 → 0	kg/s	month	YZ-basin	(lat,z/p)	1	all
ocean_meridional_overturning_mass_streamfunction	msftmrho	OMIP	level 1 → 0 & msftmrhoz → msftmrho	kg/s	month	Yρ-basin	(lat,ρ)	1	all
ocean_y_overturning_mass_streamfunction	msftyyz	OMIP	level 1 → 0	kg/s	month	YZ-basin	(native,z/p)	1	all
ocean_y_overturning_mass_streamfunction	msftyrho	OMIP	level 1 → 0 & msftyrhoz → msftyrho	kg/s	month	Yρ-basin	(native,ρ)	1	all
ocean_meridional_overturning_mass_streamfunction_due_to_parameterized_mesoscale_advection	msftmyzmpa	OMIP	new	kg/s	month	YZ-basin	(lat,z/p)	1	all
ocean_meridional_overturning_mass_streamfunction_due_to_parameterized_mesoscale_advection	msftmyrhompa	OMIP	new	kg/s	month	Yρ-basin	(lat,ρ)	1	all
ocean_y_overturning_mass_streamfunction_due_to_parameterized_mesoscale_advection	msftmympa	OMIP	new	kg/s	month	YZ-basin	(native, z/p)	1	all
ocean_y_overturning_mass_streamfunction_due_to_parameterized_mesoscale_advection	msftmyrhompa	OMIP	new	kg/s	month	Yρ-basin	(native, ρ)	1	all
ocean_meridional_overturning_mass_streamfunction_due_to_parameterized_submesoscale_advection	msftmyzsmpa	OMIP	new	kg/s	month	YZ-basin	(lat,z/p)	1	all
ocean_y_overturning_mass_streamfunction_due_to_parameterized_submesoscale_advection	msftmysmpa	OMIP	new	kg/s	month	YZ-basin	(native, z/p)	1	all
ocean_heat_x_transport	hfx	OMIP	XY → XYZ	W	month	XYZ	(native, z/p)	2	all
ocean_heat_y_transport	hfy	OMIP	XY → XYZ	W	month	XYZ	(native, z/p)	2	all
northward_ocean_heat_transport	hfbasin	OMIP	same	W	month	Y-basin	(lat)	1	all
northward_ocean_heat_transport_due_to_parameterized_mesoscale_advection	hfbasinpmadv	OMIP	new	W	month	Y-basin	(lat)	1	all
northward_ocean_heat_transport_due_to_parameterized_submesoscale_advection	hfbasinpsmadv	OMIP	new	W	month	Y-basin	(lat)	1	all
northward_ocean_heat_transport_due_to_parameterized_mesoscale_diffusion	hfbasinpmdiff	OMIP	new	W	month	Y-basin	(lat)	1	all
northward_ocean_heat_transport_due_to_parameterized_eddy_advection	hfbasinpadv	OMIP	new	W	month	Y-basin	(lat)	1	all
northward_ocean_heat_transport_due_to_gyre	htovgyre	OMIP	same	W	month	Y-basin	(lat)	2	all
northward_ocean_heat_transport_due_to_overturning	htovovrt	OMIP	same	W	month	Y-basin	(lat)	2	all
northward_ocean_salt_transport_due_to_gyre	sltovgyre	OMIP	same	kg/s	month	Y-basin	(lat)	2	all
northward_ocean_salt_transport_due_to_overturning	sltovovrt	OMIP	same	kg/s	month	Y-basin	(lat)	2	all

Table 2.3: Vector fields, or components of vector fields, that should be saved from the ocean component in CMIP6 simulations. Listed are the CF standard name, CMOR name, main community sponsoring the diagnostic (Section 2.2), relation to the CMIP5 request (same, new, modification), units, time sampling, spatial shape of the field, spatial grid (spherical longitude-latitude and/or model native, depth/pressure or isopycnal, with details in Section 1.5), prioritization (Section 2.1), and experiment for which to archive the diagnostic. The column indicating the experiment for saving the diagnostics generally says "all", in which we recommend the diagnostic be saved for ALL experiments in which there is an ocean model component. Blank entries signal a characteristic that is not applicable for this particular diagnostic. Certain of the fields in this table should be partitioned into Atlantic-Arctic, Indian-Pacific, and Global regions. Spherical remapping (mapping to north-south and east-west vector components) is discussed in Sections 1.5.3 and 1.5.4. See Section 3.3 for further details on entries to this table.

MASS TRANSPORT THROUGH SECTIONS									
CF STANDARD NAME	CMOR NAME	SPONSOR	CMIP5/CMIP6	UNITS	TIME	SHAPE	GRID	PRIORITY	EXPT
sea_water_transport_across_line (barents_opening)	mfo	OMIP	same	kg/s	month	0		2	all
sea_water_transport_across_line (bering_strait)	mfo	OMIP	same	kg/s	month	0		2	all
sea_water_transport_across_line (canadian_archipelago)	mfo	OMIP	same	kg/s	month	0		2	all
sea_water_transport_across_line (caribbean_windward_passage)	mfo	OMIP	same	kg/s	month	0		2	all
sea_water_transport_across_line (denmark_strait)	mfo	OMIP	same	kg/s	month	0		2	all
sea_water_transport_across_line (drake_passage)	mfo	OMIP	same	kg/s	month	0		2	all
sea_water_transport_across_line (english_channel)	mfo	OMIP	same	kg/s	month	0		2	all
sea_water_transport_across_line (faroe_scotland_channel)	mfo	OMIP	same	kg/s	month	0		2	all
sea_water_transport_across_line (florida_bahamas_strait)	mfo	OMIP	same	kg/s	month	0		2	all
sea_water_transport_across_line (fram_strait)	mfo	OMIP	same	kg/s	month	0		2	all
sea_water_transport_across_line (iceland_faroe_channel)	mfo	OMIP	same	kg/s	month	0		2	all
sea_water_transport_across_line (indonesian_throughflow)	mfo	OMIP	same	kg/s	month	0		2	all
sea_water_transport_across_line (mozambique_channel)	mfo	OMIP	same	kg/s	month	0		2	all
sea_water_transport_across_line (pacific_equatorial_undercurrent)	mfo	OMIP	same	kg/s	month	0		2	all
sea_water_transport_across_line (taiwan_and_luzon_straits)	mfo	OMIP	same	kg/s	month	0		2	all

Table 2.4: This table summarizes the sections for archiving the vertically integrated mass transport from the ocean component in CMIP6 simulations, to be identified by the CF standard name sea_water_transport_across_line. Each geographical region has an associated string-valued coordinate given by the name in this table. See Section 3.4 for further details on these mass transports. Listed are the CF standard name, CMOR name, main community sponsoring the diagnostic (Section 2.2), relation to the CMIP5 request (same, new, modification), units, time sampling, spatial shape of the field, spatial grid (spherical longitude-latitude and/or model native, depth/pressure or isopycnal, with details in Section 1.5), prioritization (Section 2.1), and experiment for which to archive the diagnostic. The column indicating the experiment for saving the diagnostics generally says "all", in which we recommend the diagnostic be saved for ALL experiments in which there is an ocean model component. Blank entries signal a characteristic that is not applicable for this particular diagnostic.

BOUNDARY MASS FLUXES									
CF STANDARD NAME	CMOR NAME	SPONSOR	CMIP5/CMIP6	UNITS	TIME	SHAPE	GRID	PRIORITY	EXPT
rainfall_flux	pr	OMIP/FAFMIP	same	kg/(m^2 s)	month	XY	native	2	all
snowfall_flux	prsn	OMIP/FAFMIP	same	kg/(m^2 s)	month	XY	native	2	all
water_evaporation_flux	evs	OMIP/FAFMIP	same	kg/(m^2 s)	month	XY	native	2	all
water_flux_into_sea_water_from_rivers	friver	OMIP/FAFMIP	same	kg/(m^2 s)	month	XY	native	2	all
water_flux_into_sea_water_from_icebergs	ficeberg	OMIP/FAFMIP	same	kg/(m^2 s)	month	XYZ	native, z/p	2	all
water_flux_into_sea_water_due_to_sea_ice_thermodynamics	fsitherm	OMIP/FAFMIP	same	kg/(m^2 s)	month	XY	native	2	all
water_flux_into_sea_water	wfo	OMIP	same	kg/(m^2 s)	month	XY	native & sphere	1	all
water_flux_into_sea_water_without_flux_correction	wfonocorr	OMIP	same	kg/(m^2 s)	month	XY	native & sphere	1	all
water_flux_correction	wfcorr	OMIP	same	kg/(m^2 s)	month	XY	native & sphere	1	all

Table 2.5: This table provides a summary of the air-sea and ice-sea boundary fluxes of water mass that should be saved from the ocean model component in CMIP6 simulations. Positive fluxes are into the ocean, with the single exception of evaporation, which is positive for water leaving the liquid ocean. Listed are the CF standard name, CMOR name, main community sponsoring the diagnostic (Section 2.2), relation to the CMIP5 request (same, new, modification), units, time sampling, spatial shape of the field, spatial grid (spherical longitude-latitude and/or model native, depth/pressure or isopycnal, with details in Section 1.5), prioritization (Section 2.1), and experiment for which to archive the diagnostic. The column indicating the experiment for saving the diagnostics generally says "all", in which we recommend the diagnostic be saved for ALL experiments in which there is an ocean model component. Blank entries signal a characteristic that is not applicable for this particular diagnostic. As noted in Section 1.5.2, we recommend these boundary fluxes be conservatively mapped to a latitude-longitude grid. See Section 3.5.1 for details on these boundary mass fluxes.

BOUNDARY SALT FLUXES									
CF STANDARD NAME	CMOR NAME	SPONSOR	CMIP5/CMIP6	UNITS	TIME	SHAPE	GRID	PRIORITY	EXPT
virtual_salt_flux_into_sea_water_due_to_rainfall	vsfpr	OMIP/FAFMIP	same	kg/(m^2 s)	month	XY	native	2	all
virtual_salt_flux_into_sea_water_due_to_evaporation	vsfevap	OMIP/FAFMIP	same	kg/(m^2 s)	month	XY	native	2	all
virtual_salt_flux_into_sea_water_from_rivers	vsfriver	OMIP/FAFMIP	same	kg/(m^2 s)	month	XY	native	2	all
virtual_salt_flux_into_sea_water_due_to_sea_ice_thermodynamics	vsfsit	OMIP/FAFMIP	same	kg/(m^2 s)	month	XY	native	2	all
virtual_salt_flux_into_sea_water	vsf	OMIP/FAFMIP	same	kg/(m^2 s)	month	XY	native	2	all
virtual_salt_flux_correction	vsfcorr	OMIP/FAFMIP	same	kg/(m^2 s)	month	XY	native	2	all
downward_sea_ice_basal_salt_flux	sfdsi	OMIP	same	kg/(m^2 s)	month	XY	native & sphere	1	all
salt_flux_into_sea_water_from_rivers	sfriver	OMIP	same	kg/(m^2 s)	month	XY	native & sphere	1	all

Table 2.6: This table provides a summary of the air-sea and ice-sea boundary fluxes of salt mass that should be saved from the ocean model component in CMIP6 simulations. Positive fluxes are into the ocean. Listed are the CF standard name, CMOR name, main community sponsoring the diagnostic (Section 2.2), relation to the CMIP5 request (same, new, modification), units, time sampling, spatial shape of the field, spatial grid (spherical longitude-latitude and/or model native, depth/pressure or isopycnal, with details in Section 1.5), prioritization (Section 2.1), and experiment for which to archive the diagnostic. The column indicating the experiment for saving the diagnostics generally says "all", in which we recommend the diagnostic be saved for ALL experiments in which there is an ocean model component. Blank entries signal a characteristic that is not applicable for this particular diagnostic. As noted in Section 1.5.2, we recommend these boundary fluxes be conservatively mapped to a latitude-longitude grid. See Section 3.5.2 for details on these boundary salt fluxes.

BOUNDARY HEAT FLUXES									
CF STANDARD NAME	CMOR NAME	SPONSOR	CMIP5/CMIP6	UNITS	TIME	SHAPE	GRID	PRIORITY	EXPT
upward_geothermal_heat_flux_at_sea_floor	hfgeou	OMIP/FAFMIP	same	W/m^2	month	XY	native & sphere	1	all
temperature_flux_due_to_rainfall_expressed_as_heat_flux_into_sea_water	hfrainds	OMIP/FAFMIP	same	W/m^2	month	XY	native	2	all
temperature_flux_due_to_evaporation_expressed_as_heat_flux_out_of_sea_water	hfevapds	OMIP/FAFMIP	same	W/m^2	month	XY	native	2	all
temperature_flux_due_to_runoff_expressed_as_heat_flux_into_sea_water	hfrunoffds	OMIP/FAFMIP	same	W/m^2	month	XYZ	native, z/p	2	all
heat_flux_into_sea_water_due_to_snow_thermodynamics	hfsnthermds	OMIP/FAFMIP	same	W/m^2	month	XYZ	native,z/p	2	all
heat_flux_into_sea_water_due_to_frazil_ice_formation	hfsifrazil	OMIP/FAFMIP	same	W/m^2	month	XYZ	native,z/p	2	all
heat_flux_into_sea_water_due_to_sea_ice_thermodynamics	hfsithermds	OMIP/FAFMIP	same	W/m^2	month	XYZ	native,z/p	2	all
heat_flux_into_sea_water_due_to_iceberg_thermodynamics	hfibthermds	OMIP/FAFMIP	same	W/m^2	month	XYZ	native, z/p	2	all
surface_net_downward_longwave_flux	rlds	OMIP/FAFMIP	same	W/m^2	month	XY	native	2	all
surface_downward_latent_heat_flux	hfls	OMIP/FAFMIP	same	W/m^2	month	XY	native	2	all
surface_downward_sensible_heat_flux	hfss	OMIP/FAFMIP	same	W/m^2	month	XY	native	2	all
net_downward_shortwave_flux_at_sea_water_surface	rsntds	OMIP/FAFMIP	same	W/m^2	month	XY	native	2	all
downwelling_shortwave_flux_in_sea_water	rsdo	OMIP/FAFMIP	same	W/m^2	month	XYZ	native, z/p	2	all
heat_flux_correction	hfcorr	OMIP	same	W/m^2	month	XY	native & sphere	1	all
surface_downward_heat_flux_in_sea_water	hfds	OMIP	same	W/m^2	month	XY	native & sphere	1	all

Table 2.7: This table provides a summary of the air-sea and ice-sea boundary fluxes of heat that should be saved from the ocean component from the ocean component in CMIP6 simulations. Positive fluxes are into the ocean. Listed are the CF standard name, CMOR name, main community sponsoring the diagnostic (Section 2.2), relation to the CMIP5 request (same, new, modification), units, time sampling, spatial shape of the field, spatial grid (spherical longitude-latitude and/or model native, depth/pressure or isopycnal, with details in Section 1.5), prioritization (Section 2.1), and experiment for which to archive the diagnostic. The column indicating the experiment for saving the diagnostics generally says "all", in which we recommend the diagnostic be saved for ALL experiments in which there is an ocean model component. Blank entries signal a characteristic that is not applicable for this particular diagnostic. As noted in Section 1.5.2, we recommend these boundary fluxes be conservatively mapped to a latitude-longitude grid. For the geothermal heating, most models use a static geothermal heating, in which case only one time step need be archived. If time dependent, then monthly fields are requested. Note that many climate models place boundary fluxes at the ocean surface. However, more general couplings are being considered (e.g., a sea ice model that interacts with more than the surface ocean cell). To allow for such generality, we note that many of the fluxes can be three-dimensional. Note that the field "rsdo" was mistakenly included in the CMIP5 diagnostic excel spreadsheet as "rsds". See Section 3.5.3 for details on these boundary heat fluxes.

BOUNDARY MOMENTUM FLUXES									
CF STANDARD NAME	CMOR NAME	SPONSOR	CMIP5/CMIP6	UNITS	TIME	SHAPE	GRID	PRIORITY	EXPT
surface_downward_x_stress	tauuo	OMIP	same	N/m^2	month	XY	native & sphere	1	all
surface_downward_y_stress	tauvo	OMIP	same	N/m^2	month	XY	native & sphere	1	all
surface_downward_x_stress_correction	tauucorr	OMIP	same	N/m^2	month	XY	native & sphere	1	all
surface_downward_y_stress_correction	tauvcorr	OMIP	same	N/m^2	month	XY	native & sphere	1	all

Table 2.8: This table presents the net surface stress applied at the liquid ocean surface by air-sea plus ice-sea interactions that should saved from the ocean model component in CMIP6 simulations. Positive fluxes accelerate the ocean. Listed are the CF standard name, CMOR name, main community sponsoring the diagnostic (Section 2.2), relation to the CMIP5 request (same, new, modification), units, time sampling, spatial shape of the field, spatial grid (spherical longitude-latitude and/or model native, depth/pressure or isopycnal, with details in Section 1.5), prioritization (Section 2.1), and experiment for which to archive the diagnostic. The column indicating the experiment for saving the diagnostics generally says "all", in which we recommend the diagnostic be saved for ALL experiments in which there is an ocean model component. Blank entries signal a characteristic that is not applicable for this particular diagnostic. Note the recommendation to map each momentum flux component to an A-grid on the sphere. The units N/m^2 are identical to Pa. See Section 3.5.4 for further details on these momentum fluxes.

BOUNDARY CHEMICAL (GAS EXCHANGE) FLUXES									
CF STANDARD NAME	CMOR NAME	SPONSOR	CMIP5/CMIP6	UNITS	TIME	SHAPE	GRID	PRIORITY	EXPT
surface_downward_cfc11_flux	fgcfc11	OMIP	same	$mol/(sec\ m^2)$	month	XY	native & sphere	1	hist & omip
surface_downward_cfc11_flux	fgcfc12	OMIP	same	$mol/(sec\ m^2)$	month	XY	native & sphere	2	hist & omip
surface_downward_sf6_flux	fgsf6	OMIP	same	$mol/(sec\ m^2)$	month	XY	native & sphere	2	hist & omip

Table 2.9: This table presents the net surface gas exchange fluxes for inert chemical tracers, applied at the liquid ocean surface by air-sea plus ice-sea interactions. Positive fluxes enter the ocean. Listed are the CF standard name, CMOR name, main community sponsoring the diagnostic (Section 2.2), relation to the CMIP5 request (same, new, modification), units, time sampling, spatial shape of the field, spatial grid (spherical longitude-latitude and/or model native, depth/pressure or isopycnal, with details in Section 1.5), prioritization (Section 2.1), and experiment for which to archive the diagnostic. The column indicating the experiment for saving the diagnostics says "hist & omip", as these fields should be saved just for the CMIP6/historical and CMIP6/OMIP simulations. Blank entries signal a characteristic that is not applicable for this particular diagnostic. See Section 3.5.5 for further details on these boundary fluxes.

3D HEAT AND SALT BUDGET TERMS									
STANDARD NAME	CMOR NAME	SPONSOR	CMIP5/CMIP6	UNITS	TIME	SHAPE	GRID	PRIORITY	EXPT
tendency_of_sea_water_potential_temperature_expressed_as_heat_content	opottemptend	FAFMIP	new	W m^{-2}	annual	XYZ	native, z/p	3	all
tendency_of_sea_water_potential_temperature_expressed_as_heat_content_due_to_advection	opottempadvect	FAFMIP	new	W m^{-2}	annual	XYZ	native, z/p	3	all
tendency_of_sea_water_potential_temperature_expressed_as_heat_content_due_to_parameterized_eddy_advection	opottemppadvect	FAFMIP	new	W m^{-2}	annual	XYZ	native, z/p	3	all
tendency_of_sea_water_potential_temperature_expressed_as_heat_content_due_to_parameterized_mesoscale_advection	opottemppmadvect	FAFMIP	new	W m^{-2}	annual	XYZ	native, z/p	3	all
tendency_of_sea_water_potential_temperature_expressed_as_heat_content_due_to_parameterized_mesoscale_diffusion	opottemppmdiff	FAFMIP	new	W m^{-2}	annual	XYZ	native, z/p	3	all
tendency_of_sea_water_potential_temperature_expressed_as_heat_content_due_to_parameterized_submesoscale_advection	opottemppsmadvect	FAFMIP	new	W m^{-2}	annual	XYZ	native, z/p	3	all
tendency_of_sea_water_potential_temperature_expressed_as_heat_content_due_to_parameterized_dianeutral_mixing	opottempdiff	FAFMIP	new	W m^{-2}	annual	XYZ	native, z/p	3	all
tendency_of_sea_water_conservative_temperature_expressed_as_heat_content	ocontemptend	FAFMIP	new	W m^{-2}	annual	XYZ	native, z/p	3	all
tendency_of_sea_water_conservative_temperature_expressed_as_heat_content_due_to_advection	ocontempadvect	FAFMIP	new	W m^{-2}	annual	XYZ	native, z/p	3	all
tendency_of_sea_water_conservative_temperature_expressed_as_heat_content_due_to_parameterized_eddy_advection	ocontemppadvect	FAFMIP	new	W m^{-2}	annual	XYZ	native, z/p	3	all
tendency_of_sea_water_conservative_temperature_expressed_as_heat_content_due_to_parameterized_mesoscale_advection	ocontemppmadvect	FAFMIP	new	W m^{-2}	annual	XYZ	native, z/p	3	all
tendency_of_sea_water_conservative_temperature_expressed_as_heat_content_due_to_parameterized_mesoscale_diffusion	ocontemppmdiff	FAFMIP	new	W m^{-2}	annual	XYZ	native, z/p	3	all
tendency_of_sea_water_conservative_temperature_expressed_as_heat_content_due_to_parameterized_submesoscale_advection	ocontemppsmadvect	FAFMIP	new	W m^{-2}	annual	XYZ	native, z/p	3	all
tendency_of_sea_water_conservative_temperature_expressed_as_heat_content_due_to_parameterized_dianeutral_mixing	ocontempdiff	FAFMIP	new	W m^{-2}	annual	XYZ	native, z/p	3	all
tendency_of_sea_water_salinity_expressed_as_salt_content	osalttend	FAFMIP	new	kg m^{-2} s^{-1}	annual	XYZ	native, z/p	3	all
tendency_of_sea_water_salinity_expressed_as_salt_content_due_to_advection	osaltadvect	FAFMIP	new	kg m^{-2} s^{-1}	annual	XYZ	native, z/p	3	all
tendency_of_sea_water_salinity_expressed_as_salt_content_due_to_parameterized_eddy_advection	osaltpadvect	FAFMIP	new	kg m^{-2} s^{-1}	annual	XYZ	native, z/p	3	all
tendency_of_sea_water_salinity_expressed_as_salt_content_due_to_parameterized_mesoscale_advection	osaltpmadvect	FAFMIP	new	kg m^{-2} s^{-1}	annual	XYZ	native, z/p	3	all
tendency_of_sea_water_salinity_expressed_as_salt_content_due_to_parameterized_mesoscale_diffusion	osaltpmdiff	FAFMIP	new	kg m^{-2} s^{-1}	annual	XYZ	native, z/p	3	all
tendency_of_sea_water_salinity_expressed_as_salt_content_due_to_parameterized_submesoscale_advection	osaltpsmadvect	FAFMIP	new	kg m^{-2} s^{-1}	annual	XYZ	native, z/p	3	all
tendency_of_sea_water_salinity_expressed_as_salt_content_due_to_parameterized_dianeutral_mixing	osaltdiff	FAFMIP	new	kg m^{-2} s^{-1}	annual	XYZ	native, z/p	3	all

Table 2.10: This table summarizes fields that support the study of three-dimensional ocean heat and salt budgets, listing here terms contributing to the time tendency of heat and salt in a model grid cell. For models with prognostic temperature given by potential temperature, then these models should fill the potential_temperature fields and leave the conservative_temperature fields blank; conversely for models with Conservative Temperature as the prognostic temperature field. Listed are the CF standard name, CMOR name, main community sponsoring the diagnostic (Section 2.2), relation to the CMIP5 request (same, new, modification), units, time sampling, spatial shape of the field, spatial grid (spherical longitude-latitude and/or model native, depth/pressure or isopycnal, with details in Section 1.5), prioritization (Section 2.1), and experiment for which to archive the diagnostic. The column indicating the experiment for saving the diagnostics generally says "all", in which we recommend the diagnostic be saved for ALL experiments in which there is an ocean model component. Blank entries signal a characteristic that is not applicable for this particular diagnostic. Note that due_to_parameterized_eddy_advection = due_to_parameterized_mesoscale_advection + due_to_parameterized_submesoscale_advection. Annual means are requested, rather than monthly means. See Section 3.6 for details on these diagnostics.

VERTICAL SGS PARAMETERIZATIONS									
CF STANDARD NAME	CMOR NAME	SPONSOR	CMIP5/CMIP6	UNITS	TIME	SHAPE	GRID	PRIORITY	EXPT
ocean_vertical_heat_diffusivity	difvho	OMIP/FAFMIP	(month → annual) and (hist → all)	m^2/s	annual	XYZ	native & sphere, z/p	3	all
ocean_vertical_salt_diffusivity	difvso	OMIP/FAFMIP	(month → annual) and (hist → all)	m^2/s	annual	XYZ	native & sphere, z/p	3	all
tendency_of_ocean_potential_energy_content	tnpeo	OMIP/FAFMIP	(month → annual) and (hist → all)	W/m^2	annual	XY	native & sphere, z/p	3	all

Table 2.11: This table summarizes some fields that support the study of vertical/dianeutral SGS parameterizations. These fields should be saved from the ocean model component in CMIP6 simulations. Listed are the CF standard name, CMOR name, main community sponsoring the diagnostic (Section 2.2), relation to the CMIP5 request (same, new, modification), units, time sampling, spatial shape of the field, spatial grid (spherical longitude-latitude and/or model native, depth/pressure or isopycnal, with details in Section 1.5), prioritization (Section 2.1), and experiment for which to archive the diagnostic. The column indicating the experiment for saving the diagnostics generally says "all", in which we recommend the diagnostic be saved for ALL experiments in which there is an ocean model component. Blank entries signal a characteristic that is not applicable for this particular diagnostic. See Section 3.7 for details of these SGS diagnostics. We ask only for annual means from these fields, rather than the monthly means requested for most other diagnostics. Additionally, this table has been reduced from the 12 fields requested in CMIP5 to the three requested here. Furthermore, the field tnpeo was requested as a 3d field in CMIP5, whereas for CMIP6 it is requested as a depth integrated 2d field.

LATERAL SGS PARAMETERIZATIONS									
CF STANDARD NAME	CMOR NAME	SPONSOR	CMIP5/CMIP6	UNITS	TIME	SHAPE	GRID	PRIORITY	EXPT
ocean_tracer_diffusivity_due_to_parameterized_mesoscale_advection	diftrblo	OMIP/FAFMIP	(month → annual) and (hist → all)	m^2/s	annual	XYZ	native, z/p	3	all
ocean_tracer_epineutral_laplacian_diffusivity	diftrelo	OMIP/FAFMIP	(month → annual) and (hist → all)	m^2/s	annual	XYZ	native, z/p	3	all
tendency_of_ocean_eddy_kinetic_energy_content_due_to_parameterized_eddy_advection	tnkebto	OMIP/FAFMIP	(month → annual) and (hist → all)	W/m^2	annual	XY	native	3	all
ocean_momentum_xy_laplacian_diffusivity	difmxylo	OMIP/FAFMIP	(month → annual) and (hist → all)	m^2/s	annual	XYZ	native, z/p	3	all
ocean_momentum_xy_biharmonic_diffusivity	difmxybo	OMIP/FAFMIP	(month → annual) and (hist → all)	m^4/s	annual	XYZ	native, z/p	3	all
ocean_kinetic_energy_dissipation_per_unit_area_due_to_xy_friction	dispkexyfo	OMIP/FAFMIP	(month → annual) and (hist → all)	W/m^2	annual	XY	native	3	all

Table 2.12: This table summarizes some fields that support the study of lateral SGS parameterizations. These fields should be saved from the ocean model component in CMIP6 simulations. Listed are the CF standard name, CMOR name, main community sponsoring the diagnostic (Section 2.2), relation to the CMIP5 request (same, new, modification), units, time sampling, spatial shape of the field, spatial grid (spherical longitude-latitude and/or model native, depth/pressure or isopycnal, with details in Section 1.5), prioritization (Section 2.1), and experiment for which to archive the diagnostic. The column indicating the experiment for saving the diagnostics generally says "all", in which we recommend the diagnostic be saved for ALL experiments in which there is an ocean model component. Blank entries signal a characteristic that is not applicable for this particular diagnostic. See Section 3.8 for details on these diagnostics. We ask only for annual means from these fields, rather than the monthly means requested for most other diagnostics. Additionally, this table has been reduced from the ten fields requested in CMIP5 to the six requested here. Furthermore, note that the fields tnkebto and dispkexyfo were requested as 3d fields for CMIP5, whereas they are now requested as depth integrated 2d fields.

Notes

[6]CMIP5 priority=0 diagnostics are now termed CMIP6 priority=1 diagnostics, and so on for the other priorities. This change in prioritization nomenclature aims to agree with the other MIPs in CMIP6.

[7]Downes and Hogg (2013) is an attempt to analyze the mesoscale parameterizations, with a focus on the Southern Ocean. Unfortunately, only a few models were submitted with the relevant eddy diffusivities and overturning streamfunctions.

[8]XYZ is a shorthand for the more detailed prescription of both horizontal and vertical grids, with details given in Section 1.5. For example, isopycnal coordinate ocean models must submit three-dimensional fields on both XYZ and their native XYρ. In contrast, pressure coordinate models need not remap their output to geopotential, so that XYZ represents a shorthand for XYp.

Chapter 3

Details of the ocean diagnostics

Contents

In this chapter, we present details of the physical ocean diagnostics requested for CMIP6.

3.1 Static fields and functions

This section presents recommendations for certain static fields and functions that are needed to describe elements of the ocean model. A summary of the diagnostic names is given in Table 2.1.

3.1.1 Equation of state

- sea_water_equation_of_state

This diagnostic is in fact a mere citation to the literature source for the model's equation of state used to compute *in situ* density (kg/m^3). It should also be noted what variables are used (see IOC et al. (2010)):

- temperature
  - potential temperature θ, or
  - Conservative Temperature Θ
- salinity
  - practical salinity S_P, or
  - Absolute Salinity S_A.
- pressure (in dbars) or depth (in metres).

3.1.2 Temperature for seawater freezing

- sea_water_freezing_temperature_equation

Ocean models use a variety of equations to determine when liquid seawater freezes to form frazil and then sea ice (McDougall et al., 2014). It is thus useful for studies of high latitude processes to document the equation used to compute the freezing point (in degrees C) of seawater, as a function of salinity and pressure.

3.1.3 Boussinesq reference density

- reference_sea_water_density_for_boussinesq_approximation

Many ocean climate models employ the Boussinesq approximation, in which there appears a constant reference density ρ_o within budgets for tracer and momentum, and volume is conserved rather than mass. It is useful to have an archive of this constant for CMIP6.

As noted on page 47 of Gill (1982), with the exception of only a small percentage of the ocean, *in situ* density in the World Ocean varies by no more than 2% from $1035\,\mathrm{kg\ m^{-3}}$. Hence, $\rho_o = 1035\,\mathrm{kg\ m^{-3}}$ is a sensible choice for the reference density used in a Boussinesq ocean climate model. However, some models may use a different value. For example, early versions of the GFDL ocean model (Cox, 1984) set $\rho_o = 1000\,\mathrm{kg\ m^{-3}}$. Others choose the average density corresponding to the thermocline region. Roquet et al. (2014) present a summary of various choices.

3.1.4 Seawater heat capacity

- specific_heat_capacity_of_sea_water

As detailed in McDougall (2003) and IOC et al. (2010), the heat capacity of seawater is a constant when measuring the heat content of a parcel in terms of Conservative Temperature, with a value given by

$$c_p^o = 3991.86795711963\ \mathrm{J\ kg^{-1}\ K^{-1}}. \tag{3.1}$$

As discussed in Section 1.7.2, not all models choose to use Conservative Temperature as their prognostic heat variable. However, all ocean models use a constant heat capacity, C_p^o, to convert between prognostic model temperature and heat content, though not all models use the TEOS-10 value for heat capacity. Hence, to enable accurate comparisons between ocean model heat contents, we ask that all models archive their choice for the constant seawater heat capacity, C_p^o.

A particularly useful method to archive this constant is to include it as part of the metadata for the temperature diagnostic thetao (Section 3.2.10), *as well as* for all heat related diagnostics (e.g., boundary heat fluxes in Table 2.7 and heat budget terms in Table 2.10). Doing so will facilitate computation of ocean heat content consistent with how the model computes converts boundary enthalpy fluxes into temperature tendencies.

3.1.5 Bathymetry

- sea_floor_depth_below_geoid
- sea_floor_depth_below_geoid_velocity

For global primitive equation ocean models, the geoid is assumed to correspond to the geopotential surface $z = 0$. The distance from $z = 0$ to the ocean bottom defines the ocean depth field, $H(x, y)$, or the ocean *bathymetry*, and the vertical position of the bottom is

$$z = -H(x, y). \tag{3.2}$$

This solid earth boundary used by the model should be archived. Precisely, the bathymetry representing the ocean bottom from the perspective of the model's tracer fields defines the field sea_floor_depth_below_geoid. For non-isopycnal models, it is also necessary to provide the bathymetry sea_floor_depth_below_geoid_velocity as seen by the velocity fields, as this depth generally differs from that seen by tracers. For isopycnal models, the bottom for the velocity field is a time and flow dependent function, and so need not be archived.

If the lateral area for exchange of fluid between columns (e.g., mass transport) is anything other than a simple function of the tracer column depths, then the modulated areas affecting the exchange should be provided. For example, this additional information is necessary for models that allow a strait to be more narrow than the nominal width of the cell.

3.1.6 Tracer and velocity cell region masks

- region

Analysis of budgets and properties over ocean basins is commonly performed for the purpose of assessing the integrity of simulations. This analysis generally involves the use of a mask that partitions the model grid into ocean basins (some enclosed seas may be missing from the model). We recommend the following mapping between ocean regions and integer, with the names corresponding to standard CF basin names found at

`http://cfconventions.org/`

1. southern_ocean
2. atlantic_ocean
3. pacific_ocean
4. arctic_ocean
5. indian_ocean
6. mediterranean_sea
7. black_sea
8. hudson_bay
9. baltic_sea
10. red_sea

These region masks are set according to the following flag_values and flag_meanings, which should be recorded as attributes of the variable:

- flag_values=1,2,3,4,5,6,7,8,9,10
- flag_meanings="southern_ocean, atlantic_ocean, pacific_ocean, arctic_ocean, indian_ocean, mediterranean_sea, black_sea, hudson_bay, baltic_sea, red_sea"

Many budget analyses require the tracer mask, so it is very useful for the analyst to have access to the regional mask. Additionally, for some grid staggering (such as B-grid), the tracer mask will differ from velocity mask, in which case a mask for the velocity cells should be provided to the CMIP6 archive as a distinct output variable, with the same standard name of region. The two variables are distinguished in netCDF by their coordinates, one being on the tracer grid and the other on the velocity grid.

3.2 Scalar fields

This section presents recommendations for scalar fields to be archived as part of CMIP6. These fields are summarized in Table 2.2.

3.2.1 Pressure at ocean bottom

- sea_water_pressure_at_sea_floor = pbo

The bottom pressure in a hydrostatic ocean is given by the gravitational acceleration acting on the mass per area of a fluid column, plus any pressure applied at the ocean surface from the overlying atmosphere or ice. In a discrete model, sea_water_pressure_at_sea_floor is given by the vertical sum over the $k-levels$ in the column

$$p_b = p_a + g \sum_k \rho \, dz \tag{3.3}$$

where p_a is the pressure applied at the ocean surface (pso discussed in Section 3.2.2), and we assumed a constant gravitational acceleration (presumably assumed for all CMIP6 simulations). Hence, $g^{-1}(p_b - p_a)$ is the mass per horizontal area of a fluid column. The bottom pressure is a prognostic field in non-Boussinesq hydrostatic models, whereas it is diagnosed in Boussinesq hydrostatic models. Anomalies of bottom pressure with respect to a suitable reference value, such as $\rho_o \, g \, H$, provide a means for measuring mass adjustments throughout the water column.

If the model is non-hydrostatic (very uncommon for global climate models), the bottom pressure is affected by the mass per area of the ocean fluid, plus non-hydrostatic fluctuations in the pressure field.

If the model is Boussinesq (very common), then an adjustment must be made to account for spurious mass sources in the Boussinesq fluid. Details of these adjustments are provided in Section D.3.3 of Griffies and Greatbatch (2012). In particular, if interested in the mass distribution of seawater, such as needed for angular momentum (Bryan, 1997), bottom pressure (Ponte, 1999), or geoid perturbations (Kopp et al., 2010), one must account for this spurious mass change that arises due to the oceanic Boussinesq approximation. Please make a note in the meta-data whether an adjustment has been made to correct for the Boussinesq error.

3.2.2 Net pressure from atmosphere, sea ice, ice shelves, etc

- sea_water_pressure_at_sea_water_surface = pso

The pressure applied to the ocean surface from the overlying atmosphere is often neglected in climate simulations. However, for those models that incorporate this effect, they provide a means to simulate the inverse barometer, which presents a rapid barotropic forcing to the ocean. In these cases, it is important to have a map of the applied pressure from the atmosphere acting on the ocean.

In addition to atmospheric mass impacting on the ocean, there is mass from overlying sea ice, ice shelves, icebergs, etc. This mass should also be included in this applied pressure field. Note that solid runoff is defined as all frozen water that enters the ocean from land, such as from snow and land-, lake- and river ice. For example, snow may enter in its frozen state when a land model has a buffer layer of a certain thickness, with all snow exceeding this buffer conveyed to the ocean. Land-ice may enter the ocean as icebergs that may result from an ice sheet/shelf model, or be formed from snow excess. There is no increase is liquid ocean water until the solid runoff melts. However, the presence of solid ice affects the pressure felt within the liquid ocean column.

In rigid lid ocean models, the term "surface pressure" refers to the hydrostatic pressure at $z = 0$ associated with the layer of liquid water between $z = 0$ and $z = \eta$. This pressure is also sometimes referred to as the "lid pressure." It can be positive or negative. This "surface pressure" field is distinctly *not* what we refer to here by sea_water_pressure_at_sea_water_surface. Instead, the field sea_water_pressure_at_sea_water_surface records the non-negative pressure applied at $z = \eta$ due to media above the ocean surface interface. Such pressure may be set to zero in some approximate model formulations, such as the rigid lid, in which case the ocean dynamics is not influenced by movement of overlying media.

3.2.3 Mass per area of grid cell

- sea_water_mass_per_unit_area = masscello

To compute tracer budgets, we require the mass of seawater in the grid cell, per horizontal area of the cell

$$\text{sea\_water\_mass\_per\_unit\_area} = \rho\, dz \qquad \text{non-Boussinesq,} \tag{3.4}$$

with units of kg/m^2. For a hydrostatic model, the mass per area is proportional to the pressure increment dp according to

$$dp = -g\,\rho\, dz \qquad \text{hydrostatic,} \tag{3.5}$$

so that

$$\text{sea\_water\_mass\_per\_unit\_area} = -g^{-1}\, dp \qquad \text{non-Boussinesq and hydrostatic.} \tag{3.6}$$

For a Boussinesq model, the *in situ* density factor, ρ, in equation (3.4) is set to the constant reference density, ρ_o, so that

$$\text{sea\_water\_mass\_per\_unit\_area} = \rho_o\, dz \qquad \text{Boussinesq,} \tag{3.7}$$

in which case the mass per area is equivalent to ρ_o times the grid cell thickness (Section 3.2.3).

3.2.4 Total mass of liquid seawater

- sea_water_mass = masso

This diagnostic is the global sum of masscello (Section 3.2.3).

For the purpose of global budgets in non-Boussinesq models, it is essential to have the total mass of liquid seawater in the ocean domain. This scalar field includes all seawater contained in the liquid ocean, including any enclosed seas that are part of the ocean model integration. As a discrete sum of the three-dimensional grid cells, sea_water_mass is given by

$$\mathcal{M} = \sum_{i,j,k} \rho\, dx\, dy\, dz \qquad \text{non-Boussinesq,} \tag{3.8}$$

with ρ the *in situ* density, $dx\,dy$ the horizontal area of a grid cell, and dz the vertical thickness. For a hydrostatic fluid (equation (3.5)), the total seawater mass in a non-Boussinesq model is given by

$$\mathcal{M} = -g^{-1} \sum_{i,j,k} dx\, dy\, dp \qquad \text{non-Boussinesq and hydrostatic.} \tag{3.9}$$

For a Boussinesq model, the density factor in equation (3.8) becomes a constant, ρ_o, so that the net mass is given by

$$\mathcal{M} = \sum_{i,j,k} \rho_o\, dx\, dy\, dz \qquad \text{Boussinesq,} \tag{3.10}$$

in which case the mass is equal to ρ_o times the total volume of liquid in the ocean (Section 3.2.6).

Theoretical considerations

In a non-Boussinesq ocean, the total mass of liquid seawater evolves according to the budget

$$\frac{d\mathcal{M}}{dt} = \sum_{i,j} Q^{m}\, dx\, dy, \tag{3.11}$$

where Q^{m} (kg m^{-2} s^{-1}) is the net mass flux that crosses the liquid ocean boundaries, per horizontal cross-sectional area, due to evaporation, precipitation, runoff, and material tracers such as salt.[9] Maintenance of this mass budget is a fundamental feature of a conservative non-Boussinesq ocean model.

3.2.5 Volume per area or thickness of grid cell

We request archiving of the cell thickness

$$\text{cell\_thickness} = thkcello = dz \tag{3.12}$$

in order to measure the distance (in metres) between surfaces of constant vertical coordinate. This information is useful, in particular, for measuring changes in thickness between pressure surfaces in a non-Boussinesq pressure-based model exposed to increasing anthropogenic radiation. We note that temporal dependence of the mass per area and the cell thickness is a function of the vertical coordinate used in the ocean model, and how the sea surface is treated.

3.2.6 Total volume of liquid seawater

- sea_water_volume = volo

As a discrete sum of the three-dimensional grid cells, sea_water_total_volume is given by

$$\mathcal{V} = \sum_{i,j,k} dx\, dy\, dz. \tag{3.13}$$

If there are no net boundary fluxes of volume, then a conservative Boussinesq model will retain a constant total volume to within computational roundoff. In contrast, a non-Boussinesq model will generally alter its volume in cases where the ocean density changes (i.e., via *steric effects*).

Theoretical considerations

In a Boussinesq fluid, the total volume of liquid seawater, $\mathcal{V}^{\text{Bouss}} = \sum_{i,j,k} dx\, dy\, dz$, evolves according to the budget

$$\frac{d\mathcal{V}^{\text{Bouss}}}{dt} = \rho_o^{-1} \sum_{i,j} Q^m \, dx\, dy. \tag{3.14}$$

Maintenance of this volume budget is a fundamental feature of a conservative Boussinesq ocean model.

3.2.7 Dynamic sea level

- sea_surface_height_above_geoid = zos

This diagnostic field has a zero global area mean, so that it measures sea level fluctuations around the present ocean geoid defined via a resting ocean state at $z = 0$. That is, sea_surface_height_above_geoid is the *dynamic sea level* as defined in Griffies and Greatbatch (2012); Griffies et al. (2014). The dynamic sea level has fluctuations due to ocean dynamics. This diagnostic is not meant for mapping the global mean sea level changes due to thermal expansion or changes in ocean mass. Rather, global mean changes due to thermosteric effects are archived in global_average_thermosteric_sea_level_change (Section 3.2.9).

We identify here various technical points regarding this diagnostic.

- NON-BOUSSINESQ VERSUS BOUSSINESQ:

  Non-Boussinesq models incorporate global steric effects contributing to sea level changes, such as those related to thermal expansion. In contrast, the prognostic sea surface height in Boussinesq models does not incorporate global steric effects (Greatbatch, 1994). When removing the global mean, sea level patterns from Boussinesq and non-Boussinesq models are directly comparable (Losch et al., 2004; Griffies and Greatbatch, 2012).

- ALGORITHM FOR COMPUTING SEA SURFACE HEIGHT

  It should be noted in the "comment" attribute whether sea_surface_height_above_geoid is obtained directly, as in a free-surface model, or has been derived, for example, from geostrophy using diagnosed velocities at some level or from geostrophy relative to an assumed level of quiescence, or some other technique. Various possible methods of estimating sea-level in rigid-lid models are described in the Appendix of Gregory et al. (2001). These methods are largely obsolete, since CMIP ocean models generally do not make the rigid lid approximation.

- INVERSE BAROMETER FROM SEA ICE LOADING

  In some coupled climate models, sea ice at a grid cell depresses the liquid seawater through its mass loading (appearing as an applied surface pressure on the ocean model). This depression occurs independent of the subgrid scale distribution of sea ice, as it is a result of the mass of sea ice in a grid cell acting on the liquid ocean. There is, however, no dynamical effect associated with these depressions in the liquid ocean sea level, so there are are no associated ocean currents. See Appendix C in Griffies and Greatbatch (2012) for a discussion of this inverse barometer effect of sea ice.

  – For CMIP, we do *not* wish to record inverse barometer responses from sea ice loading in sea_surface_height_above_geoid. Rather, sea_surface_height_above_geoid should report the effective sea level as if sea ice (and snow) at a grid cell were converted to liquid seawater, as this is the dynamically relevant sea level (Campin et al., 2008), and as if the atmosphere had zero pressure loading on the ocean.

  – A straightforward means to measure this *effective* dynamic sea level is to first remove the inverse barometer response to applied pressure loading on the ocean from sea ice (e.g., see equation (206) of Griffies and Greatbatch (2012))

  $$\eta_{\text{effective}} = \eta_{\text{model}} + \frac{p_{\text{ice loading}}}{g\, \rho_{\text{surf}}}. \tag{3.15}$$

  In this equation, η_{model} is the sea level computed by the ocean model, $p_{\text{ice loading}}/g$ is the mass per unit area of the applied surface loading on the ocean, and ρ_{surf} is the surface ocean density. For CMIP purposes, the surface ocean density can be approximated by a constant. Normalizing to zero then gives the effective dynamic sea level for CMIP

  $$\eta_{\text{cmip}} = \eta_{\text{effective}} - \left(\frac{\sum_{i,j} \eta_{\text{effective}}\, dx\, dy}{\sum_{i,j} dx\, dy} \right). \tag{3.16}$$

  It is the effective dynamic sea level, η_{cmip}, that should be reported in sea_surface_height_above_geoid.

- INVERSE BAROMETER FROM ATMOSPHERIC LOADING

  The inverse barometer from atmospheric loading has, for many applications on long time scales, minimal dynamical impact (Wunsch and Stammer, 1997). Indeed, most, if not all, ocean components of CMIP models ignore the atmospheric loading on the ocean (see (Arbic, 2005) for an exception).

  – For those models that do apply atmospheric loading, we request that such loading be part of the dynamic sea level archived in CMIP, so long as the global area integral of the dynamic sea level remains zero. That is, in contrast to the recommendation for sea ice, we should not remove the inverse barometer from atmospheric loading.

  - If the ocean model feels the effects from the applied atmospheric forcing, then include this fact in the "comments" section for the field sea_surface_height_above_geoid.
  - sea_surface_height_above_geoid should have zero global area mean even if the ocean model feels the weight of the atmosphere.

3.2.8 Squared dynamic sea level

- square_of_sea_surface_height_above_geoid = zossq

The field square_of_sea_surface_height_above_geoid is the square of the dynamic sea level and accumulated each model time step. It is requested to help measure the variability simulated in the dynamic sea level, by computing the variance

$$\langle (\eta_{\text{cmip}} - \langle \eta_{\text{cmip}} \rangle)^2 \rangle = \langle \eta^2_{\text{cmip}} \rangle - \langle \eta_{\text{cmip}} \rangle^2, \tag{3.17}$$

with η_{cmip} the field sea_surface_height_above_geoid, and the angle brackets represent monthly time means.

3.2.9 Global thermosteric sea level changes

- global_average_thermosteric_sea_level_change = zostoga

The potential for increased sea level due to global warming presents some of the most pressing issues for adaptation to a warmer world (Church et al., 2011, 2013; Gregory et al., 2013). Sea level changes also provide a baseline assessment of the changing ocean climate in the simulations (Yin et al., 2010a; Yin, 2012; Kuhlbrodt and Gregory, 2012). It is thus of primary importance to consider the effects from sea level rise as simulated in the CMIP models. Results from model simulations should be carefully documented in order to properly interpret the CMIP archive.

There are two main reasons for sea level to increase. First, there is thermal expansion due to the warming ocean (thermosteric changes). Second, there are changes in the mass of sea water in the ocean (barystatic changes), affecting an increase in ocean volume.

- The mass effect arises most importantly from increasing melt of land glaciers and ice sheets. These changes will be registered by changes in the bottom pressure (sea_water_pressure_at_sea_floor in Section 3.2.1) and ocean mass (sea_water_mass in Section 3.2.4). However, these estimates are not mature with most CMIP models, as the models generally do not include reliable interactive and evolving land glacier and ice sheet models. Estimates for mass effects generally come from specialized models focusing on these processes, using CMIP scenarios as input. Hence, any changes to global sea level due to change in mass of the ocean (barystatic sea level change) are not trustworthy within the CMIP context.
- The global halosteric effect is only a fraction of the volume change which results from adding freshwater to the ocean, and therefore this quantity is misleading (Munk, 2003; Lowe and Gregory, 2006).
- Thermal expansion of seawater accounts for roughly one-third to one-half of the observed global mean sea level rise in the 20th and early 21st centuries (Church et al., 2011, 2013; Gregory et al., 2013). There is notably no significant rise from changes in salinity, given that the global halosteric effect is very tiny in comparison (see Griffies and Greatbatch (2012) for discussion). Furthermore, net changes from the global halosteric effect in a CMIP simulation are associated with inaccurate estimates of ocean mass changes in these models. We therefore consider the present suite of CMIP models as relevant for estimating the global thermosteric sea level rise.
- For the above reasons, CMIP6 does *not* ask for the following CMIP5 diagnostics:
  - global_average_sea_level_change = zosga
  - global_average_steric_sea_level_change = zossga

  Rather, only the field global_average_thermosteric_sea_level_change = zostga is requested for CMIP6.

Theoretical considerations

To understand the basics of how the global mean sea level changes, we summarize some salient points from Section 4.5 of Griffies and Greatbatch (2012). Here, we consider the relation between the total mass of liquid seawater, total volume of seawater, and global mean seawater density,

$$\mathcal{M} = \mathcal{V} \overline{\rho}, \tag{3.18}$$

where $\mathcal{M}$ is the total liquid ocean mass (equation (3.8)), $\mathcal{V}$ is the total ocean volume (equation (3.13)), and $\overline{\rho}$ is the global mean *in situ* density

$$\overline{\rho} = \frac{\sum \rho \, dx \, dy \, dz}{\sum dx \, dy \, dz} = \frac{\mathcal{M}}{\mathcal{V}}. \tag{3.19}$$

Temporal changes in total ocean mass are affected by a nonzero net mass flux through the ocean boundaries (equation (3.11))

$$\frac{d\mathcal{M}}{dt} = \mathcal{A} \overline{Q^m} \tag{3.20}$$

where $\overline{Q^m} = \mathcal{A}^{-1} \int dx\, dy\, Q^m$ is the global mean mass per horizontal area per time of water crossing the ocean boundaries, with $\mathcal{A} = \int dx\, dy$ the area of the global ocean surface. For an ocean with a constant horizontal area (i.e., no wetting and drying, as is the case for typical CMIP models), then temporal changes in the ocean volume are associated with sea level changes via

$$\frac{d\mathcal{V}}{dt} = \mathcal{A} \frac{d\overline{\eta}}{dt}, \tag{3.21}$$

where

$$\overline{\eta} = \mathcal{A}^{-1} \int \eta\, dx\, dy \tag{3.22}$$

is the global mean sea level.[10] Bringing these results together leads to the evolution equation for the global mean sea level

$$\frac{d\overline{\eta}}{dt} = \frac{\overline{Q^m}}{\overline{\rho}} - \left(\frac{\mathcal{V}}{\mathcal{A}\overline{\rho}}\right) \frac{d\overline{\rho}}{dt}. \tag{3.23}$$

The first term in equation (3.23) alters sea level by adding or subtracting mass from the ocean. The second term arises from temporal changes in the global mean density; i.e., from *steric* effects.

We can approximate each of the terms in equation (3.23) over a finite time Δt via

$$\Delta\overline{\eta} \approx \frac{\overline{Q^m}\, \Delta t}{\overline{\rho}} - \left(\frac{\mathcal{V}}{\mathcal{A}}\right) \frac{\Delta\overline{\rho}}{\overline{\rho}}, \tag{3.24}$$

where the Δ operator is a finite difference over the time step of interest. The global steric term is defined by

$$\mathcal{S} \equiv -\left(\frac{\mathcal{V}}{\mathcal{A}}\right) \frac{\Delta\overline{\rho}}{\overline{\rho}}. \tag{3.25}$$

It is straightforward to diagnose from a model simulation, given temporal changes in the global mean density.

For CMIP, we are interested in the change in sea level in a global warming scenario experiment, with respect to a reference state defined by the initial conditions of the experiment. In this case, the steric term at a time n is given by

$$\begin{aligned} \mathcal{S} &= -\left(\frac{\mathcal{V}^0}{\mathcal{A}}\right) \frac{\overline{\rho^n} - \overline{\rho^0}}{\overline{\rho^0}} \\ &= \left(\frac{\mathcal{V}^0}{\mathcal{A}}\right) \left(1 - \frac{\overline{\rho}^n}{\overline{\rho^0}}\right), \end{aligned} \tag{3.26}$$

where $\rho^0 = \rho(\theta^0, S^0, p^0)$ is the *in situ* density for a grid cell as determined by the grid cell's reference temperature, salinity, and pressure, $\rho^n = \rho(\theta^n, S^n, p^n)$ is the *in situ* density at time step n, and $\mathcal{V}^0$ is the reference volume of seawater.

As stated earlier, we are most interested in the global steric changes from CMIP models associated with changes in ocean temperature. These thermosteric effects are recorded in global_average_thermosteric_sea_level_change, which represents that part of the global mean sea level change due to changes in ocean density arising just from changes in temperature. We can estimate this thermosteric effect via

$$\mathcal{S}^{\text{thermo}} = \left(\frac{\mathcal{V}^0}{\mathcal{A}}\right) \left(1 - \frac{\overline{\rho(\theta^n, S^0, p^0)}}{\overline{\rho^0}}\right). \tag{3.27}$$

That is, the density in the numerator is computed as a function of the local temperature, with salinity and pressure held constant at their reference value.

We note, importantly, that there is *no* appearance of sea ice in the expression (3.27) for thermosteric sea level rise. Sea ice changes impact on the steric sea level only by their impacts on the halosteric effect. As discussed, we are not concerned with global halosteric changes due to the nontrivial uncertainties in land ice melt, with such processes generally not considered in CMIP simulations.

3.2.10 Potential temperature in liquid seawater

- sea_water_potential_temperature = thetao

WGCM (2007) recommends the three dimensional monthly mean potential temperature be archived, where the reference pressure is at the ocean surface. This field is the most common prognostic tracer in ocean models used to measure heat, and so should be included in the archive. However, we note that the recommendations from IOC et al. (2010) promote the alternative prognostic field called *conservative temperature*, which is the potential enthalpy divided by a reference heat capacity. Conservative Temperature is indeed more conservative than potential temperature, and so provides a more solid foundation for prognosing heat movement in the ocean. However, as discussed in Section 1.7.2, for comparison to other models and to observational data, as well as to previous CMIPs, we recommend that ocean components in CMIP6 archive potential temperature, regardless whether the models consider this field as prognostic (most common situation) or diagnostic (as when Conservative Temperature is prognostic).

3.2.11 Global mean temperature

- sea_water_potential_temperature = thetaoga
- sea_water_conservative_temperature = bigthetaoga

In addition to the three-dimensional field of potential temperature, we ask for CMIP6 models to archive the global mean potential temperature. For models enacting TEOS-10 (see Section 1.7), they should *also* archive the global mean of Conservative Temperature. These global mean time series provide a measure of the model drift and reflect on the net heating at the ocean boundaries (see below).

For potential temperature, its global mean has the same standard name as the three-dimensional potential temperature, but is distinguished by the cell methods attribute (area and depth mean). For Conservative Temperature, the global mean is the only form of Conservative Temperature requested for CMIP6, again requested just for those models enacting TEOS-10.

The calculation of global mean prognostic temperature differs depending on the use of Boussinesq or non-Boussinesq ocean equations. In a non-Boussinesq model, the mean is given by the mass weighted mean

$$\overline{T}_{\text{non-Bouss}} = \frac{\sum_{i,j,k} \rho\, T\, \mathrm{d}x\, \mathrm{d}y\, \mathrm{d}z}{\sum_{i,j,k} \rho\, \mathrm{d}x\, \mathrm{d}y\, \mathrm{d}z}, \tag{3.28}$$

where T is the model's potential temperature, θ, or Conservative Temperture, Θ. In a Boussinesq model, the mean is computed as the volume weighted mean

$$\overline{T}_{\text{Bouss}} = \frac{\sum_{i,j,k} T\, \mathrm{d}x\, \mathrm{d}y\, \mathrm{d}z}{\sum_{i,j,k} \mathrm{d}x\, \mathrm{d}y\, \mathrm{d}z}. \tag{3.29}$$

The distinction between non-Boussinesq and Boussinesq models arises from the differences in the underlying conserved fields in the two model formulations. For both cases, it is necessary to accumulate each model time step when producing the time mean, since the mean is built from the product of time dependent terms (e.g., density and grid cell thicknesses are generally time dependent).

The global mean prognostic temperature presents the analyst with a very convenient measure of drift in the model, and a measure of the model's deviation from estimates of the observed global mean temperature. Furthermore, when combined with the boundary fluxes and total mass/volume, one can diagnose the degree to which the ocean model conserves heat.

Concerning the conservation of heat in ocean models

According to the results of Griffies et al. (2009b) and Griffies et al. (2014), one should *not* assume that all ocean models in CMIP6 are written with numerical methods that ensure the conservation of scalar fields such as mass, heat, and salt. One means to check for heat conservation is to compute the change in total heat over a specified time (say over a year), and compare that change to the total boundary heat input to the ocean system. The change in heat should agree to the heat input through the boundaries, with agreement to within numerical roundoff expected from a conservative model.

If there is a difference greater than numerical roundoff, then how significant is the difference? To answer this question, consider an order of magnitude calculation to determine the temperature trend that one may expect, given a nonzero net heat flux through the ocean boundaries. For simplicity, assume a Boussinesq fluid with constant volume (i.e., no net volume fluxes), and assume the model prognostic field is potential temperature. The global mean liquid ocean potential temperature evolves according to

$$(\mathcal{V}\, \rho_o\, C_p^o)\, \frac{\mathrm{d}\overline{\theta}}{\mathrm{d}t} = \mathcal{A}\, \overline{Q^{\mathrm{H}}} \tag{3.30}$$

where $\mathcal{V}$ is the liquid ocean volume, $\mathcal{A} = \sum \mathrm{d}x\, \mathrm{d}y$ is the surface area of the ocean, C_p^o is the model's constant heat capacity (see Section 1.7.2), ρ_o is the Boussinesq reference density, and $\overline{Q^{\mathrm{H}}} = \mathcal{A}^{-1} \sum Q^{\mathrm{H}}\, \mathrm{d}x\, \mathrm{d}y$ is the global average boundary heat flux. Typical values for the World Ocean yield $\mathcal{V}\, \rho_o\, C_p^o \approx 5.4 \times 10^{24}\, \mathrm{J/^\circ C}$ and $\mathcal{A} = 3.6 \times 10^{14}\, \mathrm{m}^2$, leading to the decadal scale potential temperature trend

$$\frac{\Delta\overline{\theta}}{\text{decade}} \approx 0.02\, \overline{Q^{\mathrm{H}}}. \tag{3.31}$$

For example, with a $1\, \mathrm{W\, m^{-2}}$ ocean area average heating of the ocean over the course of a decade (according to Otto et al. (2013), the net signal from global warming is on the order of $1\, \mathrm{W\, m^{-2}}$), we expect a global mean temperature trend of roughly $0.02^\circ C$ per decade, or $0.2^\circ C$ per century. If there is an error in the balance (3.30), we may define a global mean heat flux

$$Q^{\text{error}} \equiv \overline{Q^{\mathrm{H}}} - \left(\frac{\mathcal{V}\, \rho_o\, C_p}{\mathcal{A}} \right) \frac{\mathrm{d}\overline{\theta}}{\mathrm{d}t}. \tag{3.32}$$

To translate the error in the net heating into an error in the temperature trend, use relation (3.31) to define

$$\frac{\Delta\overline{\theta}^{\text{error}}}{\text{decade}} \approx 0.02\, Q^{\text{error}}. \tag{3.33}$$

3.2.12 Monthly mean SST of liquid water

- sea_surface_temperature = tos and tosga.

In the CMIP archive, it is quite valuable to have the full three-dimensional fields, such as potential temperature and salinity. However, for many purposes, just the top model fields are sufficient. The sea surface temperature (SST) and sea surface salinity (SSS) (Section 3.2.18) are

two such fields we recommend, as well as the daily mixing layer depth (Section 3.2.24). For this purpose, we request the monthly mean SST. In addition, to further reduce the size of the diagnostic, we request the global area average of the SST, sampled as monthly means.

We make note that the surface tracer fields produced from a climate model generally do *not* correspond to skin properties. Rather, they are bulk properties averaged over the top grid cell, which is generally no less than a metre thick.

3.2.13 Daily mean SST of liquid water

- sea_surface_temperature = tos

We recommend that daily mean SST be saved for the purpose of computing space-time diagrams to diagnose propagating signals, such as Tropical Instability Waves. The daily mean SST is also of use for understanding the potential for enhanced coral bleaching in a warming world. Coral bleaching is one of the major potential environmental consequences resulting from global warming. Remotely sensed estimates of coral bleaching have converged on a measure based on degree-heating weeks (Strong et al., 2004). Quantifying this measure in models requires an archive of daily mean sea surface temperatures.

3.2.14 Daily and monthly mean squared SST of liquid water

The field

- square_of_sea_surface_temperature = tossq

is accumulated each model time step. It is requested to help measure the variability simulated in the sea surface temperature, so that one may compute the variance

$$\langle (\theta - \langle \theta \rangle)^2 \rangle = \langle \theta^2 \rangle - \langle \theta \rangle^2, \tag{3.34}$$

with θ a shorthand for the field sea_surface_temperature, and the angle brackets represent either daily or monthly time means.

3.2.15 Bottom potential temperature

- sea_water_potential_temperature_at_sea_floor = tob

For studies of impacts on ecosystem from climate change, it is important to measure changes in bottom temperature and salinity (Cheung et al., 2013; Gehlen and Dunne, 2014). As with the request to save SST and SSS, we request for CMIP6 the archiving of bottom temperature and bottom salinity in order to facilitate easier analysis using these fields.

3.2.16 Mass integrated prognostic temperature over an ocean column

- integral_wrt_depth_of_product_of_sea_water_density_and_potential_temperature
- integral_wrt_depth_of_product_of_sea_water_density_and_conservative_temperature

To facilitate an assessment of the heat content in an ocean column, for purposes of closing the ocean model heat budget, it is useful to save monthly mean mass weighted depth integrated prognostic temperature, so that this diagnostic is computed via

$$\text{tomit} = \sum_{k=1}^{k=kmax} T \, \rho \, dz, \tag{3.35}$$

where the *in situ* density factor, ρ, is set to the reference density, $\rho = \rho_o$, for Boussinesq fluids. For models that use Conservative Temperature as their prognostic temperature field (see Section 1.7), the diagnostic

- integral_wrt_depth_of_product_of_sea_water_density_and_conservative_temperature

is computed using Conservative Temperature, Θ. This diagnostic is not saved when using potential temperature, θ, as the prognostic field. Rather, we request the diagnostic

- integral_wrt_depth_of_product_of_sea_water_density_and_potential_temperature

be saved in that case (see Section 1.7.2).

3.2.17 Salinity of liquid water

- sea_water_salinity = so
- global mean salinity = soga

We recommend archiving the three dimensional monthly mean ocean salinity field.[11] In addition, as for potential temperature, we recommend saving the global mean salinity of liquid seawater. This mean is computed in a non-Boussinesq model by the mass weighted mean

$$\overline{S}_{\text{non-Bouss}} = \frac{\sum_{i,j,k} \rho \, S \, dx \, dy \, dz}{\sum_{i,j,k} \rho \, dx \, dy \, dz}, \tag{3.36}$$

whereas for a Boussinesq model it is the volume weighted mean

$$\overline{S}_{\text{Bouss}} = \frac{\sum_{i,j,k} S \, dx \, dy \, dz}{\sum_{i,j,k} dx \, dy \, dz}. \tag{3.37}$$

In either case, the global mean salinity presents the analyst with a very useful measure of the drift in the model, a measure of the model's deviation from the estimates of the observed global mean salinity, and a means for checking for conservation of total salt. As for the global mean temperature, it is generally necessary to compute each of the terms in the average on each time step, since the average is generally built from the product of time dependent terms.

3.2.18 Sea surface salinity

- sea_surface_salinity = sos and sosga

The sea surface salinity (SSS) provides a useful means for detecting changes in the high latitude thermohaline forcing, which can present the analyst with a quick diagnosis of whether a simulation is more or less prone to modification of the overturning circulation. For example, fresh water capping can be seen by diagnosis of the SSS. In this case, signals in SSS may motivate more detailed analysis of the three-dimensional fields. Absent the SSS field in the archive, the analyst is burdened with unpacking the full three-dimensional fields to make even the most rudimentary analysis. Given the far more convenient nature of the smaller two-dimensional SSS relative to the full three-dimensional salinity, we recommend that monthly mean SSS field be archived for CMIP6. In addition, to further reduce the size of the diagnostic, we request the global area average of the SSS, sampled as monthly means.

3.2.19 Bottom salinity

- sea_water_salinity_at_sea_floor = sob

For studies of impacts on ecosystem from climate change, it is important to measure changes in bottom temperature and salinity (Cheung et al., 2013; Gehlen and Dunne, 2014). As with the request to save SST and SSS, we request for CMIP6 the archiving of bottom temperature and bottom salinity in order to facilitate easier analysis using these fields.

3.2.20 Mass integrated salinity over an ocean column

- integral_wrt_depth_of_product_of_sea_water_density_and_salinity = somint

To facilitate a quick assessment of the salt content in an ocean column, for purposes of closing the ocean model salt budget, it is useful to save monthly mean mass weighted depth integrated salinity, so that this diagnostic is computed via

$$\text{somit} = \sum_{k=1}^{k=kmax} S\,\rho\,dz, \tag{3.38}$$

where the *in situ* density factor, ρ, is set to the reference density, $\rho = \rho_o$, for Boussinesq fluids.

3.2.21 Squared ocean buoyancy frequency

- square_of_brunt_vaisala_frequency_in_sea_water = obvfsq

Potential density referenced to the ocean surface (σ_0) is a useful auxiliary field for garnering a measure of the stability of the upper ocean. WGCM (2007) recommended that the monthly mean potential density be archived for CMIP3, as did Griffies et al. (2009a) for CMIP5. However, the buoyancy frequency is in fact a more general field measuring vertical stability. Additionally, it is commonly used as part of various ocean parameterizations, such as gravity wave mixing (Simmons et al., 2004; Melet et al., 2013), and mesoscale eddy closures (Gent et al., 1995; Griffies et al., 1998). We therefore recommend that for CMIP6, models archive the squared buoyancy frequency rather than the potential density. This is a field of very high utility for many purposes, thus prompting its level=0 priority.

3.2.22 Ideal age tracer

- sea_water_age_since_surface_contact = agessc

A number of groups participating in CMIP3 included ideal age tracer (Bryan et al., 2006; Gnanadesikan et al., 2007). This tracer (Thiele and Sarmiento, 1990; England, 1995) is set to zero in the model surface level/layer at each time step, and ages at 1 yr/yr below. Ideal age is particularly useful for revealing surface-to-deep connections in regions such as the Southern Ocean where these connections have spatiotemporal variability. It can also be used to estimate uptake of anthropogenic tracers such as carbon dioxide (Russell et al., 2006).

Ideal age satisfies the following advection-diffusion-source equation

$$\frac{\partial A}{\partial t} + \nabla \cdot (\mathbf{v}\, A) = -\nabla \cdot \mathbf{F} + 1 + \gamma\,(A^* - A)\,\delta_{\text{surf}}. \tag{3.39}$$

In this equation, A is the ideal age with dimensions of time; $\mathbf{F}$ is the SGS flux; a unit source adds time to the age tracer over each time step; and a damping is applied in a surface region back to $A^* = 0$. The surface damping is often applied just to the top grid cell. Alternatively, it can be applied over a region of specified thickness. If the damping time γ^{-1} is zero (infinitely strong damping), then $A = A^*$ is specified for the surface region. Some groups take $\gamma^{-1} = 0$ whereas others use a finite value. So long as the restoring strength is sufficiently strong, there should be only minor distinctions between the two approaches.

To facilitate direct comparison of ideal age in the different model simulations, we recommend initializing age globally to zero at 01Jan1901 in the various scenario experiments. Measuring age in years, rather than seconds, is the traditional approach in ocean modeling, and is the recommended units for ideal age in CMIP6.

3.2.23 CFC-11 and CFC12

- moles_per_unit_mass_of_cfc11_in_sea_water = cfc11
- moles_per_unit_mass_of_cfc12_in_sea_water = cfc12

Chlorofluorocarbons (CFCs) have been increasingly utilized in evaluating ocean climate models, largely due to a good observational data base (the World Ocean Circulation Experiment, WOCE, upon which Global Ocean Data Analysis Project, GLODAP, Key et al. (2004) is largely based) and their well-known atmospheric concentrations. These tracers are particularly useful in assessing model mixing processes, ventilation rates, deep water formation, and circulation characteristics.

In models simulating CFCs, we recommend that surface CFC fluxes be calculated from 01Jan 1936 until the end of the CMIP6 historical simulation, and over the first years of the rcp45 simulation (until 2014) following updated protocols from the Ocean Carbon Model Intercomparison Project (OCMIP-2) (Dutay et al., 2002). Some earth system models include a prognostic calculation of CFC-11. However, for proper ocean model evaluation, models should use the observed transient atmospheric CFC-11 (mole fraction) as a boundary condition.

The units of CFC-11 and CFC-12 should be reported as the moles of CFC per kilogram of seawater. If the model units are instead moles per cubed metre, then conversion should be made using the Boussinesq reference density, ρ_o (Section 3.1.3) for Boussinesq models, or *in situ* density ρ for non-Boussinesq models.

3.2.24 Mixed layer depth

- ocean_mixed_layer_thickness_defined_by_sigma_t = mlotst

An assessment of model mixed layer depth (MLD) is useful for understanding how water-mass formation in the simulations is regulated by upper ocean stratification and surface water overturn. Unfortunately, there is no universally agreed upon criterion for defining the mixed layer depth. For the purpose of fostering a consistent comparison of simulated mixed layers from ocean model components in CMIP6, we recommend that the "sigma-t" criterion introduced by Levitus (1982) be followed. To furthermore support the direct comparison of simulated MLDs from those presented in observational analyses, we recommend that the simulated MLDs be diagnosed from the monthly mean temperature and salinity, rather than accumulated over each model time step.

Theoretical and practical considerations

The mixed layer depth is based on measuring ocean gravitational stability under a vertical displacement. To determine whether vertical transfer is favored requires a thought experiment, in which a surface ocean fluid parcel is displaced downward without changing its temperature or salinity, but feeling the local *in situ* pressure. If the density of the displaced parcel is sufficiently far from the local *in situ* density, then the displacement is not favored, and we are thus beneath the mixed layer and into the stratified interior. What determines "sufficiently far" is subjective, with convention determining the precise value.

The mixed layer has near-zero gradients of Θ and S, and density, as well as tracers such as CFCs. So most techniques to estimate the MLD rely on either a threshold gradient or a threshold change in one of these quantities, normally in potential temperature θ or density (see, for example Lorbacher et al., 2006; de Boyer Montégut et al., 2004; Monterey and Levitus, 1997). Relying solely on θ has the advantage of good observational data coverage, but this approach neglects salinity stratification associated with barrier layers (see e.g., Sprintall and Tomczak, 1992). In contrast, relying solely on density overlooks density-compensating changes in $\theta - S$, exaggerating the mixed layer depth.

The method we recommend for purposes of ocean model comparisons is that from Levitus (1982). Here, the MLD is defined based on meeting a "sigma-t" criterion. This method has the advantage that it is readily employed in off-line mode, thus supporting the use of monthly mean model fields, analogous to Levitus (1982). We here provide some details for this method.

Mathematically, we compute the difference between the following two densities

$$\rho_{\text{displaced from surface}} = \rho[S(k=1), \Theta(k=1), p(k)] \tag{3.40a}$$

$$\rho_{\text{local}} = \rho[S(k), \Theta(k), p(k)], \tag{3.40b}$$

and convert that density difference to a buoyancy difference

$$\delta B = -\left(\frac{g\,(\rho_{\text{displaced from surface}} - \rho_{\text{local}})}{\rho_{\text{local}}} \right). \tag{3.41}$$

This buoyancy difference is computed from the surface down to the first depth at which $\delta B > \Delta B_{\text{crit}}$, where the CMIP recommended value is

$$\Delta B_{\text{crit}} = 0.0003 \text{ m s}^{-2}, \tag{3.42}$$

with this value also used in Conkright et al. (2002). Other values may be more suitable for regional studies, such as for the Southern Ocean. The mixed layer depth, $H^{(\text{mld})}(x, y, t)$ is then approximated by interpolating between the depth where $\delta B > \Delta B_{\text{crit}}$ and the shallower depth. Note that with $g = 9.8$ m s^{-2} and $\rho_{\text{local}} \approx 1035$ kg m^{-3}, then $\Delta B_{\text{crit}} = 0.0003$ m s^{-2} corresponds to a critical density difference of

$$\Delta \rho_{\text{crit}} = 0.03 \text{ kg m}^{-3}, \tag{3.43}$$

as used by de Boyer Montégut et al. (2004) in their study of ocean mixed layers. We note, however, that some studies employ the larger $\Delta\rho_{\text{crit}} = 0.125$ kg m^{-3}, which will result in a deeper mixed layer depth due to the need to penetrate deeper into the stratified water.

3.2.25 Squared mixed layer depth

- square_of_ocean_mixed_layer_thickness_defined_by_sigma_t = mlotstsq

This field is accumulated each model time step. An assessment of model mixed layer depth (MLD) is useful for understanding how water-mass formation in the simulations is regulated by upper ocean stratification and surface water overturn. In addition, with the squared MLD one may deduce a measure for the variability of the simulated MLD. The squared mixed layer requested here is the square of ocean_mixed_layer_thickness_defined_by_sigma_t defined above.

3.2.26 Barotropic or quasi-barotropic streamfunction

- ocean_barotropic_mass_streamfunction = msftbarot

The barotropic streamfunction is a useful field for mapping the vertically integrated fluid transport. However, many ocean models have jettisoned the rigid lid assumption of Bryan (1969) for both computational and physical reasons. Absent a rigid lid assumption, the vertically integrated mass transport[12] $\mathbf{U}^\rho = \int_{-H}^{\eta} \rho\,\mathbf{u}\,dz$ generally has a non-zero divergence, thus precluding it from being fully specified by a single scalar field. Instead, both a streamfunction and velocity potential are needed to specify the transport. For those models that do not compute a barotropic streamfunction, we introduce the notion of a *quasi-barotropic streamfunction* ψ^U in the following theoretical considerations, with this field serving as a useful approximate alternative to the barotropic streamfunction.

In summary, we recommend either of the following scalar fields be archived for purposes of mapping the vertically integrated mass transport:

- Barotropic streamfunction for those models that compute this function using an elliptic solver.
- The quasi-barotropic streamfunction ψ^U for cases when the model does not distinguish the streamfunction from the velocity potential.

Consistent with our discussion in Section 3.3.2, we recommend that the dimensions of the streamfunction be mass transport (kg/s), rather than volume transport (m^3/s).

Theoretical considerations

For a mass conserving non-Boussinesq fluid, the vertically integrated mass transport

$$\mathbf{U}^\rho = \int_{-H}^{\eta} \mathbf{u}\,\rho\,dz \tag{3.44}$$

has a divergence given by

$$\nabla\cdot\mathbf{U}^\rho = -\frac{\partial(D\,\overline{\rho})}{\partial t} + Q^{\text{m}}, \tag{3.45}$$

where

$$D = H + \eta \tag{3.46}$$

is the thickness of a fluid column. Similarly, for a Boussinesq fluid the depth integrated velocity

$$\mathbf{U} = \int_{-H}^{\eta} \mathbf{u}\,dz \tag{3.47}$$

has a divergence

$$\nabla\cdot\mathbf{U} = -\frac{\partial\eta}{\partial t} + Q^{\text{m}}/\rho_o. \tag{3.48}$$

Given that neither $\mathbf{U}^\rho$ nor $\mathbf{U}$ are non-divergent, a barotropic streamfunction is insufficient to fully describe the vertically integrated flow. In general, it is necessary to solve an elliptic boundary value problem to diagnose the barotropic streamfunction. However, for CMIP purposes, it is sufficient to compute an approximate streamfunction, with details now given.

Consider the function

$$\psi^U(x,y) = -\int_{y_o}^{y} U^\rho(x,y')\,dy', \tag{3.49}$$

where the southern limit y_o is at Antarctica. Note that all intermediate ranges of latitude bands are included, so there are no shadow regions that may otherwise be isolated due to land/sea arrangements. By definition, the y derivative $\psi^U(x,y)$ yields the $\hat{\mathbf{x}}$-transport $\partial_y\psi^U = U^\rho$, yet the x derivative does not yield the $\hat{\mathbf{y}}$-transport due to the divergent nature of the vertically integrated flow. A complement function

$$\psi^V(x,y) = \psi^U(x_o,y) + \int_{x_o}^{x} V^\rho(x',y)\,dx', \tag{3.50}$$

yields $\partial_x\psi^V = V^\rho$. In the special case of a Boussinesq rigid lid model absent surface water fluxes, ψ^U and ψ^V reduce to the single rigid lid barotropic streamfunction. In the more general case, comparison of ψ^U and ψ^V in climate model simulations at GFDL reveal that after just a few years of spin-up, patterns for the monthly means of ψ^U and ψ^V are very similar. This

result provides evidence that much of the large-scale vertically integrated circulation is nearly non-divergent. In this case, either function ψ^U and ψ^V renders a useful map of the vertically integrated mass transport. Due to its simplicity, we recommend that the quasi-barotropic streamfunction ψ^U be archived for CMIP6.

3.3 Vectors or components to vectors

We now consider vector fields, or components to vector fields, suggested for the ocean model components to CMIP6. Refer to Table 2.3 for a summary of the fields.

3.3.1 Remapping

See Section 1.5.3 for a discussion of remapping vector fields, and Section 1.5.4 for remapping of transport components to estimate meridional transports.

3.3.2 Physical dimensions for fluid transport

An increasing number of ocean models have removed the Boussinesq approximation, and so are now mass conserving non-Boussinesq models. One benefit of non-Boussinesq models is that the sea level height is more accurate, since these models include steric effects within the prognostic equations (Greatbatch, 1994). We detail these points in Section 3.2.

A notable consequence of moving to a non-Boussinesq model involves the physical dimensions of transport fields. Namely, fluid transport is measured as a mass flux rather than a volume flux. For example, the mass transport

$$\mathcal{V}^{(\hat{\mathbf{n}})} = \rho \, \mathbf{v} \cdot \hat{\mathbf{n}} \, dA \tag{3.51}$$

is the mass per time passing through the $\hat{\mathbf{n}}$ face of a grid cell, with dA the area of the cell face. This transport is conveniently quantified using the mass Sverdrup

$$\text{mass Sv} = 10^9 \text{kg s}^{-1} \tag{3.52}$$

rather than the volume Sverdrup

$$\text{volume Sv} = 10^6 \text{m}^3 \text{ s}^{-1}. \tag{3.53}$$

For a Boussinesq model, the density factor ρ becomes a constant reference density ρ_o, which trivially allows for use of the mass Sverdrup as the unit of transport as well.

In summary, we recommend the following physical dimensions of transport fields:

- **Mass flux Units**: Fluid transport should be recorded as a mass transport (kg/s) rather than a volume transport (m^3/s).

3.3.3 Horizontal velocity field from resolved flow

- sea_water_x_velocity = uo
- sea_water_y_velocity = vo

These diagnostics are for the horizontal velocity components. They are diagnosed from the model's resolved velocity field that is time stepped as part of the model's prognostic equations. This diagnostic does *not* include extra transport that may arise from parameterized eddy-advection.

3.3.4 Horizontal mass transport from resolved plus parameterized flow

- ocean_mass_x_transport = umo
- ocean_mass_y_transport = vmo

This diagnostic asks for the total mass transport through the faces of a grid cell, where transport arises from the sum of the resolved flow plus any parameterized flow. That is, this diagnostic seeks the following mass transport

$$\mathcal{V}^{(\text{total-x})} = \rho \, u^{\dagger} \, dy \, dz \tag{3.54}$$

$$\mathcal{V}^{(\text{total-y})} = \rho \, v^{\dagger} \, dx \, dz, \tag{3.55}$$

where $\mathbf{u}^{\dagger}$ is the residual mean transport velocity (sum of Eulerian mean plus parameterized eddy-induced velocity). Note that for a Boussinesq model, the *in situ* density factor ρ is set to the constant reference density ρ_o.

3.3.5 Vertical mass transport from resolved plus parameterized flow

- upward_ocean_mass_transport = wmo = $\rho \, w^{\dagger} \, dx \, dy$.

This diagnostic is the vertical mass transport across the model's coordinate surface, diagnosed from the model's resolved velocity field plus any parameterized vertical advective transport (such as from parameterized mesoscale or submesoscale eddies). This transport (measured in kg/s) is more valuable for analysis than the vertical velocity component. Nonetheless, *if* there is reason to determine the vertical residual velocity, it can be trivially diagnosed from the net vertical mass transport in a Boussinesq model, and approximated in a non-Boussinesq model. Hence, rather than archiving the vertical velocity, or the vertical residual velocity, we recommend archiving the vertical mass transport of seawater.

3.3.6 Poleward and ŷ-ward overturning streamfunction from all transport processes

- ocean_meridional_overturning_mass_streamfunction = msftmyz and msftmrho
- ocean_y_overturning_mass_streamfunction = msftyyz and msftyrho

The transport of fluid northward in each of the basins Atlantic-Arctic, Indian-Pacific, and World Ocean, as a function of depth/pressure and density, is of interest for many purposes of ocean climate dynamics.[13] This transport is of particular interest for the study of tracers, such as heat and salt. Consequently, we are interested in transport arising from the model's resolved velocity field, as well as transport arising from all SGS processes such as Gent and McWilliams (1990); Gent et al. (1995) and the submesoscale mixed layer transport scheme from Fox-Kemper et al. (2008, 2011), amongst others. This diagnostic request is for the net transport from all processes, resolved and parameterized. It is of primary importance and interest for studies of ocean climate science.

The issue of generalized horizontal coordinates adds complexity to the diagnosis of the northward mass transport when using non-spherical grids. As stated in Section 1.5.4, instead of remapping mass fluxes to a spherical grid, and then computing the basin transports, we recommend computing the transports across native grid lines that approximate latitude circles, and reporting these as a function of latitude. Such algorithms can be implemented in a conservative manner for finite volume based models, even those with complex grids. Finite element models, in contrast, require extra care (Sidorenko et al., 2009).

For those models using a non-spherical coordinate horizontal grid, in addition to archiving the meridional overturning streamfunction, we recommend archiving the model's native grid $\hat{\mathbf{y}}$-ward overturning streamfunction, where $(\hat{\mathbf{x}}, \hat{\mathbf{y}})$ are directions defined according to the model's native grid. We also use the synonyms $(iward, jward)$, using the familiar (i, j) notation for horizontal grid indices. For many purposes and for many of the most commonly used non-spherical grids, the $\hat{\mathbf{y}}$-ward native grid streamfunction is sufficient. The following reasons can be given for those cases where the $\hat{\mathbf{y}}$-ward native grid streamfunction is sufficient:

- There are two commonly used generalized horizontal coordinates for ocean models in CMIP6. One includes the tripolar grid of Murray (1996) or Madec and Imbard (1996). As shown in Griffies et al. (2005), for the tripolar grid, all latitudes south of roughly $65^\circ N$ remain spherical. The second common grid is the displaced pole grid (see, for example, Smith and Gent, 2004), where the coordinate North Pole is moved over a land region in the northern hemisphere. In either case, northward transport, at least for regions south of the Arctic Circle, is readily approximated as the $\hat{\mathbf{y}}$-ward transport, as defined along the model's native grid lines. These streamfunctions are sensibly compared between models with varying grid choices, again since regions where the grid lines are most highly distorted from the sphere are precisely those regions where the flow is very weak and thus of less interest for scientific purposes.
- Transport in regions north of the Arctic Circle is very weak relative to transport in the south, and poorly sampled from observations. Hence, its diagnosis is often of secondary concern for comparison to observations.
- The overturning streamfunction is not a directly observed field. Instead, it is partially inferred through selected transport measurements at very few ocean sections. To constrain the recording of the simulated streamfunction to be oriented precisely along a line parallel to geographical longitude is not warranted for reasons of comparing to observations.

A general expression for the ocean mass transport overturning streamfunction is given by

$$\Psi(y, s, t) = -\int_{x_a}^{x_b} dx \int_{-H}^{z(s)} \rho\, v^\dagger\, dz, \tag{3.56}$$

where $v^\dagger$ is the native grid approximation to the resolved y-ward velocity plus parameterized eddy-induced advective transport (see ocean_mass_y_transport in Section 3.3.4). Note that the zonal integral is computed along surfaces of constant s, where s is either a geopotential/pressure surface, or a potential density surface. That is, we recommend that the following versions of the overturning streamfunction be archived at monthly time averages in the CMIP6 repository, with results for the Atlantic-Arctic, Indian-Pacific, and Global Oceans:

- **poleward-depth overturning streamfunction** and **ŷ-ward-depth overturning streamfunction**: The depth $z(s)$ corresponds to either the depth of a geopotential or the depth of a pressure surface, depending on whether the model is Boussinesq or non-Boussinesq, respectively.
- **poleward-density overturning streamfunction** and **ŷ-ward-density overturning streamfunction**: The depth $z(s)$ corresponds to the depth of a predefined set of σ_{2000} isopycnals, with the definition of these isopycnals at the modeler's discretion. This field presents complementary information relative to the $\hat{\mathbf{y}}$-ward-depth overturning streamfunction, and is very useful particularly for diagnosing water mass transformation processes.[14]
- Consistent with the discussion in Section 1.3, it is critical that the time average of the streamfunction be accumulated using each model time step, in order to avoid problems with aliasing and problems ignoring correlations.

3.3.7 Poleward and ŷ-ward overturning streamfunction from SGS transport

- ocean_meridional_overturning_mass_streamfunction_due_to_parameterized_mesoscale_advection

- ocean_y_overturning_mass_streamfunction_due_to_parameterized_mesoscale_advection
- ocean_meridional_overturning_mass_streamfunction_due_to_parameterized_submesoscale_advection
- ocean_y_overturning_mass_streamfunction_due_to_parameterized_submesoscale_advection

We follow the same philosophy as in Section 3.3.6 for diagnosing the poleward and $\hat{\mathbf{y}}$-ward overturning streamfunction arising just from SGS transport.

- The CMIP5 name for these fields is "bolus_advection". The new CMIP6 name is preferable since "bolus" advection is a specialized term that has limited applicability.
- The scheme most associated with mesoscale eddy parameterization is that from Gent et al. (1995). It is the mass transport from this, or alternative mesoscale closures, that should be archived in the fields "due_to_parameterized_mesoscale_advection".
- The scheme most associated with mixed layer submesoscale transport is the scheme from Fox-Kemper et al. (2008, 2011). It is the mass transport from this, or alternative submesoscale closures, that should be archived in the fields "due_to_parameterized_submesoscale_advection".
- Since the Fox-Kemper et al. (2008, 2011) scheme applies only in the mixed layer, only its poleward-depth and $\hat{\mathbf{y}}$-depth version is relevant.
- For the Gent et al. (1995) streamfunction, it is useful to map this in both depth and density space.
- For the Gent et al. (1995) volume transport streamfunction in a Boussinesq fluid (similar relations hold for non-Boussinesq), we have

$$\begin{aligned} \Psi^{\rm gm}(y,s,t) &= -\int_{x_a}^{x_b} \mathrm{d}x \int_{-H}^{z(s)} v^{\rm gm}\, \mathrm{d}z \\ &= \int_{x_a}^{x_b} \mathrm{d}x \int_{-H}^{z(s)} \partial_z(\kappa_{\rm gm}\, S^y)\, \mathrm{d}z \\ &= \int_{x_a}^{x_b} \kappa_{\rm gm}\, S^y(z(s))\, \mathrm{d}x, \end{aligned} \tag{3.57}$$

where $\kappa_{\rm gm} > 0$ is the eddy diffusivity, S^y is the $\hat{\mathbf{y}}$ neutral slope, and $\kappa_{\rm gm}$ vanishes at the ocean bottom. As for the streamfunction Ψ defined by equation (3.56), we recommend archiving $\Psi^{\rm gm}$ on both depth/pressure levels and isopycnal (σ_{2000}) levels.

3.3.8 Heat transport from resolved + parameterized processes

- northward_ocean_heat_transport = hfbasin
- ocean_heat_x_transport
- ocean_heat_y_transport

There are many processes in the ocean that affect heat and salt transport: resolved advective transport, diffusion, parameterized eddy-induced advection or skew diffusion, overflow parameterizations, etc. In the analysis of ocean model simulations, it is useful to have a measure of each component of the heat and salt transport, particularly in the horizontal. We follow CMIP5 in requesting the vertically integrated $\hat{\mathbf{x}}$-ward and $\hat{\mathbf{y}}$-ward heat transport from *all* processes, archived as monthly means for the Atlantic-Arctic, Indian-Pacific, and World Ocean, and maintained on the model's native grid.

In addition, following from the approach taken for the meridional overturning streamfunction, each ocean model using non-spherical coordinate horizontal grids should compute the northward heat transport in each of the basins (northward_ocean_heat_transport), approximated using the model's native grid fields without remapping. For models using a spherical latitude-longitude grid, there will be no difference. The approximated poleward transport in non-spherical grids will generally consist of transports crossing a "zig-zag" path (Section 1.5.4). The resulting poleward heat transport should be reported as a function of latitude, with latitudinal resolution comparable to the model's native grid resolution.

3.3.9 Parameterized mesocale and submesoscale heat transport

- northward_ocean_heat_transport_due_to_parameterized_mesoscale_advection = hfbasinpmadv
- northward_ocean_heat_transport_due_to_parameterized_submesoscale_advection = hfbasinpsmadv
- northward_ocean_heat_transport_due_to_parameterized_mesocale_diffusion = hfbasinpmdiff
- northward_ocean_heat_transport_due_to_parameterized_eddy_advection = hfbasinpadv

In support of understanding the importance of various SGS physical parameterizations, we recommend that heat transports should be archived as follows.

- Parameterized SGS advection from mesoscale closures (such as Gent and McWilliams (1990); Gent et al. (1995)) and submesocale closures (as in Fox-Kemper et al. (2008, 2011)). We include the contributions from these schemes in the fields with the suffix "advection", even if the implementation of the schemes appears as a skew diffusion.
- If the eddy-induced advection from the mesoscale and submesoscale closures are combined operationally in the model, and cannot be separately diagnosed, then their net effect can be archived in the fields with suffix "due_to_parameterized_eddy_advection".

- In addition to eddy-induced advection, mesocale eddies are commonly parameterized through neutral diffusion as in Solomon (1971) and Redi (1982). Contributions to heat transport from neutral diffusion should be placed in the fields with suffix "due_to_parameterized_mesoscale_diffusion".
- The vertically integrated northward transports can be approximated using the a "zig-zag" path method discussed in Section 1.5.4. The components should be archived as monthly means for the Atlantic-Arctic, Indian-Pacific, and World Ocean. The transports should be reported as a function of latitude, with the latitudinal spacing comparable to the model's native grid spacing.

3.3.10 Gyre and overturning decomposition of heat & salt transport

- northward_ocean_heat_transport_due_to_gyre = htovgyre
- northward_ocean_heat_transport_due_to_overturning = htovovrt
- northward_ocean_salt_transport_due_to_gyre = sltovgyre
- northward_ocean_salt_transport_due_to_overturning = sltovovrt

The $\hat{\mathbf{y}}$-ward advective transport of a tracer within a particular ocean basin is given by the integral

$$\mathcal{H}^{(\hat{\mathbf{y}})}(y,t) = \int_{x_1}^{x_2} \mathrm{d}x \int_{-H}^{\eta} \rho\, C\, v^{\dagger}\, \mathrm{d}z, \tag{3.58}$$

where C is the tracer concentration, $v^{\dagger}$ is the residual mean meridional velocity component (sum of resolved plus parameterized advection), $z = -H(x,y)$ is the ocean bottom, $z = \eta(x,y,t)$ is the ocean surface, and x_1 and x_2 are the boundaries of the basin or global ocean. It is useful for some analysis to decompose the transport (3.58) into "gyre" and "overturning" components, with these terms defined in the following.

We recommend that the monthly means for the components to heat and salt transport, partitioned according to Atlantic-Arctic, Indian-Pacific, and Global Oceans, be archived for all processes affecting the tracer, including resolved and SGS processes. The transports should be reported as a function of latitude, with the latitudinal spacing comparable to the model's native grid spacing.

Theoretical considerations

The total mass transport leaving the $\hat{\mathbf{y}}$-ward face of a grid cell is written

$$\mathcal{V}_{\text{total}}\, \mathrm{d}x = v^{\dagger}\, \rho\, \mathrm{d}z\, \mathrm{d}x, \tag{3.59}$$

and so $C\, \mathcal{V}_{\text{total}}\, \mathrm{d}x$ measures the mass per time of tracer leaving the $\hat{\mathbf{y}}$-ward face, including transport from resolved and parameterized advection. We now consider a decomposition of this transport by defining the basin average transport and basin average tracer concentration as follows (dropping here the "total" subscript for brevity)

$$[\mathcal{V}] = \frac{\sum_i \mathcal{V}\, \mathrm{d}x}{\sum_i \mathrm{d}x} \tag{3.60}$$

$$[C] = \frac{\sum_i C\, \mathrm{d}x}{\sum_i \mathrm{d}x}, \tag{3.61}$$

along with the deviations from basin average

$$\mathcal{V} = [\mathcal{V}] + \mathcal{V}^* \tag{3.62}$$

$$C = [C] + C^*. \tag{3.63}$$

The discrete i-sum extends over the basin or global domain of interest, so that $\sum_i \mathrm{d}x\, \mathcal{V}$ is the total $\hat{\mathbf{y}}$-ward transport of seawater at this band at a particular ocean model vertical level. The resulting $\hat{\mathbf{y}}$-ward tracer transport becomes

$$\mathcal{H}(y,t) = \sum_i \sum_k \mathcal{V}\, C\, \mathrm{d}x \tag{3.64}$$

$$= \sum_i \sum_k ([\mathcal{V}][C] + \mathcal{V}^*\, C^*)\, \mathrm{d}x, \tag{3.65}$$

where the k sum extends over the vertical cells in a column.

It is common to identify three components:

$$\text{y\_flux\_advect} = \sum_i \sum_k \mathcal{V}\, C\, \mathrm{d}x \tag{3.66}$$

$$\text{y\_flux\_over} = \sum_i \sum_k [\mathcal{V}][C]\, \mathrm{d}x \tag{3.67}$$

$$\text{y\_flux\_gyre} = \sum_i \sum_k \mathcal{V}^*\, C^*\, \mathrm{d}x, \tag{3.68}$$

with

$$\text{y\_flux\_gyre} = \text{y\_flux\_advect} - \text{y\_flux\_over}. \tag{3.69}$$

This identity follows very simply when the advective flux takes on the form of either first order upwind or second order centered differences. It becomes more involved when considering higher order, or flux limited, advection schemes. In these general cases, this result serves as a definition of the gyre component, so that the advective flux is built from the advection scheme used in the ocean model.

3.4 Mass transports through pre-defined sections

- sea_water_transport_across_line = mfo

1. barents_opening
2. bering_strait
3. canadian_archipelago
4. caribbean_windward_passage
5. denmark_strait
6. drake_passage
7. english_channel
8. faroe_scotland_channel
9. florida_bahamas_strait
10. fram_strait
11. iceland_faroe_channel
12. indonesian_throughflow
13. mozambique_channel
14. pacific_equatorial_undercurrent
15. taiwan_and_luzon_straits

There are a number of climatologically important straits, throughflows, and current systems whose vertically integrated mass transport is measured observationally (though some have wide uncertainties). These mass transports provide a useful means to characterize the simulation.

Pre-defined transports were not archived in CMIP3, thus necessitating a diagnostic calculation from the archived velocity field and/or the barotropic streamfunction. Such diagnoses, however, can be subject to uncertainty, especially for models with complex horizontal and vertical grids. It is thus more direct and accurate to have these transports computed by each participating model group, and archived as part of CMIP. Table 2.4 provides a list of recommended transports for CMIP6, with this table identical to the CMOP5 request. Each geographical region has an associated string valued coordinate given by the name.

We make the following recommendations regarding the recording of integrated mass transports.

- The depth integrated mass transport vanishes for mesoscale closures based on Gent et al. (1995), and the submesocale closures based on Fox-Kemper et al. (2008). Hence, the depth integrated transport involves *only* the resolved advective transport.
- In the following, we note the approximate geographical longitude and latitude coordinates of the straits and currents. Given considerations of model grid resolution and grid orientation, precise values for the coordinates may differ for any particular model. *In general, we recommend computing the simulated transport where the strait is narrowest and shallowest in the model configuration, and where the model grid is closely aligned with the section*.
- For most ocean model grids, the requested transports can be diagnosed by aligning the section along a model grid axis. In this case, it is straightforward to assign a positive sign to transports going in a pseudo-north or pseudo-east direction, and negative signs for the opposite direction. We use the term *pseudo* here as it refers to an orientation according to the model grid lines, which in general may not agree with geographical longitude and latitude lines. In general, the sign convention chosen for the recorded transport should be clearly indicated in the metadata information for the transport field.
- Some models may have a strait artificially closed, due to inadequate grid resolution. In this case, a zero transport should be recorded for this strait.
- We present references to observational estimates for the mass transports. Notably, there are some straits with large uncertainties. Even so, recording transport results from the various models will present the community with a valuable means to characterize the model flow fields.
- Some of the following transports are defined in accordance with the Global Ocean Data Assimilation Experiment (GODAE), as detailed in the report by the MERSEA project (MERCATOR, 2006).

The following provides details for the various regions where integrated mass transport is requested for CMIP6.[15]

1. BARENTS OPENING: The Barents Opening separates Spitsbergen from Norway. Vertically integrated transport through the Barents Opening occurs geographically roughly between the points

- Barents opening = $(16.8°E, 76.5°N)$ to $(19.2°E, 70.2°N)$.

Observational estimates range from 1.5-2.0 Sv northwards, with large variability, thus necessitating longer time series to get a zero order estimate.

2. Bering Strait: The Bering Strait separates Alaska from Siberia. Vertically integrated transport through the Bering Strait provides the only exchange between Pacific and Arctic waters. It is defined geographically from

   - Bering Strait = $(171°W, 66.2°N)$ to $(166°W, 65°N)$.

   An observational estimate from Roach et al. (1995) is 0.8Sv northward from the Pacific into the Arctic Ocean.

3. Canadian Archipelago: The Canadian Archipelago refers to the wide range of Arctic islands in northern Canada. The transport through these islands connects waters of the open Arctic to the North Atlantic through the Davis Strait and into the Labrador Sea. Vertically integrated transport through the Canadian Archipelego can be defined according to the following geographic region

   - Canadian Archipelego = $(128.2°W, 70.6°N)$ to $(59.3°W, 82.1°N)$.

   Observational estimates range from 0.7 to 2.0Sv southward (Sadler, 1976; Fissel et al., 1998; Melling, 2000).

4. Caribbean Windward Passage: The Caribbean Windward Passage lies between the easternmost region of Cuba and the northwest of Haiti, and is defined approximately by

   - Caribbean Windward Passage = $(75°W, 20.2°N)$ to $(72.6°W, 19.7°N)$.

5. Denmark Strait: The Denmark Strait separates Greenland from Iceland. Vertically integrated transport between Iceland and Greenland occurs over the following geographical region

   - Denmark Strait = $(37°W, 66.1°N)$ to $(22.5°W, 66°N)$.

   Observational estimates are 0.8Sv for the net northward transport (Osterhus et al., 2005) and 3Sv for the net southward transport (Olsen et al., 2008).

6. Drake Passage: The Drake Passage separates South America from Antarctica. It presents the narrowest constriction for the Antarctic Circumpolar Current. Vertically integrated transport in the Southern Ocean through the Drake Passage is determined by flow through the region

   - Drake Passage = $(68°W, 54°S)$ to $(60°W, 64.7°S)$.

   An observational estimate from Cunningham et al. (2003) is an eastward transport of 135Sv.

7. English Channel: The English Channel separates Britain from the European continent. Vertically integrated transport in the English Channel occurs geographically through the region

   - English Channel = $(1.5°E, 51.1°N$ to $1.7°E, 51.0°N)$.

   Observational estimates from Otto et al. (1990) are roughly 0.1 – 0.2Sv northward.

8. Faroe-Scotland Channel: The Faroe-Scotland Channel separates the Faroe Islands from Scotland. Vertically integrated transport between the Faroe Islands and Scotland occurs geographically through the region between

   - Faroe-Scotland Channel = $(6.9°W, 62°N)$ to $(5°W, 58.7°N)$

   Observational estimates are 3.8Sv for the net northward transport (Osterhus et al., 2005) and 2.1Sv for the net southward transport (Olsen et al., 2008).

9. Florida-Bahamas Strait: Since 1982 cables have been used to measure the transport of the Florida Current between Florida and the Bahamas near 27N. We thus define this transport according to the following geographical locations

   - Florida-Bahamas Strait = $(78.5°W, 26°N)$ to $(80.5°W, 27°N)$.

   Observational estimates range from 29Sv-35Sv (Leaman et al., 1987). Updated information is available from AOML at `www.aoml.noaa.gov/phod/floridacurrent/`. See also Figure 2-6 from the MERSEA project (MERCATOR, 2006).

10. Fram Strait: The Fram Strait separates Spitsbergen from Greenland. Vertically integrated transport in the Fram Strait occurs geographically through the region

    - Fram Strait = $(11.5°W, 81.3°N$ to $10.5°E, 79.6°N)$.

    Observational estimates from Schauer et al. (2004) are 4 ± 2Sv southwards.

11. Iceland Faroe Channel: The Iceland Faroe Channel separates Iceland from the Faroe Islands. Vertically integrated transport between Iceland and the Faroe Islands occurs geographically through the region between

    - Iceland-Faroe Channel = $(13.6°W, 64.9°N)$ to $(7.4°W, 62.2°N)$

    Observational estimates are 3.8Sv for the net northward transport (Osterhus et al., 2005) and 1Sv for the net southward transport (Olsen et al., 2008).

12. Indonesian Throughflow: Vertically integrated transport through the Indonesian Archipelogo is defined approximately by

    - Indonesian Throughflow = $(100°E, 6°S)$ to $(140°E, 6°S)$.

    An observational estimate from Gordon et al. (2003) is roughly 10Sv from the Pacific to the Indian Oceans.

13. MOZAMBIQUE CHANNEL: The Mozambique Channel separates Madagascar from the African continent. Vertically integrated transport through the Mozambique channel separating Madagascar from Southeast Africa is defined approximately by

    - MOZAMBIQUE CHANNEL = $(39°E, 16°S)$ to $(45°E, 18°S)$.

14. PACIFIC EQUATORIAL UNDERCURRENT: A commonly used region to measure transport in the equatorial undercurrent is given by the region

    - PACIFIC EQUATORIAL UNDERCURRENT = $(155°W, 3°S)$ to $(155°W, 3°N)$ over the depth range 0-350m.

    Observational estimates range between 24Sv-36Sv in an eastward direction (Lukas and Firing, 1984; Sloyan et al., 2003).

15. TAIWAN-LUZON STRAITS: We ask here for the vertically integrated transport giving the combined inflow to the South China Sea through the Taiwan and Luzon straits. The value from observations is positive when entering the South China Sea, and Yaremchuk et al. (2009) present a review of observed values.

3.5 Boundary fluxes

The ocean is a forced-dissipative system, with forcing largely at its boundaries. To develop a mechanistic understanding of ocean simulations, it is critical to have a clear sampling of the many forcing fields. Some of the following fields can be found in other parts of the CMIP6 archive as part of the sea ice or atmosphere components. However, these fields are typically on grids distinct from the ocean model grid. Fluxes on grids distinct from the ocean make accurate budget analyses difficult to perform, and such was a major shortcoming of the CMIP3 archive (WGCM, 2007). Following the CMIP5 approach, for CMIP6 we request an archive of the precise boundary fluxes used to force the ocean model.

We offer the following general comments regarding the boundary flux fields. Details of the requested fluxes are given in the subsequent subsections.

- All fluxes (water mass, salt mass, heat, momentum) are normalized according to the horizontal area of the ocean model grid cell. In some cases (e.g., rainfall), the flux computation requires integrating the rainfall over the ice-free sea (to get a mass per time of rainfall) and then dividing by the ocean grid cell area (to get mass per time per area). For these fluxes, according to the CF metadata conventions, the cell_methods attribute for the fields should read

  - area: mean where ice_free_sea over all_area_types.

  In other cases (e.g., melting sea ice) the flux computation requires integrating the sea ice melt over the sea ice covered portion of the ocean grid cell, and then dividing by the ocean grid cell area. For these fluxes, according to the CF metadata conventions, the cell_methods attribute for the fields should read

  - area: mean where sea_ice over all_area_types.

- Multiplication of a boundary flux by the ocean model grid cell area allows for the mass, heat, or momentum passed to the ocean, per time, to be computed. This property must be maintained whether the fluxes are archived on the native model grid, or on a remapped grid according to the recommendations of Section 1.5.

- Many climate models place boundary fluxes just at the ocean surface. However, more general couplings are being considered (e.g., penetrative shortwave heating; sea ice models that interact with more than the surface ocean cell). To allow for such generality, we ask that those fluxes that are three-dimensional be archived with their full three dimensional structure.

- The term "flux correction" in Tables 2.5, 2.6, 2.7, and 2.8 refers to the imposition of a prescribed flux that has at most a monthly variability (sometimes only an annual mean adjustment is imposed). Flux corrections (also called flux adjustments) have no interannual variability. They are added to some climate models for the purpose of reducing model drift. However, flux corrections are becoming less common as models are improved, in which case they are zero (see, for example, Section 8.4.2 of McAvaney et al., 2001).

- Some ocean models do not allow for the passage of water mass across the liquid ocean boundaries. Virtual salt fluxes are instead formulated to parameterize the effects of changes in salinity on the density field (Huang, 1993; Griffies et al., 2001; Yin et al., 2010b). The models that use virtual fluxes do not have a physically correct water cycle, as there is zero exchange of water between the ocean and other components of the climate system. Correspondingly, they do not have a physically correct salt budget, since the real ocean system has a trivial net flux of salt across the ocean surface boundary, contrasting with the nontrivial virtual salt fluxes. Additionally, they are missing the Goldsborough-Stommel circulation (Goldsbrough (1933), Stommel (1957), and Huang and Schmitt (1993)).

- The passage of water across an ocean boundary (via precipitation, evaporation, and runoff) corresponds to a transfer of tracer across the boundary, since the water generally carries tracer (e.g., carbon, heat). Heat from this water transport (relative to $0°C$) is requested in the Table 2.7. Notably, this heat transport is distinct from the heat transport associated with phase changes. Instead, the heat transport is due solely to the nontrivial

heat present in water that moves between the ocean and other components of the climate system. Models that artificially preclude water to cross the ocean boundary (e.g., rigid lid models, or models with a virtual tracer flux) have zero contributions to these transport induced heat fluxes.

For precipitation and evaporation, the heat flux associated with water transport across the ocean boundaries generally provides a global net cooling of the ocean, since evaporation transfers water away from the ocean at a temperature typically higher than precipitation adds water. In a steady state, this net heat loss is compensated by ocean heat transport, and the ocean heat transport is in turn balanced by atmospheric heat transport. However, most atmospheric models do not carry the temperature of its moisture field, thus precluding the atmospheric component in a climate model from representing the heat transport. There is a resulting non-conservative heat budget in the simulated climate system.

The size of the atmospheric heat transport associated with the temperature of its moisture field is small relative to the atmospheric heat fluxes associated with phase changes of water in the atmosphere. It is the dominance of heating associated with phase change that has motivated atmospheric modelers to ignore the temperature of its moisture field. In contrast, ocean water must be tagged with its temperature field in order to simulate the ocean fluid, providing a generally nonzero heat associated with water that passes across ocean boundaries. This topic is discussed in Section 3 of the coupled model paper from Delworth et al. (2006), where an estimate for the heat flux is given. Section D.2 of the ocean model comparison paper by Griffies et al. (2009b) also provides a discussion of this heat flux, as does Section A.4 in the sea level comparison paper of Griffies et al. (2014).

3.5.1 Boundary fluxes of water mass

- rainfall_flux = pr
- snowfall_flux = prsn
- water_evaporation_flux = evs
- water_flux_into_sea_water_from_rivers = friver
- water_flux_into_sea_water_from_icebergs = ficeberg
- water_flux_into_sea_water_due_to_sea_ice_thermodynamics = fsitherm
- water_flux_into_sea_water = wfo
- water_flux_into_sea_water_without_flux_correction = wfonocorr
- water_flux_correction = wfcorr

These fluxes (Table 2.5) aim to present the analyst with sufficient information to perform a water mass budget on the liquid ocean, and to map regionally where water enters or leaves the ocean through various physical processes. Models that employ a virtual salt flux, and so do not allow for the transfer of water mass across the liquid ocean boundary, will report zero for each of these fields. The following presents some general comments.

- Liquid runoff is defined as liquid water that enters the ocean from land, such as through rainwater in rivers, or snow and ice meltwater in rivers. It may also incorporate melt water from sea ice and icebergs.
- An iceberg model exports a certain amount of calved land ice away from the coasts. It is thus important to record where the icebergs melt (horizontal position and depth), hence the suggestion to include iceberg melt (Table 2.5).

We now present detailed comments about each of the fields. As discussed in the first bulleted item at the beginning of Section 3.5, the fluxes, which may be defined only over a portion of each ocean grid cell, are normalized by the full area of each ocean grid cell. As a result, the product of the ocean horizontal area and the flux will render the mass per time of water entering or leaving the liquid ocean.

- rainfall_flux: The mass flux of liquid precipitation from the atmosphere entering the ice-free portion of an ocean grid cell.
- snowfall_flux: The mass flux of frozen precipitation from the atmosphere entering the ice-free portion of an ocean grid cell.
- water_evaporation_flux: This is a flux that is positive for water leaving the liquid ocean. It measures the rate at which water vapor leaves the liquid ocean and enters the atmosphere, through the ice-free portion of an ocean grid cell.
- water_flux_into_sea_water_from_rivers: This field measures the mass of liquid water runoff entering the ocean from land-surface boundaries.
- water_flux_into_sea_water_from_icebergs: The solid mass that enters the ocean from land-ocean boundaries will eventually melt in the ocean. This melt may occur just at the ocean-land boundary, be distributed seawards by a spreading scheme, or participate in the transport via icebergs. It is this mass flux that is requested.
- water_flux_into_sea_water_due_to_sea_ice_thermodynamics: This is the contribution to liquid ocean mass due to the melt (positive flux) or freezing (negative flux) of sea ice.
- water_flux_into_sea_water: This is the net flux of liquid water entering the liquid ocean.
- water_flux_correction: This field stores the mass flux due to flux corrections. It will be zero for models with no flux corrections.
- water_flux_into_sea_water_without_flux_correction: This field stores the mass flux due to physical processes absent the flux corrections.

Note that the following equality is satisfied by the requested water flux fields

$$\begin{aligned}&\text{water\_flux\_into\_sea\_water} = \\ &\text{water\_flux\_into\_sea\_water\_without\_flux\_correction} + \text{water\_flux\_correction.}\end{aligned} \tag{3.70}$$

3.5.2 Boundary fluxes of salt

- virtual_salt_flux_into_sea_water_due_to_rainfall = vsfpr
- virtual_salt_flux_into_sea_water_due_to_evaporation = vsfevap
- virtual_salt_flux_into_sea_water_from_rivers = vsfriver
- virtual_salt_flux_into_sea_water_due_to_sea_ice_thermodynamics = vsfsit
- virtual_salt_flux_into_sea_water = vsf
- virtual_salt_flux_correction = vsfcorr
- downward_sea_ice_basal_salt_flux = sfdsi
- salt_flux_into_sea_water_from_rivers = sfriver

These fluxes (Table 2.6) aim to present the analyst with sufficient information to perform a salt budget on the liquid ocean, and to map regionally where salt enters or leaves the ocean through various physical processes. The following presents some details about the fields. Note that for models using real water fluxes, the virtual salt flux fields are ALL zero.

- virtual_salt_flux_into_sea_water_due_to_rainfall: This field measures the virtual salt flux associated with liquid precipitation.
- virtual_salt_flux_into_sea_water_due_to_evaporation: This field measures the virtual salt flux associated with the evaporation of liquid water.
- virtual_salt_flux_into_sea_water_from_rivers: This field measures the virtual salt flux associated with the liquid runoff from land processes.
- virtual_salt_flux_into_sea_water_due_to_sea_ice_thermodynamics: This field measures the virtual salt flux associated with the melting or freezing of sea ice.
- virtual_salt_flux_correction: This field measures the virtual salt flux arising from a salt flux correction.
- virtual_salt_flux_into_sea_water: This field measures the total virtual salt flux entering the ocean. It is the sum of all of the above virtual salt fluxes, including the salt flux correction.
- Salt transport from sea-ice to the ocean is measured in the field downward_sea_ice_basal_salt_flux. The field downward_sea_ice_basal_salt_flux arises since sea ice has a nonzero salinity, so it exchanges salt with the liquid ocean upon melting and freezing. This field is distinct from the virtual salt flux into sea water due to sea ice thermodynamics.
- Rivers may contain a nonzero salinity, in which case salt_flux_into_sea_water_from_rivers will be nonzero.

3.5.3 Boundary fluxes of heat

- upward_geothermal_heat_flux_at_sea_floor = hfgeou
- temperature_flux_due_to_rainfall_expressed_as_heat_flux_into_sea_water = hfrainds
- temperature_flux_due_to_evaporation_expressed_as_heat_flux_out_of_sea_water = hfevapds
- temperature_flux_due_to_runoff_expressed_as_heat_flux_into_sea_water = hfrunoffds
- heat_flux_into_sea_water_due_to_snow_thermodynamics = hfsnthermds
- heat_flux_into_sea_water_due_to_frazil_ice_formation = hfsifrazil
- heat_flux_into_sea_water_due_to_sea_ice_thermodynamics = hfsithermds
- heat_flux_into_sea_water_due_to_iceberg_thermodynamics = hfibthermds
- surface_net_downward_longwave_flux = rlds
- surface_downward_latent_heat_flux = hfls
- surface_downward_sensible_heat_flux = hfss
- net_downward_shortwave_flux_at_sea_water_surface = rsntds
- downwelling_shortwave_flux_in_sea_water = rsdo[16]
- heat_flux_correction = hfcorr
- surface_downward_heat_flux_in_sea_water = hfds

These fluxes (Table 2.7) aim to present the analyst with sufficient information to perform a heat budget on the liquid ocean, and to map regionally where heat enters or leaves the ocean through various physical processes. The following presents some details about the fields.

The net heat flux crossing the liquid ocean boundaries is given by

$$\begin{aligned} Q_{\text{net}} &= Q_{\text{geothermal}} \\ &+ Q_{\text{precip heat content}} + Q_{\text{evap heat content}} + Q_{\text{river heat content}} \\ &+ Q_{\text{latent heat snow melt}} + Q_{\text{latent heat ice berg melt}} \\ &+ (Q_{\text{sea ice thermo}} - Q_{\text{frazil ice flux}}) + Q_{\text{frazil ice flux}} \\ &+ Q_{\text{longwave}} + Q_{\text{shortwave}} \\ &+ Q_{\text{latent heat evap}} + Q_{\text{sensible}} \\ &+ Q_{\text{flux correction}} \cdot \end{aligned} \tag{3.71}$$

In the following, we detail these fields and connect them to the long-names presented in the above itemized list.

- $Q_{\text{geothermal}}$ = upward_geothermal_heat_flux_at_sea_floor: Some ocean model components in CMIP6 employ geothermal heating through the ocean bottom. This heating is typically unchanging over the course of climate simulations, in which case the geothermal heat flux is a constant. For those models that use a time dependence for the geothermal heating, they should archive the monthly heat flux. It is assumed that models considering a geothermal heating will inject this heating at the sea-floor.

- $Q_{\text{precip heat content}}$ = temperature_flux_due_to_rainfall_expressed_as_heat_flux_into_sea_water: This field measures the heat carried by the transfer of liquid and frozen precipitation into the liquid ocean. This heat computed is with respect to $0°C$. For liquid rainfall, it is computed in the following manner:

$$\text{rainfall heat } (\text{W/m}^2) = Q_{\text{rain}}\, C_p\, T_{\text{rain}}, \tag{3.72}$$

  where Q_{rain} is the rainfall mass flux in kg/(m^2 sec), C_p is the rainfall heat capacity, and T_{rain} is the temperature of rainfall in degrees Celsius. Most climate models choose the rainfall temperature to equal the ocean sea surface temperature. The reason for this assumption is that atmospheric models tend not to carry the temperature of their moisture field. But this assumption need not be applicable for more complete atmospheric models that carry the heat content of its precipitation.

  Since we measure this heat flux with respect to $0°C$, there is no need to record an analogous heat flux due to snowfall, $Q_{\text{snow heat}}$, if we assume the snow enters the ocean at $0°C$. However, for more general cases, the snowfall may have a heat content that is determined by the atmospheric model, in which case this heat content will be included in $Q_{\text{precip heat content}}$.

  For models employing a virtual tracer flux, in which there is no mass or volume transport of water across the ocean surface, this field is zero.

- $Q_{\text{evap heat content}}$ = temperature_flux_due_to_evaporation_expressed_as_heat_flux_out_of_sea_water: This field measures the heat carried by the transfer of water away from the liquid ocean through the process of evaporation. This heat is distinct from latent heat flux, and it is computed with respect to $0°C$ in the following manner:

$$Q_{\text{evap heat}}\ (\text{W/m}^2) = Q_{\text{evap}}\, C_p\, T_{\text{evap}}, \tag{3.73}$$

  where Q_{evap} is the evaporative mass flux in kg/(m^2 sec), C_p is the water heat capacity, and T_{evap} is the temperature of evaporating water in degrees Celsius, with T_{evap} generally equal to the ocean sea surface temperature.

  For models employing a virtual salt flux, in which there is no mass transport of water across the ocean surface, this field is zero.

- $Q_{\text{river heat content}}$ = temperature_flux_due_to_runoff_expressed_as_heat_flux_into_sea_water: This field measures the heat of runoff that enters the liquid ocean, with respect to $0°C$. This heat is computed as

$$Q_{\text{runoff heat}}\ (\text{W/m}^2) = Q_{\text{runoff}}\, C_p\, T_{\text{runoff}}, \tag{3.74}$$

  where Q_{runoff} is the liquid runoff mass flux in kg/(m^2 sec), C_p is the ocean heat capacity, and T_{runoff} is the temperature of liquid runoff in degrees Celsius. Note that this "runoff" mass flux may include mass flux from sea ice and from icebergs, in which case the name "runoff" is inappropriate, but is retained as a placeholder.

  For models employing a virtual tracer flux, in which there is no mass transport of water across the ocean surface, this field is zero.

- $Q_{\text{frazil ice flux}}$ = heat_flux_into_sea_water_due_to_frazil_ice_formation: As the temperature of seawater cools to the freezing point, sea ice is formed, initially through the production of frazil. Operationally in an ocean model, liquid water can be supercooled at any particular time step through surface fluxes and transport. An adjustment process heats the liquid water back to the freezing point, with this positive frazil heat flux extracted from the ice model as frazil sea ice is formed. This term is necessary to close the heat budget of the liquid ocean, and so it is requested for CMIP6.

- $Q_{\text{sea ice thermo}}$ = heat_flux_into_sea_water_due_to_sea_ice_thermodynamics: This field accounts for two terms. First, there is the heat gain by the liquid ocean when sea ice is formed, or heat loss from the liquid ocean when sea ice melts. This first term in fact is the same as the frazil heat term, Q_{frazil}. The second term the conductive heat flux from the ice-ocean interface into the sea ice. This term is a sensible heating term, and is sometimes bundled inside of the sensible heat term from air-sea interactions.

The field upward_sea_ice_basal_heat_flux was asked for in CMIP3, and this field is closely related to the field asked for here. Whereas CMIP3 asked for the total heating of ice, in Watts, we ask for heating per horizontal area of ocean an ocean grid cell.

The reason to bundle two heat fluxes together is that many ocean-ice models partition these terms in different manners. To expose some details, consider the discussion in Winton (2000), where we here consider heating of the liquid ocean to be positive. Equation (23) in Winton (2000) then reads

$$F_b = M_b - 4K(T_f - T_i)/h_i, \tag{3.75}$$

where F_b is the net heat flux into the liquid ocean associated with sea ice melt and formation, as well as conduction. The term $M_b > 0$ is the heat flux entering the liquid ocean during the formation of sea ice, whereas $M_b < 0$ is the heat flux lost from the liquid ocean upon melting sea ice. The second term on the right hand side is the conductive term, with K the thermal conductivity of sea ice. A value of $K = 2.03\,\mathrm{W/(m\,°C)}$ is typical. T_f is the freezing temperature of seawater, with the ice-ocean interface assumed to be constantly at this temperature. T_i is the temperature of the sea ice. Finally, h_i is the sea ice thickness. The conductive term contributes a negative heat flux to the liquid ocean when the freezing temperature T_f is greater than the ice temperature T_i, and a positive heat flux for an oppositely signed temperature difference.

Finally, we note that this term, $Q_{\text{sea ice thermo}}$, is more often diagnosed from within the ice model than within the ocean model. Its placement in the CMIP ocean diagnostic request is historical.

- $Q_{\text{latent heat ice berg melt}}$ = heat_flux_into_sea_water_due_to_iceberg_thermodynamics: Icebergs transport calved land ice from the land into the ocean. A rudimentary "iceberg" model may simply be the insertion of calving land ice/snow into the ocean. More realistic iceberg models are now becoming more common (Jongma et al., 2009; Martin and Adcroft, 2010). Melting of the icebergs into the liquid ocean is associated with a transfer of the latent heat of fusion from liquid ocean, and so represents a cooling of the liquid ocean in regions where the icebergs melt. It is this heat flux that is to be archived in the field heat_flux_into_sea_water_due_to_iceberg_thermodynamics.
- $Q_{\text{latent heat melt snow}}$ = heat_flux_into_sea_water_due_to_snow_thermodynamics: Snow entering the liquid ocean is assumed to melt upon transferring its latent heat of fusion from the ocean. This cooling of the liquid ocean is what is to be archived in heat_flux_into_sea_water_due_to_snow_thermodynamics.
- Q_{longwave} = surface_net_downward_longwave_flux: This field measures the net downward flux of longwave radiation that enters the liquid ocean. Negative values cool the ocean.
- $Q_{\text{latent heat evap}}$ = surface_downward_latent_heat_flux: This field measures the net flux of latent heating associated with the phase change from liquid ocean to water vapor. Negative values cool the ocean, as occurs when liquid water evaporates.
- Q_{sensible} = surface_downward_sensible_heat_flux: This field measures the net downward flux of sensible heating acting on the liquid ocean. Positive values warm the ocean and negative values cool.
- $Q_{\text{shortwave}}$ = net_downward_shortwave_flux_at_sea_water_surface: This field measures the net downward flux of shortwave heating that enters the liquid ocean surface. Positive values warm the ocean.
- $Q_{\text{flux correction}}$ = heat_flux_correction: This field records the heat flux correction acting at the liquid ocean surface. This field is zero for nearly all CMIP6 models.
- $Q_{\text{net}} - Q_{\text{geothermal}}$ = surface_downward_heat_flux_in_sea_water: This field records the net heat flux passing across the ocean surface due to radiative, turbulent, and heat content fluxes.
- downwelling_shortwave_flux_in_sea_water: This field measures the downwelling flux of shortwave heating within the three-dimensional liquid ocean. Shortwave radiation penetrates into the ocean column, with this penetration of fundamental importance for many ocean processes.

3.5.4 Boundary fluxes of momentum

- surface_downward_x_stress = tauuo
- surface_downward_y_stress = tauvo
- surface_downward_x_stress_correction = tauucorr
- surface_downward_y_stress_correction = tauvcorr

These fluxes (Table 2.8) aim to present the analyst with sufficient information to quantify the net momentum imparted to the liquid ocean surface from the overlying atmosphere, sea ice, ice shelf, etc.

3.5.5 Boundary gas exchange for inert chemical species

- surface_downward_mole_flux_of_cfc11 = fgcfc11
- surface_downward_mole_flux_of_cfc12 = fgcfc12
- surface_downward_mole_flux_of_fs6 = fgfsf6

These fluxes (Table 2.9) quantify the net surface flux of CFC11, CFC12, and SF6 crossing the liquid ocean surface. These fluxes should be saved for the CMIP6 historical experiment and for the CMIP6/OMIP experiment.

3.6 Budget terms for heat and salt

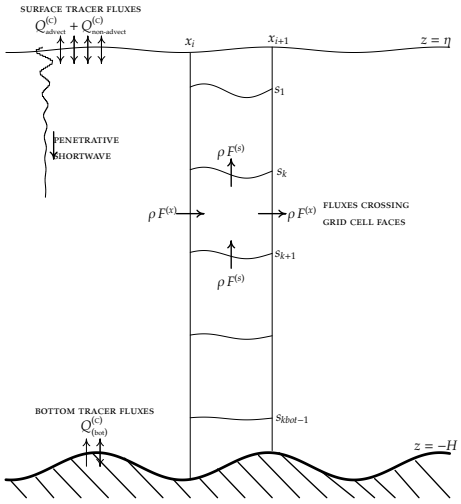

Figure 3.1: A longitudinal-vertical slice of ocean fluid from the surface at $z = \eta(x, y, t)$ to bottom at $z = -H(x, y)$, along with a representative column of discrete grid cells (a latitudinal-vertical slice is analogous). Most ocean models used for large-scale climate studies assume the horizontal boundaries of a grid cell at x_i and x_{i+1} are static, meaning that the horizontal cross-sectional area is time independent. In contrast, the vertical extent, defined by surfaces of constant generalized vertical coordinate s_k and s_{k+1}, are generally time dependent (e.g., pressure surfaces, isopycnal surfaces, sigma surfaces, etc.). A general tracer flux $\rho \mathbf{F}$ (e.g., advective or SGS flux) is decomposed into horizontal and dia-surface components, with the convergence of these fluxes onto a grid cell determining the evolution of tracer content within the cell. Amongst the fluxes crossing the ocean surface, the shortwave flux penetrates into the ocean column as a function of the optical properties of seawater (e.g., Manizza et al., 2005). This figure is based on Figure 1 of Griffies and Treguier (2013).

There are an increasing number of papers that perform detailed budget analyses for heat and salt, which in turn provide mechanistic understanding of model simulations. Such studies include the following: Gregory (2000), Palter et al. (2014), Griffies et al. (2014), Exarchou et al. (2014) and Kuhlbrodt et al. (2014). Hence, we are motivated to request heat and salt budget terms in CMIP6. This request is based on the premise that analysis of budget terms will render a far more mechanistic information about model behaviour than possible without such terms. The bulk of the science resulting from these budgets has thus far come from use of the annual mean fields, hence the request here is only for annual mean budget terms.

When combined with the boundary fluxes in Section 3.5.3 and 3.5.2, the following 3d tendencies (see Table 2.10 for a summary of the budget terms) provide the analyst with all terms required to perform a detailed 3d heat and salt budget for the liquid ocean. In the following, we detail how these terms are to be saved, and recommend methods for their analysis. Note that the terms saved for heat depend on whether the model uses potential temperature as a prognostic variable, or conservative temperature.

Here are the diagnostic terms for heat content budgets if the ocean model uses potential temperature as a prognostic field.

- tendency_of_sea_water_potential_temperature_expressed_as_heat_content
- tendency_of_sea_water_potential_temperature_expressed_as_heat_content_due_to_advection
- tendency_of_sea_water_potential_temperature_expressed_as_heat_content_due_to_parameterized_eddy_advection
- tendency_of_sea_water_potential_temperature_expressed_as_heat_content_due_to_parameterized_mesoscale_advection
- tendency_of_sea_water_potential_temperature_expressed_as_heat_content_due_to_parameterized_mesoscale_diffusion
- tendency_of_sea_water_potential_temperature_expressed_as_heat_content_due_to_parameterized_submesoscale_advection
- tendency_of_sea_water_potential_temperature_expressed_as_heat_content_due_to_parameterized_dianeutral_mixing

Here are the diagnostic terms for heat content budgets if the ocean model uses conservative temperature as a prognostic field.

- tendency_of_sea_water_conservative_temperature_expressed_as_heat_content
- tendency_of_sea_water_conservative_temperature_expressed_as_heat_content_due_to_advection
- tendency_of_sea_water_conservative_temperature_expressed_as_heat_content_due_to_parameterized_eddy_advection
- tendency_of_sea_water_conservative_temperature_expressed_as_heat_content_due_to_parameterized_mesoscale_advection
- tendency_of_sea_water_conservative_temperature_expressed_as_heat_content_due_to_parameterized_mesoscale_diffusion
- tendency_of_sea_water_conservative_temperature_expressed_as_heat_content_due_to_parameterized_submesoscale_advection
- tendency_of_sea_water_conservative_temperature_expressed_as_heat_content_due_to_parameterized_dianeutral_mixing

Here are the diagnostic terms for the salt budgets.

- tendency_of_sea_water_salinity_expressed_as_salt_content
- tendency_of_sea_water_salinity_expressed_as_salt_content_due_to_advection
- tendency_of_sea_water_salinity_expressed_as_heat_content_due_to_parameterized_eddy_advection
- tendency_of_sea_water_salinity_expressed_as_salt_content_due_to_parameterized_mesocale_advection
- tendency_of_sea_water_salinity_expressed_as_salt_content_due_to_parameterized_mesocale_diffusion
- tendency_of_sea_water_salinity_expressed_as_salt_content_due_to_parameterized_submesocale_advection
- tendency_of_sea_water_salinity_expressed_as_salt_content_due_to_parameterized_dianeutral_mixing

3.6.1 Tracer budgets for a grid cell

In order to ensure proper archival and use of budget terms, we provide here a brief tutorial for the sourcel-less tracer budget equation in an ocean model.[17] The following semi-discrete equations are the basis for an ocean model tracer budget in surface, interior, and bottom grid cells

$$\frac{\partial (C\,\rho\,dz)}{\partial t} = -\nabla_s \cdot [\rho\, dz\, (\mathbf{u}\, C + \rho \mathbf{F})] + \left[(w\,\rho\, C + \rho\, F^{(s)}) \right]_{s=s_{k=1}} + Q^{(C)}_{\text{advect}} + Q^{(C)}_{\text{non-advect}} \tag{3.76a}$$

$$\frac{\partial (C\,\rho\,dz)}{\partial t} = -\nabla_s \cdot [\rho\, dz\, (\mathbf{u}\, C + \mathbf{F})] - [\rho\, (w\, C + F^{(s)})]_{s=s_{k-1}} + [\rho\, (w\, C + F^{(s)})]_{s=s_k} \tag{3.76b}$$

$$\frac{\partial (C\,\rho\,dz)}{\partial t} = -\nabla_s \cdot [\rho\, dz\, (\mathbf{u}\, C + \mathbf{F})] - \left[\rho\, (w\, C + F^{(s)}) \right]_{s=s_{kbot-1}} + Q^{(C)}_{(\text{bot})}. \tag{3.76c}$$

These budgets are formulated as finite volume contributions to the tracer mass per horizontal area (or heat per area) of a grid cell, with the horizontal area of the grid cell assumed constant in time. The left hand side of these equations represents the time tendency for the net tracer content in a grid cell, per horizontal area of the cell. The right hand side arises from the convergence of advective and SGS fluxes crossing the faces of a grid cell, as well as the boundary fluxes.

A schematic of ocean model grid cells over an ocean column is shown in Figure 3.1. Grid cells generally have a non-constant thickness and non-constant density (although Boussinesq budgets have constant density factor $\rho \to \rho_0$). The lateral convergence operator acting on an advective or SGS flux is formulated numerically so that multiplication by the respective area of a grid cell face leads to a difference operator acting on the lateral flux components crossing the tracer grid cell faces. That is, the numerical discretization satisfies Gauss's Law (Section 3.6.7), as doing so allows us to retain the familiar finite volume budgets within the numerical model. We now detail terms in these budgets.

- C is the potential (or conservative) temperature of a grid cell, or the mass of tracer (e.g., salt or another material tracer) per mass of seawater within the cell (i.e., tracer concentration).
- $\rho\, dz$ is the mass of seawater per horizontal area in a grid cell, with ρ the *in situ* density and dz the thickness. For models that makes the Boussinesq approximation, the ρ factor is replaced by a constant reference density ρ_o whose value depends on the ocean model, but which is typically close to the global averaged density or $\rho_o = 1035$ kg m^{-3}. For models with fixed grid cell thicknesses, the thickness factor dz is a temporal constant.
- The product $C\,\rho\, dz$ is the mass per unit horizontal area of a grid cell if C is a material tracer such as salinity. Since the horizontal area of the cell is constant in time, we may multiply by the horizontal area to recover a budget for the mass in the cell.
- The product $C\,\rho\, dz$ is the heat per horizontal area if C is potential or conservative temperature multiplied by the heat capacity. Since the horizontal area of the cell is constant in time, we may multiply by the horizontal area to recover a budget for the heat within the grid cell, in SI units of Joule.
- The generalized level vertical coordinate is denoted by s, and its discrete values s_k determine the vertical grid cell.
- The horizontal velocity component is $\mathbf{u}$ and dia-surface component is w. For geopotential coordinate models, w is the usual vertical velocity component. More generally, for generalized coordinate models, w is the dia-surface component.
- The horizontal subgrid scale transport is $\rho\,\mathbf{F}$ and dia-surface component is $\rho\, F^{(s)}$.
- Tracer flux associated with the boundary water flux is accounted for by the term $Q^{(C)}_{\text{advect}}$. That is, this term accounts for the heat content of the mass crossing the ocean surface, with discussion of this term given in Section 3.5.3.
- $Q^{(C)}_{(\text{bot})}$ is the flux of tracer passed into the liquid ocean through the solid bottom boundary, such as through geothermal heating (Section 3.5.3).
- $Q^{(C)}_{\text{non-advect}}$ is the non-advective flux of tracer crossing the ocean surface boundary. The sign is defined so that a positive value represents a flux of tracer into the ocean; e.g., positive sign adds heat, salt, carbon, or other tracers to the ocean. For the heat budget, this term arises from such terms as shortwave, longwave, latent, and sensible heat fluxes (Section 3.5.3).

3.6.2 Processes to be diagnosed for the budgets

There are numerous physical processes contributing to the evolution of heat and salt in a grid cell. Unfortunately, it is not practical to request all such terms be archived for CMIP. Rather, we aim to archive a suite of terms whose physical content is interesting, and whose contributions to the heat and salt budgets generally nontrivial, at least in regions. In addition to the boundary salt fluxes detailed in Sections 3.5.2, and the boundary heat fluxes and penetrative shortwave radiation detailed in Section 3.5.3, we recommend archiving the following terms associated with ocean advective and subgrid scale transport. We list here the terms for salt, merely since the CF names are shorter, with the same terms applying to heat content.

- tendency_of_sea_water_salinity_expressed_as_salt_content = net time tendency for salt in a grid cell due to *all* processes.
- tendency_of_sea_water_salinity_expressed_as_salt_content_due_to_advection = convergence of the three dimensional advective fluxes acting to alter salt in a grid cell.

- tendency_of_sea_water_salinity_expressed_as_salt_content_due_to_parameterized_eddy_advection = convergence of the three dimensional parameterized advective fluxes acting to alter salt in a grid cell, with examples including parameterizations due to mesoscale and/or submesoscale processes. We have the identity due_to_parameterized_eddy_advection = due_to_parameterized_mesocale_advection + due_to_parameterized_submesocale_advection, so there is no need to archive all three.
- tendency_of_sea_water_salinity_expressed_as_salt_content_due_to_parameterized_mesocale_advection = convergence of the three dimensional parameterized advective (or skew diffusive) salt fluxes due to mesoscale eddy parameterizations (e.g., Gent and McWilliams (1990); Gent et al. (1995); Griffies (1998)).
- tendency_of_sea_water_salinity_expressed_as_salt_content_due_to_parameterized_mesocale_diffusion = convergence of the three dimensional parameterized diffusive heat fluxes associated with mesoscale closures. Such diffusion is usually oriented according to neutral directions or isopycnal directions (Solomon (1971), Redi (1982), Griffies et al. (1998)). Care should be taken to include all components of this convergence, including the vertical flux convergence.
- tendency_of_sea_water_salinity_expressed_as_salt_content_due_to_parameterized_submesocale_advection = convergence of the three dimensional parameterized advective (or skew diffusive) heat fluxes due to submesoscale eddy parameterizations present in the heat equation (e.g., Fox-Kemper et al. (2008, 2011)). Note that there has been thus far no proposal to parameterize submesoscale processes according to diffusion, thus motivating only the archival of an advective term.
- tendency_of_sea_water_salinity_expressed_as_salt_content_due_to_parameterized_dianeutral_mixing = convergence of the parameterized heat fluxes associated with dia-neutral (or diapycnal) processes, including convection implemented via an enhanced vertical diffusivity; convection implemented via convective adjustment (Rahmstorf, 1993); boundary layer mixing; interior shear driven mixing; gravity wave induced mixing; background diffusion.
- Contributions from remaining processes can be inferred as a residual by taking the difference of all diagnosed processes from the net tendency. Residual processes may include non-local KPP mixing (Large et al., 1994) and mixing from overflow schemes (Beckmann and Döscher, 1997; Campin and Goosse, 1999; Danabasoglu et al., 2010; Bates et al., 2012).
- For heat, note that penetrative shortwave radiation should be saved in the diagnostic downwelling_shortwave_flux_in_sea_water = rsdo (Table 2.7 and Section 3.5.3).

Again, the heat budget terms are analogous to these salt budget terms. Note that by archiving the net heat and salt terms, we can determine a residual that accounts for all terms not diagnosed by the terms listed here. Presumably these other missing processes are sub-dominant, though such may depend on specifics of the model.

3.6.3 Conventions for the heat budget terms

Following from the tracer budget given by equations (3.76a)-(3.76c), all heat budget terms for archiving into CMIP take the general form[18]

$$Q^{(\Theta)}_{\text{process(n)}} = C^{o}_{p} \left(\frac{\partial(\rho \, dz \, \Theta)}{\partial t} \right)_{\text{process(n)}} \qquad \text{Watt m}^{-2}, \tag{3.77}$$

where n labels the particular physical process. The heat capacity C^{o}_{p} is generally assumed constant. The physical units for the heat budget terms are thus given by

$$Q^{(\Theta)}_{\text{process(n)}} \; [\equiv] \; \text{Watt m}^{-2}. \tag{3.78}$$

The area normalization for each budget term corresponds to the horizontal area of the tracer grid cell. Multiplication of any budget term by the tracer grid cell horizontal area thus yields the heat content change for that grid cell in units of Watts.

3.6.4 Conventions for the salt budget terms

Following from the tracer budget given by equations (3.76a)-(3.76c), all salt budget terms for archiving into CMIP take the general form

$$Q^{(S)}_{\text{process(n)}} = \frac{1}{1000} \left(\frac{\partial(\rho \, dz \, S)}{\partial t} \right)_{\text{process(n)}} \qquad \text{kg m}^{-2} \, \text{s}^{-1}, \tag{3.79}$$

where S is the salinity in units of ppt = gram of salt per kilogram of seawater or psu, depending on the model native field, and n labels the particular physical process. Division by 1000 converts grams to kilograms. Multiplication of any budget term by the tracer grid cell horizontal area thus yields the salt content change for that grid cell in units of kilogram per second.

3.6.5 Temperature tendency terms

The heat budget term (3.77) scales according to the thickness of a cell. This is expected, since the budget determines the change in heat content per horizontal area of a cell, and this is the prognostic term in the ocean model.

For diagnostic purposes, it may be useful to diagnose a temperature tendency corresponding to the heat budget terms, with the temperature tendency in units of K s^{-1}. Doing so removes the dependence on the grid cell thickness. That is, we may choose to consider the tendency for an intensive quantity, temperature, rather than the budget for an extensive quantity,

heat. For this purpose, we recommend dividing the heat budget terms in equation (3.77) by the annual mean mass per horizontal area of a grid cell, according to

$$\delta\Theta_{\text{process(n)}} = \frac{Q^{(\Theta)}_{\text{process(n)}}}{C^o_p\, \rho\, dz} \; [\equiv] \; \text{K s}^{-1}. \tag{3.80}$$

The factor $\rho\, dz$ is the annual mean mass per unit area of a grid cell, requested in Section 3.2.3. In this way, we can map vertical sections of the tendency terms a thus remove dependence on the grid cell thicknesses. Note that for a Boussinesq model with grid cell thicknesses that are time independent, temperature tendency terms are trivially related to the heat budget terms.

3.6.6 Salinity tendency terms

Likewise, we may convert the salt budget terms into salinity tendencies in units of ppt/s. For this purpose, we may divide the salt budget terms in equation (3.79) according to

$$\delta S_{\text{process(n)}} = \frac{Q^{(S)}_{\text{process(n)}}}{\rho\, dz} \; [\equiv] \; \text{ppt s}^{-1}. \tag{3.81}$$

The $\rho\, dz$ array is the annual mean mass per unit area of a grid cell, requested in Section 3.2.3. Note that for a Boussinesq model with grid cell thicknesses that are time independent, salinity tendency terms are trivially related to the salt budget terms.

3.6.7 Fluxes versus their convergence

In the mechanistic analysis of budgets, one is often interested in assessing budgets over a region, such as an ocean basin or within a subregion of a basin. These regional budgets help to identify dominant processes contributing to changes in heat and salt within the region, which in turn can help characterize physical mechanisms. For many purposes, this sort of analysis may involve characterizing the fluxes of heat and salt crossing the regional boundaries, in which case the three components of a flux vector may be required.

However, it is ultimately the convergence of a flux vector into a region that causes the change in heat or salt in that region. Additionally, fluxes remain arbitrary up to the curl of a scalar, since the curl of a scalar has zero convergence. One therefore must be careful when focusing an analysis on fluxes. Further words of caution in these regards are summarized in the appendix of Gregory (2000).

We are not advocating outright abandonment of flux components for mechanistic analyses, rather cautioning in their use absent consideration for their convergences into a region. It is largely for this reason that we are compelled for CMIP6 to recommend saving budget terms comprised of the convergence of fluxes associated with various physical processes. Besides saving archive space relative to saving fluxes (by a factor of three), we are assured that the budget analysis is making use of terms that directly contribute to the changes in heat and salt within a region.

We furthermore note that integration of the divergence over a region leads, through Gauss's Law, to the sum of the fluxes crossing the boundary of the region

$$\iiint_{\mathcal{V}} \nabla \cdot \mathbf{F}\, dV = \oiint_{\mathcal{S}} \hat{\mathbf{n}} \cdot \mathbf{F}\, dS, \tag{3.82}$$

where $\mathcal{V}$ is an arbitrary volume of fluid, $\mathcal{S}$ is the boundary of $\mathcal{V}$, and $\hat{\mathbf{n}}$ is the outward normal on the boundary. Hence, by integrating a flux divergence (negative of the convergence) over a chosen volume (left hand side), one can garner mechanistic insight into the impacts from various physical processes in that region, without having to make direct use of flux components (right hand side).

3.7 Vertical/dianeutral SGS parameterizations

Thus far, we have recommended some fields that provide insight into the workings of various ocean subgrid scale (SGS) parameterizations. Table 2.11 presents additional fields to further characterize the parameterizations and their impact on the simulation, with focus on the vertical/dianeutral SGS parameterizations. In Section 3.7, we present fields helping to characterize lateral SGS parameterizations in the ocean models (see Table 2.12). In both cases, the CMIP6 request is *less* than for CMIP5.

There is one limitation of the fields requested here that is worth highlighting. Although we recommend saving diffusivities and work terms, what is of more fundamental importance for characterizing the effects the SGS has on a field is the flux that it produces. Many fluxes are formulated as a diffusivity times a gradient. However, some parameterizations of fluxes are not expressed as such. Indeed, downgradient diffusion is not a good model for many SGS processes. It is for this reason that we ask for "buoyancy work from sgs parameterization" rather than just that from diffusivity. More generally, the protocols for saving fluxes rather than diffusivities and work need to be developed as more nontrivial SGS parameterizations become common.

3.7.1 Vertical/dianeutral tracer diffusivities

- ocean_vertical_heat_diffusivity = difvho
- ocean_vertical_salt_diffusivity = difvso

Vertical/dianeutral tracer diffusivities used in modern CMIP models typically consist of a static background value and a dynamically determined value. For the background diffusivity, some modelers choose a globally constant value, whereas others impose spatial dependence. There is evidence that the background diffusivity influences such processes as ENSO variability and overturning strength in model simulations. Hence, it is very important to have this field archived.

There are an increasingly large number of physical processes used by CMIP-class models that affect the vertical tracer diffusivity. For example, vigorous mixing processes in the upper ocean are associated with large mixing coefficients; more quiescent processes in the ocean pycnocline region lead to much smaller coefficients; and enhanced mixing near the ocean bottom generally increases the mixing coefficients. For CMIP6, we are asking for the net diffusivity resulting from the accumulation of all these processes.

It is difficult to anticipate the full suite of physical processes affecting the vertical/dianeutral diffusivity. As a start, we identify the following processes that are commonly found in CMIP class models, whose corresponding diffusivities would be of use in the CMIP6 archive:

- Static background tracer diffusivity meant to parameterize the background internal wave field;
- Tidal induced tracer diffusivity, with all relevant tidal constituents contributing to the mixing (e.g., Simmons et al., 2004; Lee et al., 2006);
- Boundary layer diffusivity meant to parameterize mixing at or near the ocean boundaries.
- Total vertical/dianeutral diffusivity for temperature and salinity associated with all physical processes, including the background diffusivity.

The background, tidal, and boundary layer diffusivities are the same for temperature, salinity, and other tracers. The total diffusivities may differ, however, if including a parameterization of double diffusive processes. In many implementations of boundary layer processes, the effects from double diffusion are wrapped into the boundary layer diffusivities. Hence, we write the diffusivities κ for temperature and salinity in the following form

$$\kappa^{\theta} = \kappa_{\text{back}} + \kappa_{\text{tides}} + \kappa^{\theta}_{\text{boundary+dd}} \tag{3.83}$$

$$\kappa^{S} = \kappa^{S}_{\text{back}} + \kappa_{\text{tides}} + \kappa^{S}_{\text{boundary+dd}} \tag{3.84}$$

We request archival of just the net diffusivities

- κ^{θ}= ocean_vertical_heat_diffusivity
- κ^{S}= ocean_vertical_salt_diffusivity.

3.7.2 Rate of work done against stratification

- tendency_of_ocean_potential_energy_content = tnpeo

A vertical/dianeutral diffusivity impacts the solution only in regions where there are nontrivial vertical tracer gradients. A measure of the impact can be deduced by mapping the rate at which work is done against the stratification by the tracer diffusivity. This work against stratification also impacts the potential energy budget, hence the name for the variables. We recommend mapping this work rate per horizontal area as a three-dimensional field.

Theoretical considerations

The non-negative rate of work done against stratification by vertical/dianeutral diffusion of density is given by

$$\mathcal{P} \equiv \int \kappa_{\text{d}} N^2 \rho \, \text{d}V, \tag{3.85}$$

where N^2 is the squared buoyancy frequency and κ_{d} is the vertical/dianeutral diffusivity corresponding to a particular SGS process. Equation (3.85) assumes the heat and salt diffusivities are the same, which is the case for tidal and background diffusivities. However, the full heat diffusivity, $\kappa^{\theta}_{\text{d}}$, and salt diffusivity, κ^{S}_{d}, can differ through the effects from double diffusion. In this case, we may wish to split the integral as follows

$$\mathcal{P} \equiv -g \int \left(\kappa^{\theta}_{\text{d}} \frac{\partial \rho}{\partial \theta} \frac{\partial \theta}{\partial z} + \kappa^{S}_{\text{d}} \frac{\partial \rho}{\partial S} \frac{\partial S}{\partial z} \right) \text{d}V. \tag{3.86}$$

In the following, we refer to the form (3.85) for brevity, but recommend the more general form (3.86) when distinguishing heat and salt diffusivities.

We request that this work term should be archived as a two-dimensional map of depth integrated mixing work

$$\text{rate of work against stratification per horiz area from vertical diffusion}(\text{W/m}^2) = \int_{-H}^{\eta} \kappa_{\text{d}} N^2 \rho \, \text{d}z. \tag{3.87}$$

Horizontal maps of the column integrated work can thus be compared with this field. This depth integrated field also provide a means for directly comparing the work done by diffusion against the heat fluxes crossing the ocean boundaries. Furthermore, multiplication by the horizontal grid area, then summing over the globe, provides the global amount of work done by mixing. If there are sufficient contributions of this field for CMIP6, we anticipate future CMIPs to request the three-dimensional field $\kappa_{\text{d}} \rho N^2$, providing the work per volume from vertical mixing.

3.8 Lateral SGS parameterizations

In this section, we present fields helping to characterize lateral SGS parameterizations in the ocean, with Table 2.12 summarizing the fields. As for the vertical/dianeutral SGS parameterizations, we propose that dominant scientific use of the fields discussed in this subsection are realized by archiving *just* the annual mean fields.

3.8.1 Lateral tracer diffusivities

- ocean_tracer_diffusivity_due_to_parameterized_mesoscale_advection = diftrblo
- ocean_tracer_epineutral_laplacian_diffusivity = diftrelo

It is important to archive diffusivities used for neutral diffusion (Solomon, 1971; Redi, 1982), and eddy-induced transport (Gent and McWilliams, 1990; Gent et al., 1995). We thus ask for the following diffusivities to be archived for CMIP6:

- ocean_tracer_diffusivity_due_to_parameterized_mesoscale_advection = eddy induced advective transport diffusivity for a Laplacian operator;
- ocean_tracer_epineutral_laplacian_diffusivity = epineutral or isopycnal diffusivity for a Laplacian operator;

Note that for isopyncal models, the distinction between epineutral and along-coordinate diffusivities is often blurred, though there is in general a distinction. Also note that the diffusivity ocean_tracer_diffusivity_due_to_parameterized_mesoscale_advection was formerly called ocean_tracer_bolus_laplacian_diffusivity in CMIP5. The CMIP5 name, with the term "bolus", is not appropriate physically (see Hirst and McDougall (1998)).

3.8.2 Eddy kinetic energy source from Gent et al. (1995)

- tendency_of_ocean_eddy_kinetic_energy_content_due_to_parameterized_eddy_advection = tnkebto

An energetic analysis of the extraction of potential energy from the Gent and McWilliams (1990); Gent et al. (1995) scheme indicates that it affects an increase in the eddy kinetic energy (Aiki and Richards, 2008). The rate of eddy kinetic energy increase, per unit horizontal area over an ocean column, is

$$\text{rate of eddy kinetic energy increase from GM per unit horiz area}(\text{W/m}^2) = \int_{-H}^{\eta} \kappa\,(N\,S)^2\,\rho\,\text{dz}. \tag{3.88}$$

In this expression, N is the buoyancy frequency, S is the magnitude of the neutral slope, κ is the diffusivity setting the overall strength of the parameterization, $\rho\,\text{dz}$ is the grid cell mass per horizontal area, with dz the cell thickness. In a Boussinesq model, the *in situ* density factor should be set to the constant Boussinesq reference density ρ_o used by the model. Note that the CMIP5 request asked for the full three-dimensional field, whereas for CMIP6 we only ask for the depth integrated two-dimensional field, in hopes that there will be more submissions of this diagnostic. If there are sufficient contributions of this field for CMIP6, we anticipate future CMIPs to request the three-dimensional field $\kappa\,(N\,S)^2\,\rho$, providing the work per volume from GM.

Horizontal maps of the column integrated work from the GM mesoscale parameterization (3.88) can be readily compared across the suite of CMIP models. This depth integrated field also provide a means for directly comparing the work done by vertical diffusion (Section 3.7.2). Furthermore, multiplication by the horizontal grid area, then summing over the globe, provides the global amount of work associated with GM.

3.8.3 Lateral momentum viscosities

- ocean_momentum_xy_laplacian_diffusivity = difmxylo
- ocean_momentum_xy_biharmonic_diffusivity = difmxybo

We do not make the distinction between various methods used to compute the lateral momentum viscosities. Hence, we only recommend the total fields be archived from the ocean models in CMIP6:

- ocean_momentum_xy_laplacian_diffusivity = total lateral momentum Laplacian diffusivity
- ocean_momentum_xy_biharmonic_diffusivity = total lateral momentum biharmonic diffusivity.

3.8.4 Kinetic energy dissipation by lateral viscosity

- ocean_kinetic_energy_dissipation_per_unit_area_due_to_xy_friction = dispkexyfo

As for the vertical/dianeutral viscosity, we recommend archiving the maps of energy dissipation integrated over a full ocean column, induced by the total lateral viscous friction.

Theoretical considerations

The local energy dissipated in a hydrostatic model by a lateral Laplacian friction with isotropic viscosity A and anisotropic viscosity D (see Section 17.8.2 of Griffies, 2004) is given by the non-positive quantity

$$\mathcal{D} = -(\rho \, dV) \left[A \, (e_T^2 + e_S^2) + 2 \, D \, \Delta^2 \right], \tag{3.89}$$

where $e_T = (dy)(u/dy)_{,x} - (dx)(v/dx)_{,y}$ and $e_S = (dx)(u/dx)_{,y} + (dy)(v/dy)_{,x}$ are the deformation rates, θ is an angle that sets the alignment of the generally anisotropic viscosity (Large et al., 2001; Smith and McWilliams, 2003), $2\Delta = e_S \cos 2\theta - e_T \sin 2\theta$, and dx and dy are the horizontal grid elements. We recommend archiving depth integrated dissipation per horizontal area

$$\text{dissipation per horiz area from lateral laplacian friction}(W/m^2) = -\int_{-H}^{\eta} (\rho \, dz) \left[A \, (e_T^2 + e_S^2) + 2 \, D \, \Delta^2 \right]. \tag{3.90}$$

The local energy dissipated in a hydrostatic model by a lateral biharmonic friction is given by the non-positive quantity (see Section 17.9.2 of Griffies, 2004)

$$\mathcal{D} = -(\rho \, dV) \, \mathbf{F} \cdot \mathbf{F}, \tag{3.91}$$

where $\rho \, dV \, \mathbf{F}$ is the lateral Laplacian friction vector used to build up the biharmonic operator. As for the dissipation from vertical viscosity, we recommend mapping the dissipation per horizontal area for each column of seawater, as given by

$$\text{dissipation per horizontal area from lateral biharmonic friction}(W/m^2) = -\int_{-H}^{\eta} (\rho \, dz) \, \mathbf{F} \cdot \mathbf{F}. \tag{3.92}$$

Notes

[9] Most ocean models do not add or remove mass associated with the transfer of material tracers across the ocean surface.

[10] Contrary to the dynamic sea level η_{cmip} considered in Section 3.2.7, we are interested here in the evolution of the global mean of the sea level η, with this global mean distinctly nonzero due to thermosteric effects.

[11] We discuss issues related to salinity and TEOS-10 in Section 1.7.2.

[12] The density factor ρ in a non-Boussinesq fluid becomes the constant ρ_o for Boussinesq fluids.

[13] WGCM (2007) recommend partitioning the poleward overturning streamfunction into the Atlantic, Pacific, and Indian Oceans. However, to separate the Indian and Pacific Oceans is not sensible, since there is no meridional boundary separating these basins. Instead, the Atlantic-Arctic, Indian-Pacific, and World Ocean are physically relevant, and thus are recommended here. We make the same recommendation for the partioning of $\hat{\mathbf{y}}$-ward tracer transport into basins.

[14] We choose not to recommend plotting overturning on the neutral density coordinate from McDougall and Jackett (2005) in order to facilitate direct comparison of the density overturning streamfunction between isopycnal models, which are based on σ_{2000}, and non-isopycnal models.

[15] Some of the observed mass transport values need to be updated.

[16] Note that in CMIP5, there was a mistake in the variables Xcel spread-sheet, with rsdo incorrectly listed as rsds, with rsds an atmospheric field.

[17] Sources are trivial to add to the formulation, with sources critical for the treatment of biogeochemical tracers. As sources do not contribute to the evolution of heat and salt, we omit sources to reduce clutter.

[18] We use Θ in this section, as appropriate for TEOS-10 models. For preTEOS-10 models, they should archive tendencies appearing in the potential temperature, θ equation. See Section 1.7.2 for discussion.

Chapter 4

Loose ends

We highlight certain questions that remain unanswered by this document. These questions generally aim to support those analysts pursuing process-level mechanistic understanding of model results.

- **Eddy statistics**: Ocean model resolutions of 1/4° or finer are actively being considered by various groups for CMIP6, and no doubt finer grids will be used afterward. In this document, we made no comment on the needs for sampling fields to develop robust eddy statistics. However, by archiving budget terms (Table 2.10 and Section 3.6), in particular the convergence of tracer advective fluxes, as well as native mass transport and native tracer fields, we enable the inference of eddy flux convergences as considered in, for example, Griffies et al. (2014). Nonetheless, further work is required to prescribe general recommendations suitable for a model comparison project, particularly with the aim to have the eddy statistics span model vertical grid choices.
- **3d Term Balances**: A mechanistic understanding of ocean processes typically requires the analysis of detailed budget terms, in addition to boundary forcing. For tracer budgets, one generally requires grid cell tendencies from advection and all SGS processes. Notably, CMIP6 requested, for the first time, terms from the heat and salt budgets (Section 3.6). However, these budgets are only a start.
  - There are more refined budgets available than requested here, with terms to be split apart to garner even more detailed budget information.
  - There are other tracer budgets that may be considered, particularly for biogeochemical tracers, where interior sources and sinks are also of central importance. Details for heat and salt budgets identified here will be of use for the ocean biogeochemical diagnostics saved in CMIP6.
  - Momentum budgets are absent here. Such budgets require information about forces and transport processes acting to alter momentum.
  - One may wish to consider budgets for other dynamically relevant fields, such as potential vorticity.
  - Budgets are of interest over certain time dependent regions, such as the upper ocean mixed layer. We did not address this issue here.

References

Adcroft, A. and Campin, J.-M.: Rescaled height coordinates for accurate representation of free-surface flows in ocean circulation models, Ocean Modelling, 7, 269–284, 2004.

Aiki, H. and Richards, K.: Energetics of the global ocean: the role of layer-thickness form drag, Journal of Physical Oceanography, 38, 1845–1869, 2008.

Arbic, B.: Atmospheric forcing of the oceanic semidiurnal tide, Geophysical Research Letters, 32, L02610, doi:10.1029/2004GL021 668, 2005.

Bates, M., Griffies, S. M., and England, M.: A dynamic, embedded Lagrangian model for ocean climate models, Part II: Idealised overflow tests, Ocean Modelling, 59-60, 60–76, 2012.

Beckmann, A. and Döscher, R.: A method for improved representation of dense water spreading over topography in geopotential-coordinate models, Journal of Physical Oceanography, 27, 581–591, 1997.

Bryan, F., Danabasoglu, G., Gent, P., and Lindsay, K.: Changes in ocean ventilation during the 21st century in the CCSM3, Ocean Modelling, 15, 141–156, 2006.

Bryan, F. O.: The axial angular momentum balance of a global ocean general circulation model, Dynamics of Atmospheres and Oceans, 25, 191–216, 1997.

Bryan, K.: A numerical method for the study of the circulation of the world ocean, Journal of Computational Physics, 4, 347–376, 1969.

Campin, J.-M. and Goosse, H.: Parameterization of density-driven downsloping flow for a coarse-resolution ocean model in z-coordinate, Tellus, 51A, 412–430, 1999.

Campin, J.-M., Marshall, J., and Ferreira, D.: Sea ice-ocean coupling using a rescaled vertical coordinate z^*, Ocean Modelling, 24, 1–14, 2008.

Cheung, W. W. L., Sarmiento, J. L., Dunne, J. P., Frölicher, T. L., Lam, V. W. Y., Palomares, M. L. D., Watson, R., and Pauly, D.: Shrinking of fishes exacerbates impacts of global ocean changes on marine ecosystems, Nature Climate Change, 3, 2013.

Church, J., White, N., Konikow, L., Domingues, C., Cogley, J., Rignot, E., Gregory, J., van den Broeke, M., Monaghan, A., and Velicogna, I.: Revisiting the Earth's sea-level and energy budgets from 1961 to 2008, Geophysical Research Letters, 38, L18601, doi:10.1029/2011GL048 794, 2011.

Church, J., White, N., Domingues, C., and Monselesan, D.: Sea-level change and ocean heat-content change, in Ocean Circulation and Climate, 2nd Edition: A 21st Century Perspective, edited by G. Siedler, S. M. Griffies, J. Gould, and J. Church, vol. 103 of International Geophysics Series, Academic Press, 2013.

Conkright, M., Antonov, J., Baranova, O., Boyer, T., Garcia, H., Gelfeld, F., Johnson, D., Locarnini, R., Murphy, P., O'Brien, T., Smolyar, I., and Stephens, C.: World Ocean Database 2001, Volume 1: Introduction, NOAA Atlas NESDIS 42, U.S. Government Printing Office 13, NOAA, Washington, D.C., 167 pp., 2002.

Cox, M. D.: A Primitive Equation, 3-Dimensional Model of the Ocean, NOAA/Geophysical Fluid Dynamics Laboratory, Princeton, USA, 1984.

Cunningham, S., Alderson, S., King, B., and Brandon, M.: Transport and variability of the Antarctic Circumpolar Current in Drake Passage, Journal of Geophysical Research, 108, Art. 8084, 2003.

Danabasoglu, G., Large, W., and Briegleb, B.: Climate impacts of parameterized Nordic Sea overflows, Journal of Geophysical Research, 115, C11005, doi:10.1029/2010JC006 243, 2010.

Danabasoglu, G., Yeager, S. G., Bailey, D., Behrens, E., Bentsen, M., Bi, D., Biastoch, A., Böning, C. W., Bozec, A., Canuto, V. M., Cassou, C., Chassignet, E., Coward, A. C., Danilov, S., Diansky, N., Drange, H., Farneti, R., Fernandez, E., Fogli, P. G., Forget, G., Fujii, Y., Griffies, S. M., Gusev, A., Heimbach, P., Howard, A., Jung, T., Kelley, M., Large, W. G., Leboissetier, A., Lu, J., Madec, G., Marsland, S. J., Masina, S., Navarra, A., Nurser, A. G., Pirani, A., y Mélia, D. S., Samuels, B. L., Scheinert, M., Sidorenko, D., Treguier, A.-M., Tsujino, H., Uotila, P., Valcke, S., Voldoire, A., and Wang, Q.: North Atlantic simulations in Coordinated Ocean-ice Reference Experiments phase II (CORE-II). Part I: Mean states, Ocean Modelling, 73, 76–107, http://www.sciencedirect.com/science/article/pii/S1463500313001868, 2014.

de Boyer Montégut, C., Madec, G., Fischer, A., Lazar, A., and Iudicone, D.: Mixed layer depth over the global ocean: An examination of profile data and a profile based climatology, Journal of Geophysical Research, 109, doi:10.1029/2004JC002 378, 2004.

Delworth, T. L., Broccoli, A. J., Rosati, A., Stouffer, R. J., Balaji, V., Beesley, J. A., Cooke, W. F., Dixon, K. W., Dunne, J., Dunne, K. A., Durachta, J. W., Findell, K. L., Ginoux, P., Gnanadesikan, A., Gordon, C., Griffies, S. M., Gudgel, R., Harrison, M. J., Held, I. M., Hemler, R. S., Horowitz, L. W., Klein, S. A., Knutson, T. R., Kushner, P. J., Langenhorst, A. L., Lee, H.-C., Lin, S., Lu, L., Malyshev, S. L., Milly, P., Ramaswamy, V., Russell, J., Schwarzkopf, M. D., Shevliakova, E., Sirutis, J., Spelman, M., Stern, W. F., Winton, M., Wittenberg, A. T., Wyman, B., Zeng, F., and Zhang, R.: GFDL's CM2 Global Coupled Climate Models - Part 1: Formulation and Simulation Characteristics, Journal of Climate, 19, 643–674, 2006.

DeSzoeke, R. A. and Samelson, R. M.: The duality between the Boussinesq and Non-Boussinesq Hydrostatic Equations of Motion, Journal of Physical Oceanography, 32, 2194–2203, 2002.

Downes, S. M. and Hogg, A. M.: Southern Ocean circulation and eddy compensation in CMIP5 models, Journal of Climate, 26, 7198–7220, 2013.

Dukowicz, J. K. and Smith, R. D.: Implicit free-surface method for the Bryan-Cox-Semtner ocean model., Journal of Geophysical Research, 99, 7991–8014, 1994.

Dutay, J.-C., Bullister, J., Doney, S., Orr, J., Najjar, R., Caldeira, K., Campin, J.-M., Drange, H., Follows, M., Gao, Y., Gruber, N., Hecht, M., Ishida, A., Joos, F., Lindsay, K., Madec, G., Maier-Reimer, E., Marshall, J., Matear, R., Monfray, P., Mouchet, A., Plattner, G.-K., Sarmiento, J., Schlitzer, R., Slater, R., Totterdell, I., Weirig, M.-F., Yamanaka, Y., and Yool, A.: Evaluation of ocean model ventilation with CFC-11: comparison of 13 global ocean models, Ocean Modelling, 4, 89–120, 2002.

England, M. H.: The age of water and ventilation timescales in a global ocean model, Journal of Physical Oceanography, 25, 2756–2777, 1995.

Exarchou, E., Kuhlbrodt, T., Gregory, J., and Smith, R.: Ocean Heat Uptake Processes: A Model Intercomparison, Climate Dynamics, submitted, 2014.

Fissel, D., Birch, J., Melling, H., and Lake, R.: Non-tidal flows in the Northwest Passage, in Canadian Technical Report of Hydrography and Ocean Sciences, p. 142pp, Institute of Ocean Sciences, Sidney, Canada, 1998.

Fox-Kemper, B., Ferrari, R., and Hallberg, R.: Parameterization of mixed layer eddies. I: Theory and diagnosis, Journal of Physical Oceanography, 38, 1145–1165, 2008.

Fox-Kemper, B., Danabasoglu, G., Ferrari, R., Griffies, S. M., Hallberg, R. W., Holland, M., Peacock, S., and Samuels, B.: Parameterization of Mixed Layer Eddies. III: Global Implementation and Impact on Ocean Climate Simulations, Ocean Modelling, 39, 61–78, 2011.

Gehlen, M. and Dunne, J. P.: Projected pH reductions by 2100 might put deep North Atlantic biodiversity at risk, Biogeosciences Discussions, 2014.

Gent, P. R. and McWilliams, J. C.: Isopycnal mixing in ocean circulation models, Journal of Physical Oceanography, 20, 150–155, 1990.

Gent, P. R., Willebrand, J., McDougall, T. J., and McWilliams, J. C.: Parameterizing eddy-induced tracer transports in ocean circulation models, Journal of Physical Oceanography, 25, 463–474, 1995.

Gill, A.: Atmosphere-Ocean Dynamics, vol. 30 of International Geophysics Series, Academic Press, London, 662 + xv pp, 1982.

Gnanadesikan, A., Russell, J., and Zeng, F.: How does ocean ventilation change under global warming?, Ocean Science, 3, 43–53, 2007.

Goldsbrough, G.: Ocean currents produced by evaporation and precipitation, Proceedings of the Royal Society of London, A141, 512–517, 1933.

Gordon, A., Susanto, R., and Vranes, K.: Cool Indonesian throughflow as a consequence of restricted surface layer flow, Nature, 425, 824–828, 2003.

Graham, F. and McDougall, T.: Quantifying the nonconservative production of Conservative Temperature, potential temperature, and entropy, Journal of Physical Oceanography, 43, 838–862, 2013.

Greatbatch, R. J.: A note on the representation of steric sea level in models that conserve volume rather than mass, Journal of Geophysical Research, 99, 12 767–12 771, 1994.

Gregory, J.: Vertical heat transports in the ocean and their effect on time-dependent climate change, Climate Dynamics, 15, 501–515, 2000.

Gregory, J., Church, J., Boer, G., Dixon, K., Flato, G., Jackett, D., Lowe, J., O'Farrell, S., Roeckner, E., Russell, G., Stouffer, R., and Winton, M.: Comparison of results from several AOGCMs for global and regional sea-level change 1900–2100, Climate Dynamics, 18, 225–240, 2001.

Gregory, J., White, N., Church, J., Bierkens, M., Box, J., van den Broeke, R., Cogley, J., Fettweis, X., Hanna, E., Huybrechts, P., Konikow, L., Leclercq, P., Marzeion, B., Orelemans, J., Tamisiea, M., Wada, Y., Wake, L., and van den Wal, R.: Twentieth-century global-mean sea-level rise: is the whole greater than the sum of the parts?, Journal of Climate, pp. 4476–4499, 2013.

Griffies, S. M.: The Gent-McWilliams skew-flux, Journal of Physical Oceanography, 28, 831–841, 1998.

Griffies, S. M.: Fundamentals of Ocean Climate Models, Princeton University Press, Princeton, USA, 518+xxxiv pages, 2004.

Griffies, S. M. and Greatbatch, R. J.: Physical processes that impact the evolution of global mean sea level in ocean climate models, Ocean Modelling, 51, 37–72, 2012.

Griffies, S. M. and Treguier, A.-M.: Ocean Models and Ocean Modeling, in Ocean Circulation and Climate, 2nd Edition: A 21st Century Perspective, edited by G. Siedler, S. M. Griffies, J. Gould, and J. Church, vol. 103 of International Geophysics Series, Academic Press, 2013.

Griffies, S. M., Gnanadesikan, A., Pacanowski, R. C., Larichev, V., Dukowicz, J. K., and Smith, R. D.: Isoneutral diffusion in a z-coordinate ocean model, Journal of Physical Oceanography, 28, 805–830, 1998.

Griffies, S. M., Pacanowski, R., Schmidt, M., and Balaji, V.: Tracer Conservation with an Explicit Free Surface Method for z-coordinate Ocean Models, Monthly Weather Review, 129, 1081–1098, 2001.

Griffies, S. M., Gnanadesikan, A., Dixon, K. W., Dunne, J. P., Gerdes, R., Harrison, M. J., Rosati, A., Russell, J., Samuels, B. L., Spelman, M. J., Winton, M., and Zhang, R.: Formulation of an ocean model for global climate simulations, Ocean Science, 1, 45–79, 2005.

Griffies, S. M., Adcroft, A. J., Aiki, H., Balaji, V., Bentson, M., Bryan, F., Danabasoglu, G., Denvil, S., Drange, H., England, M., Gregory, J., Hallberg, R., Legg, S., Martin, T., McDougall, T. J., Pirani, A., Schmidt, G., Stevens, D., Taylor, K., and Tsujino, H.: Sampling Physical Ocean Fields in WCRP CMIP5 Simulations, vol. available from http://www-pcmdi.llnl.gov, ICPO Publication Series 137, WCRP Informal Report No. 3/2009, 2009a.

Griffies, S. M., Biastoch, A., Böning, C. W., Bryan, F., Danabasoglu, G., Chassignet, E., England, M. H., Gerdes, R., Haak, H., Hallberg, R. W., Hazeleger, W., Jungclaus, J., Large, W. G., Madec, G., Pirani, A., Samuels, B. L., Scheinert, M., Gupta, A. S., Severijns, C. A., Simmons, H. L., Treguier, A. M., Winton, M., Yeager, S., and Yin, J.: Coordinated Ocean-ice Reference Experiments (COREs), Ocean Modelling, 26, 1–46, 2009b.

Griffies, S. M., Winton, M., Anderson, W. G., Benson, R., Delworth, T. L., Dufour, C., Dunne, J. P., Goddard, P., Morrison, A. K., Rosati, A., Wittenberg, A. T., and Yin, J.: Impacts on ocean heat from transient mesoscale eddies in a hierarchy of climate models, Journal of Climate, accepted, 2014.

Griffies, S. M., Yin, J., Durack, P. J., Goddard, P., Bates, S., Behrens, E., Bentsen, M., Bi, D., Biastoch, A., Böning, C., Bozec, A., Cassou, C., Chassignet, E., Danabasoglu, G., Danilov, S., Domingues, C., Drange, H., Farneti, R., Fernandez, E., Greatbatch, R. J., Holland, D. M., Ilicak, M., Lu, J., Marsland, S. J., Mishra, A., Large, W. G., Lorbacher, K., Nurser, A. G., Salas y Mélia, D., Palter, J. B., Samuels, B. L., Schröter, J., Schwarzkopf, F. U., Sidorenko, D., Treguier, A.-M., heng Tseng, Y., Tsujino, H., Uotila, P., Valcke, S., Voldoire, A., Wang, Q., Winton, M., and Zhang, Z.: An assessment of global and regional sea level for years 1993-2007 in a suite of interannual CORE-II simulations, Ocean Modelling, 78, 35–89, 2014.

Hirst, A. C. and McDougall, T. J.: Meridional overturning and dianeutral transport in a z-coordinate ocean model including eddy-induced advection,, Journal of Physical Oceanography, 28, 1205–1223, 1998.

Huang, R. X.: Real freshwater flux as a natural boundary condition for the salinity balance and thermohaline circulation forced by evaporation and precipitation, Journal of Physical Oceanography, 23, 2428–2446, 1993.

Huang, R. X. and Schmitt, R. W.: Goldsbrough-Stommel circulation of the World Oceans, Journal of Physical Oceanography, 23, 1277–1284, 1993.

Huang, R. X., Jin, X., and Zhang, X.: An oceanic general circulation model in pressure coordinates, Advances in Atmospheric Physics, 18, 1–22, 2001.

IOC, SCOR, and IAPSO: The international thermodynamic equation of seawater-2010: calculation and use of thermodynamic properties, Intergovernmental Oceanographic Commission, Manuals and Guides No. 56, UNESCO, available from http://www.TEOS-10.org, 196pp, 2010.

Jongma, J., Driesschaert, E., Fichefet, T., Goosse, H., and Renssen, H.: The effect of dynamic-thermodynamic icebergs on the Southern Ocean climate in a three-dimensional model, Ocean Modelling, 26, 104–113, 2009.

Key, R., Kozyr, A., Sabine, C., Lee, K., Wanninkhof, R., Bullister, J., Feely, R., Millero, F., Mordy, C., and Peng, T.-H.: A global ocean carbon climatology: results from GLODAP, Global Biogeochemical Cycles, 18, GB4031, 2004.

Kopp, R. E., Mitrovica, J. X., Griffies, S. M., Yin, J., Hay, C. C., and Stouffer, R. J.: The impact of Greenland melt on regional sea level: a preliminary comparison of dynamic and static equilibrium effects, Climatic Change Letters, 103, 619–625, 2010.

Kuhlbrodt, T. and Gregory, J. M.: Ocean heat uptake and its consequences for the magnitude of sea level and climate change, Geophysical Research Letters, 38, L18608, doi: 10.1029/2012GL052 952, 2012.

Kuhlbrodt, T., Gregory, J. M., and Shaffrey, L.: A process-based analysis of ocean heat uptake in an AOGCM with an eddy-permitting ocean component, Climate Dynamics, submitted, 2014.

Large, W., McWilliams, J., and Doney, S.: Oceanic vertical mixing: a review and a model with a nonlocal boundary layer parameterization, Reviews of Geophysics, 32, 363–403, 1994.

Large, W. G., Danabasoglu, G., McWilliams, J. C., Gent, P. R., and Bryan, F. O.: Equatorial circulation of a global ocean climate model with anisotropic horizontal viscosity, Journal of Physical Oceanography, 31, 518–536, 2001.

Leaman, K., Molinari, R., and Vertes, P.: Structure and variability of the Florida Current at 27N: April 1982-July 1984, Journal of Physical Oceanography, 17, 565–583, 1987.

Lee, H.-C., Rosati, A., and Spelman, M.: Barotropic tidal mixing effects in a coupled climate model: Oceanic conditions in the northern Atlantic, Ocean Modelling, 3-4, 464–477, 2006.

Levitus, S.: Climatological atlas of the world ocean, U.S. Government Printing Office 13, NOAA, Washington, D.C., 163 pp., 1982.

Lewis, E. and Perkin, R.: The Practical Salinity Scale 1978: conversion of existing data, Deep Sea Research, 28A, 307–328, 1981.

Lorbacher, K., Dommenget, D., Niiler, P. P., and Köhl, A.: Ocean mixed layer depth: A subsurface proxy of ocean-atmosphere variability, Journal of Geophysical Research, 111-C07010, doi:10.1029/2003JC002 157, 2006.

Losch, M., Adcroft, A., and Campin, J.-M.: How sensitive are coarse general circulation models to fundamental approximations in the equations of motion?, Journal of Physical Oceanography, 34, 306–319, 2004.

Lowe, J. A. and Gregory, J. M.: Understanding projections of sea level rise in a Hadley Centre coupled climate model, Journal of Geophysical Research: Oceans, 111, n/a–n/a, http://dx.doi.org/10.1029/2005JC003421, 2006.

Lukas, R. and Firing, E.: The geostrophic balance of the Pacific equatorial undercurrent, Deep-Sea Research, 31, 61–66, 1984.

Madec, G. and Imbard, M.: A global ocean mesh to overcome the North Pole singularity, CD, 12, 381–388, 1996.

Manizza, M., Le Quere, C., Watson, A., and Buitenhuis, E.: Bio-optical feedbacks among phytoplankton, upper ocean physics and sea-ice in a global model, Geophysical Research Letters, 32, doi:10.1029/2004GL020 778, 2005.

Marshall, J., Adcroft, A., Campin, J.-M., Hill, C., and White, A.: Atmosphere-Ocean modeling exploiting fluid isomorphisms, Monthly Weather Review, 132, 2882–2894, 2004.

Martin, T. and Adcroft, A.: Parameterizing the fresh-water flux from land ice to ocean with interactive icebergs in a coupled climate model, Ocean Modelling, 34, 111–124, 2010.

McAvaney, B., Covey, C., Joussaume, S., Kattsov, V., Kitoh, A., Ogana, W., Pitman, A. J., Weaver, A. J., Wood, R. A., Zhao, Z.-C., AchutaRao, K., Arking, A., Barnston, A., Betts, R., Bitz, C., Boer, G., Braconnot, P., Broccoli, A., Bryan, F., Claussen, M., Colman, R., Delecluse, P., Genio, A. D., Dixon, K., Duffy, P., Dmenil, L., England, M., Fichefet, T., Flato, G., Fyfe, J. C., Gedney, N., Gent, P., Genthon, C., Gregory, J., Guilyardi, E., Harrison, S., Hasegawa, N., Holland, G., Holland, M., Jia, Y., Jones, P. D., Kageyama, N., Keith, D., Kodera, K., Kutzbach, J., Lambert, S., Legutke, S., Madec, G., Maeda, S., Mann, M. E., Meehl, G., Mokhov, I., Motoi, T., Phillips, T., Polcher, J., Potter, G. L., Pope, V., Prentice, C., Roff, G., Semazzi, F., Sellers, P., Stensrud, D. J., Stockdale, T., Stouffer, R., Taylor, K. E., Trenberth, K., Tol, R., Walsh, J., Wild, M., Williamson, D., Xie, S.-P., Zhang, X.-H., , and Zwiers, F.: Model Evaluation, in Climate Change 2001: The Scientific Basis. Contribution of Working Group I to the Third Assessment Report of the Intergovernmental Panel on Climate Change, pp. 472–523, Cambridge University Press, Cambridge, UK, 2001.

McDougall, T. J.: Potential enthalpy: a conservative oceanic variable for evaluating heat content and heat fluxes, Journal of Physical Oceanography, 33, 945–963, 2003.

McDougall, T. J. and Jackett, D. R.: The material derivative of neutral density, Journal of Marine Research, 63, 159–185, 2005.

McDougall, T. J., Barker, P. M., Feistel, R., and Galton-Fenzi, B. K.: Melting of Ice and Sea Ice into Seawater and Frazil Ice Formation, Journal of Physical Oceanography, 44, 1751–1775, 2014.

Melet, A., Hallberg, R., Legg, S., and Polzin, K.: Sensitivity of the Pacific Ocean state to the vertical distribution of internal-tide driven mixing, Journal of Physical Oceanography, 43, 602–615, 2013.

Melling, H.: Exchanges of freshwater through the shallow straits of the North American Arctic, in The freshwater budget of the Arctic Ocean, pp. 472–523, Kluwer Academic Publisher, 2000.

MERCATOR: List of internal metrics for the MERSEA-GODAE Global Ocean: Specification for implementation, in Integrated System Design and Assessment, France, 2006.

Monterey, G. and Levitus, S.: Climatological cycle of mixed layer depth in the world ocean, U.S. government printing office, NOAA NESDIS, Washington, D.C., 5 pp., 1997.

Munk, W.: Ocean freshening, sea level rising, Science, 300, 2041–2043, 2003.

Murray, R.: Explicit generation of orthogonal grids for ocean models, Journal of Computational Physics, 126, 251–273, 1996.

Olsen, S., Hansen, B., Quadfasel, D., and Osterhus, S.: Observed and modelled stability of overflow across the Greenland-Scotland ridge, Nature, 455, doi:10.1038/nature07 302, 2008.

Osterhus, S., Turrell, W., Jonsson, S., and Hansen, B.: Measured volume, heat, and salt fluxes from the Atlantic to the Arctic Mediterranean, Geophysical Research Letters, 32, doi:10.1029/2004GL022 188, 2005.

Otto, A., Otto, F., Boucher, O., Church, J., Hegerl, G., Forster, P., Gillett, N., Gregory, J., Johnson, G., Knutti, R., Lewis, N., Lohmann, U., Marotzke, J., Myhre, G., Shindell, D., Stevens, B., and Allen, M.: Energy budget constraints on climate response, Nature Geosciences, 6, 415–416, 2013.

Otto, L., Zimmerman, J., Furnes, G., Mork, M., Saetre, R., and Becker, G.: Review of the physical oceanography of the North Sea, Netherlands Journal of Sea Research, 26, 161–238, 1990.

Palter, J. B., Griffies, S. M., Galbraith, E. D., Gnanadesikan, A., Samuels, B. L., and Klocker, A.: The deep ocean buoyancy budget and its temporal variability, Journal of Climate, 27, 551–573, 2014.

Pinardi, N., Rosati, A., and Pacanowski, R. C.: The sea surface pressure formulation of rigid lid models. Implications for altimetric data assimilation studies, Journal of Marine Systems, 6, 109–119, 1995.

Ponte, R. M.: A preliminary model study of the large-scale seasonal cycle in bottom pressure over the global ocean, Journal of Geophysical Research, 104, 1289–1300, 1999.

Rahmstorf, S.: A fast and complete convection scheme for ocean models, Ocean Modelling, 101, 9–11, 1993.

Redi, M. H.: Oceanic isopycnal mixing by coordinate rotation., Journal of Physical Oceanography, 12, 1154–1158, 1982.

Roach, A., Aagard, K., Pease, C., Salo, S., Weingartner, T., Pavlov, V., and Kulakov, M.: Direct measurements of transport and water properties through Bering Strait, Journal of Geophysical Research, 100, 18 443–18 457, 1995.

Roberts, C., Jackson, L., and McNeall, D.: Is the 2004-2012 reduction of the Atlantic meridional overturning circulation significant?, Geophysical Research Letters, 41, 32043210, 2014.

Roberts, C. D., Garry, F., and Jackson, L.: A multi-model study of sea surface temperature and sub-surface density fingerprints of the Atlantic Meridional Overturning Circulation, Journal of Climate, 26, 91559174, 2013.

Roquet, F., Madec, G., McDougall, T. J., and Barker, P. M.: Accurate polynomial expressions for the density and specific volume of seawater using the TEOS-10 standard, Ocean Modelling, under review, 2014.

Roullet, G. and Madec, G.: Salt conservation, free surface, and varying volume. A new formulation for OGCMs, JGR, 105, 23 927–23 947, 2000.

Russell, J., Dixon, K., Gnanadesikan, A., Stouffer, R., and Toggweiler, J.: Southern Ocean Westerlies in a warming world: Propping open the door to the deep ocean, Journal of Climate, 19, 6381–6390, 2006.

Sadler, H.: Water, heat and salt transports through Nares Strait, Ellesmere Island, Fisheries Research Board of Canada, 33, 22862295, 1976.

Schauer, U., Fahrbach, E., Osterhus, S., and Rohardt, G.: Arctic warming through the Fram Strait: Oceanic heat transport from 3 years of measurements, Journal of Geophysical Research, 109, doi:10.1029/2003JC001 823, 2004.

Sidorenko, D., Danilov, S., Wang, Q., Huerta-Casas, A., and Schröter, J.: On computing transports in finite-element models, Ocean Modelling, 28, 60–65, 2009.

Simmons, H. L., Jayne, S. R., St.Laurent, L. C., and Weaver, A. J.: Tidally driven mixing in a numerical model of the ocean general circulation, Ocean Modelling, 6, 245–263, 2004.

Slangen, A., Katsman, C., van de Wal, R., Vermeersen, L., and Riva, R.: Towards regional projections of twenty-first century sea-level change based on IPCC SRES scenarios, Climate Dynamics, pp. 10.1007/s00 382–011–1057–6, 2012.

Slangen, A., son, Katsman, C., van de Wal, R., Hoehl, A., Vermeersen, L., and Stammer, D.: Projecting twenty-first century regional sea-level changes, Climatic Change, pp. 317–332, 2014.

Sloyan, B., Johnson, G., and Kessler, W.: The Pacific Cold Tongue: A pathway for interhemispheric exchange, Journal of Physical Oceanography, 33, 1027–1043, 2003.

Smith, R. and Gent, P.: Reference Manual for the Parallel Ocean Program (POP), Los Alamos Technical Report No. LAUR-02-2484, 2004.

Smith, R. D. and McWilliams, J. C.: Anisotropic horizonal viscosity for ocean models, Ocean Modelling, 5, 129–156, 2003.

Solomon, H.: On the representation of isentropic mixing in ocean models, Journal of Physical Oceanography, 1, 233–234, 1971.

Sprintall, J. and Tomczak, M.: Evidence of the Barrier Layer in the Surface Layer of the Tropics, Journal of Geophysical Research, 97, 7305–7316, 1992.

Stacey, M. W., Pond, S., and Nowak, Z. P.: A Numerical Model of the Circulation in Knight Inlet, British Columbia, Canada, Journal of Physical Oceanography, 25, 1037–1062, 1995.

Stommel, H.: A survey of ocean current theory, Deep Sea Research, 4, 149–184, 1957.

Strong, A., Liu, G., Meyer, J., Hendee, J., and Sasko, D.: Coral Reef Watch 2002, Bulletin of Marine Science, 75, 259–268, 2004.

Thiele, G. and Sarmiento, J. L.: Tracer dating and ocean ventilation, Journal of Geophysical Research, 95, 9377–9391, 1990.

WGCM: IPCC Standard Output from Coupled Ocean-Atmosphere GCMs, CLIVAR WGCM Document, available from http://www-pcmdi.llnl.gov/ipcc/standard_output.html, 2007.

Winton, M.: A reformulated three-layer sea ice model, Journal of Atmospheric and Oceanic Technology, 17, 525–531, 2000.

Wunsch, C. and Stammer, D.: Atmospheric loading and the oceanic "inverted barometer" effect, Reviews of Geophysics, 35, 79–107, 1997.

Yaremchuk, M., McCreary, J., Yu, Z., and Furue, R.: The South China Sea throughow retrieved from climatological data, Journal of Physical Oceanography, 39, 753–767, 2009.

Yin, J.: Century to multi-century sea level rise projections from CMIP5 models, Geophysical Research Letters, 39, 10.1029/2012GL052 947, http://dx.doi.org/10.1029/2012GL052947, 2012.

Yin, J., Griffies, S. M., and Stouffer, R.: Spatial Variability of Sea-Level Rise in 21st Century Projections, Journal of Climate, 23, 4585–4607, 2010a.

Yin, J., Stouffer, R., Spelman, M. J., and Griffies, S. M.: Evaluating the Uncertainty Induced by the Virtual Salt Flux Assumption in Climate Simulations and Future Projections, Journal of Climate, 23, 80–96, 2010b.